Surface effects in dry powders for inhalation

Dissertation zur Erlangung des Doktorgrades der Mathematisch-Naturwissenschaftlichen Fakultät der Christian-Albrechts-Universität zu Kiel

Vorgelegt von:

Nicholas Bungert

Kiel, 2022

This work was carried out from January 2019 until April 2022 at the Department of Pharmaceutics and Biopharmaceutics, Kiel University, Kiel, Germany. The thesis was prepared under supervision of Prof. Dr. Regina Scherließ.

1st Referee: Prof. Dr. Regina Scherließ

2nd Referee: Prof. Dr. Dr. Dr. Thomas Rades

Submission of the PhD Application:	29.04.2022
Date of examination:	29.06.2022
Accepted for publication:	29.06.2022

Meiner Familie gewidmet.

“Start where you are. Use what you have. Do what you can.”

-Arthur Ashe-

Publication list

Peer-reviewed publications contributing to this thesis:

Nicholas Bungert, Mirjam Kobler, Regina Scherließ
In-Depth Comparison of Dry Particle Coating Processes Used in DPI Particle Engineering
Pharmaceutics **2021**, 13, 580.

Nicholas Bungert, Mirjam Kobler, Regina Scherließ
Surface energy considerations in ternary powder blends for inhalation
International Journal of Pharmaceutics **2021**, 609, 121189.

Nicholas Bungert, Mirjam Kobler, Regina Scherließ
The role of intrinsic fines in the decreasing performance of expired lactose carriers for DPI applications
European Journal of Pharmaceutics and Biopharmaceutics **2022**, 175, 7-12.

Nicholas Bungert, Mirjam Kobler, Regina Scherließ
Proof-of-concept for artificial surface energies and modified extrinsic fines as a novel particle engineering approach in DPI formulations
Pharmaceutics **2022**, 14(5), 951.

Further publications not being part of this thesis:

Regina Scherließ, Simon Bock, Nicholas Bungert, Anna Neustock, Lena Valentin
Particle engineering in dry powders for inhalation
European Journal of Pharmaceutical Sciences **2022,** 172, 10658.

Conference contributions:

Nicholas Bungert, Mirjam Kobler, Regina Scherließ
The influence of the carrier surface energy on the aerodynamic performance of interactive blends revisited
Respiratory Drug Delivery 2020, virtual
April 26th – 30th (scientific poster)

Nicholas Bungert, Mirjam Kobler, Regina Scherließ
The influence of surface energies on the suitability of additional fines
Drug Delivery to the Lungs 2020, virtual
December 9th – 11th (oral presentation)

Nicholas Bungert
Surface energy considerations in formulation development: An example of SEA applications in dry powder inhalation
European Sorption Science Symposium 2021, virtual
September 22nd – 23rd (oral presentation)

Nicholas Bungert
Surface energy determinations as formulation development tool in dry powder inhalation
DPhG Annual PhD and Postdoc Meeting 2022, virtual
February 24th – 25th (oral presentation)

Nicholas Bungert, Mirjam Kobler, Regina Scherließ
Proof-of-concept: Surface energy alterations as particle engineering strategy in DPI formulations
PBP World Meeting 2022, Rotterdam, The Netherlands
March 28th – 31st (scientific poster)

Nicholas Bungert, Mirjam Kobler, Regina Scherließ
On the performance affecting mechanisms of long-time stored lactose carriers for inhalation
Respiratory Drug Delivery 2022, Orlando, Florida
May 1st – 5th (scientific poster) – accepted for presentation

Nicholas Bungert, Mirjam Kobler, Thomas Rades, Regina Scherließ
On the origin of the double peak of lactose-monohydrate dehydration events
Nordic POP Annual Meeting 2022, Helsinki, Finland
August 10th – 12th (scientific poster) – accepted for presentation

Kristoffer S. Sjögren, Nicholas Bungert, Ingunn Tho, Regina Scherließ
Performance defining properties in reservoir DPIs: An evaluation of powder flow optimizations
Nordic POP Annual Meeting 2022, Helsinki, Finland
August 10th – 12th (scientific poster) – accepted for presentation

Table of contents:

Chapter 1: Aim of thesis and introduction

Aim of thesis

Despite of impressing advances in computational tools, formulation scientists still do not have a universally applicable predictive model for dry powder inhaler (DPI) formulation performance. If a new drug candidate shall be delivered to the lung, the formulation composition is typically evaluated using internal company guidelines (based upon experiences of specific formulations, established devices, patents, etc.). Thereby, solid-state characterisation facilitates the understanding of resulting drug delivery performance. Multiple references provide information on the influence of physical properties of carrier [1,2] and drug [3] on the aerodynamic performance of respective DPI formulations. The complexity of solid-solid interactions causes a lack of transferability from one drug or carrier to another, further complicated by the crucial influence of the drug delivery device [4]. For future prediction techniques being valid, we need further understanding of the underlying mechanisms. Therefore, fundamental research is permanently focused on understanding the characteristics of particles and how they interact with each other.

The aim of this thesis is to further establish the inverse gas chromatography as a formulation development tool. It offers a comparably easy and sensitive analysis of adhesion affecting bulk properties. The complexity of respiratory drug delivery systems complicates a straight-forward prediction of formulation performance solely derived from surface energy (SE) parameters; hence experiment noise reduction is of crucial importance. Nevertheless, the surface energy determination is a valuable addition since it provides information on properties apart from well-established techniques like particle sizing or surface area determinations, which were already investigated in the past.

In the following chapters I will cover different aspects of surface energy related events in DPI formulations.

Regarding the carrier in adhesive mixtures, formulation scientists usually aim for low adhesive properties (low surface energies). This can be achieved by screening a variety of materials for the one with the lowest surface energy, or by altering the surface energy of well-established materials in a targeted manner. Apart from the formulation optimisation aspect, altering existing excipient qualities also offers an opportunity for extended understanding of surface energy effects. The second chapter of my work thus covers the evaluation of suitable methods to specifically modify surface energies of lactose carriers. Thereby I will focus on the decrease of surface energies with the least impact on morphology, particle size distribution or crystallinity.

The third chapter addresses surface energies of fine lactose excipients without the specific modification. Differences in their surface energies are solely based on their origin, so their manufacturing route and state of expiry. Here, I am aiming to figure out which surface energy levels are most beneficial for these fines. The term “fines“ is not clearly defined, but I will refer to fines as particles substantially smaller than 30 µm. Such fines in the carrier bulk are ubiquitous (intrinsic fines), while their extent depends on the processing of the lactose quality. Chapter four brings the conclusions from chapter two and three together and continues the common storyline. The first sections address the reversibility of surface energy modifications by dry particle engineering and shows that there is a causal connection between surface energy and adhesion. Furthermore, I present an idea of engineering fines to tailor their surface energy, according to specific requirements. Herewith, a variety of tools is part of this thesis, which are suitable to match SEs of formulation components to adjust adhesion strength in DPI formulations. I hypothesise that there is an optimum of SE interaction between respective blend components, which promotes the optimal blend dispersion and hence, drug delivery.

Within the fifth chapter I followed up on the long-time storage/ expiry effects of chapter three. This study covers the role of the intrinsic fine excipients of the lactose carrier bulk in the decreasing aerodynamic performance after long-time storage. I applied a systematic approach to assess their direct influence by removing and re-adding fine excipients from/to the carrier bulk.

1. Respiratory drug delivery: The current status

The lung as a therapeutic target can be traced back thousands of years [5]. Ancient Egyptian people were already aware that the vapour, which was produced by heating black henbane, could improve their breathing. Nowadays, anticholinergic drugs are still used for the treatment of asthma and chronic obstructive pulmonary disease (COPD). Asthma and COPD are both chronic respiratory diseases whose global burden increased dramatically within the last decades [6], and will most likely increase further within the following. The reason for the expected increase is in the intensification of the respective trigger factors, which are urbanisation and industrial evolution dependent (mainly air pollution) [7,8]. Both diseases are not curable at the moment, but treatable. According to the German therapy guideline for asthma and COPD [9] the therapeutic regime is fundamentally based on respiratory drug delivery. Acute exacerbations are typically treated with pressurised metered dose inhalers (pMDIs), whereas dry powder inhalers are the devices of choice to control the chronic inflammation of the lung tissue.

During an acute worsening of the breathing (e.g., asthma attack), pMDIs are necessary due to their independence of the patients peak inspiratory flow. By expansion of the propellant, the liquid formulation disperses, and droplets will exit the inhaler with high velocities. Hence, the patient needs to coordinate the actuation of the device with his inspiration. Otherwise, these high velocities will lead to high impaction rates in the upper throat region and thus less deposition in the targeted lung tissue. Upper throat deposition in turn, could result in more side effects since the drug will be swallowed and will likely act systemically. In the urgent case of an exacerbation, the patient needs to accept this disadvantage.

In contrast, dry powder inhalers (DPIs) are breath actuated. By pressing the actuator of the device, a single dose is prepared for inhalation either by metering from a reservoir, piercing a capsule or opening a blister cup. As soon as the patient starts to inhale, the airstream disperses the powder and carries (parts of) the formulation into the lung. The breath actuation allows for higher deposition rates in the target tissue since no coordination by the patient is necessary. Furthermore, DPIs contain no propellants, which makes them superior considering the greenhouse effect and the ongoing climate crisis. In addition, dry powder formulations are typically more stable than liquid ones, microbiologically as well as physically. The permanently expanding portfolio of DPIs can be therefore attributed to their benefits over pMDIs [10]. The Novolizer®, which is the DPI device used in this thesis, is a reservoir-based inhaler.

The third big category of inhalation devices are the nebulisers. Nebulisers need a power supply, since they actively disperse a liquid formulation into small, inhalable droplets. At the moment, the need for an external power source restricts their use to at-home therapies, being especially suitable for kids and elderly people. An intermediate between classical nebulisers

and the above mentioned handheld DPIs and pMDIs is the soft mist inhaler (Respimat®, MRX004 by Merxin® or Rescya). It combines the propellant free dispersion of a liquid formulation with the independency of an external power source.

However, based on the restricted applicability of nebulisers and the present disadvantages of pMDIs, DPIs are a well-accepted inhaler class and still hold great potential for the future. Beside local drug therapy (bronchiole deposition), this future potential is also strongly derived from the possibility to deliver a drug to the systemic blood circulation (alveolar deposition). The systemic application via the respiratory tract is promising, especially for drugs with high first pass effects, e.g., peptides. The large absorption site is characterised by high absorption rates and low metabolic activity and offers an opportunity for needle-free self-administration of systemic drugs [11].

An example for the feasibility of respiratory peptide delivery is the inhalable insulin Exubera®. The FDA and EMA approval in 2006 was unfortunately not followed by economic success. The main reasons were the costs, side effects and the applicability. Exubera® needed a bulky device, which complicated its use during the day, or on the go. Pfizer announced the withdrawal of Exubera in 2007. Another attempt of inhalable insulin is Afrezza® from MannKind (FDA approval in 2014). Even though the device is in a typical inhaler size, it still has negligible economic success. The main reason is most likely the hard market entry (highly developed, low-cost insulin pen technology) and negligible advantages over established administration strategies. Although being an economical backlash, both products proved that there is the possibility for respiratory delivery of peptide hormones as a dry powder, and it paved the way for future innovations.

Apart from curative peptide delivery, systemic inhaled therapies for Parkinson's disease, schizophrenia or migraine (nasally inhaled) are available on the market today [12].

In addition, respiratory vaccine delivery is a current research focus. Mucosal vaccination utilising the respiratory route holds great potential. Delivering an antigen via the lung or nose mimics its intended entry route and activates the mucosal immune system. Hence, directly after entry of the pathogen into the human body the acquired defence mechanisms come into play and hamper the reproduction of the pathogen. Furthermore, the application of the vaccine is more convenient since no injection is needed [13].

2. Dry powder formulations for inhaled therapy

In DPI formulation technology, scientists focus on the delivery of solid drug particles using the respiratory system. To follow the inhalation airstream into the deep lung tissue (alveolar region), the drug particles need to have an aerodynamic diameter below 5 µm. In contrast to

a geometric diameter, the aerodynamic diameter (D_{ae}) characterises the flight behaviour instead of just geometrical properties. It is defined as the diameter of a sphere (1 g/cm^3, ρ_0) with the same sedimentation velocity (in air) as the particle under investigation. The flight behaviour is strongly dependent on particle shape and density. The dependency is described accordingly, at best it is determined experimentally (Equation 1).

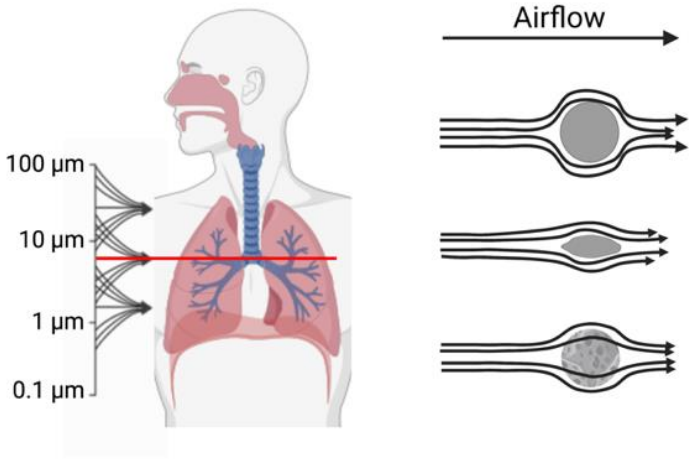

Figure 1: Particle deposition in the lungs depends on aerodynamic particle size. The aerodynamic particle size is defined by size, shape and density.

$$D_{ae} = D_{eq}\sqrt{\frac{\rho_p}{\rho_0 * X}} \quad (1)$$

X is the particle shape, D_{eq} represents the geometric diameter and ρ_P the respective density. Notwithstanding, a prerequisite for an API to be “inhalation grade” is generally a d_{90} value smaller than 5 µm measured as a geometric diameter (e.g. by laser diffraction). Thus, “inhalation grade” drugs are typically micronised.

After micronisation, particles are highly cohesive and practically impossible to process without further improvements. Hence, formulation scientists constantly develop powder formulations to enable the drug delivery of micronised powders to the lung.

In general, powder formulations for respiratory drug delivery are categorised in three strategies. The interactive blend, also known as adhesive or ordered mixture, is marketwise the most important, i.e., the most represented one [14]. Typically, these formulations are based on well-established excipients as carriers mainly lactose-monohydrate. Mannitol is a promising alternative since it is generally recognised as safe for pulmonal application and was also approved by the FDA in 2020 as active ingredient [15]. As a result, it is currently evaluated as an alternative to lactose [16].

Interactive blends build the fundament of respiratory therapies worldwide. To obtain an effective DPI formulation comparably low effort is needed: One needs a carrier (in the size range from 50 µm to 200 µm) [17], which is approved for respiratory application, and a micronised drug (< 5 µm). By blending both, the highly adhesive drug will attach onto the carrier surface. However, these binary formulations usually suffer two main disadvantages which are I) a very limited drug loading capacity and II) insufficient drug detachment during inhalation. The latter results in respirable fractions of mostly < 50% in currently marketed products [18]. The former is the main reason for interactive blends being just suitable for low-dose therapies. Drug carriers may be loaded with up to 15% (w/w) of drug [19]. Combined with the low respirable fractions, the delivery of multiple milligrams of drug (e.g. 20 mg rifampicin for the respiratory treatment of tuberculosis [20]) is simply not feasible utilising interactive blends. Scientists constantly evaluate and address both challenges to provide more safe and effective respiratory therapies.

To deliver such high drug doses to the lung, spheronised powders are a formulation strategy which is superior to interactive blends. One uses the high agglomeration tendency of micronised drug particles to form spherical agglomerates. Since these agglomerates show some appearance similarities to pellets, they are also called softpellets. The main advantage here is the drug content of up to 100%.

The third category of DPI formulations is called engineered powders. Usually, it is associated with the Pulmosphere™ technology, a spray-dried, highly porous particle formulation [21]. These low-density particles have significantly decreased contact area between the single particles. Hence, these particles show sufficient flow properties in a particle size, which is usually associated with poor flowability and dosability. Engineered powders do not have to be spray dried. The term generally covers the specific design of particles, to tailor their properties. Even though spray-drying is a useful and widely used technique to do so [22], there are numerous approaches, which are also covered by the collective term “engineered particles“. We recently published an extensive review article, discussing the wide range of engineered particles [23]. Within our review, we elaborated on particle engineering also being applicable to carrier-based blends. It offers the opportunity to address the earlier mentioned disadvantages of adhesive mixtures. The insufficient drug detachment from the carrier is still the main optimisation focus in carrier-based, respiratory formulation development. Most of the current strategies to increase that detachment have evolved over the past decades but are basically trial and error strategies. The reason is that we are missing a clear strategy to categorise adhesion properties of drugs or excipients. Consequently, understanding the mechanisms is crucial for structured formulation development approaches.

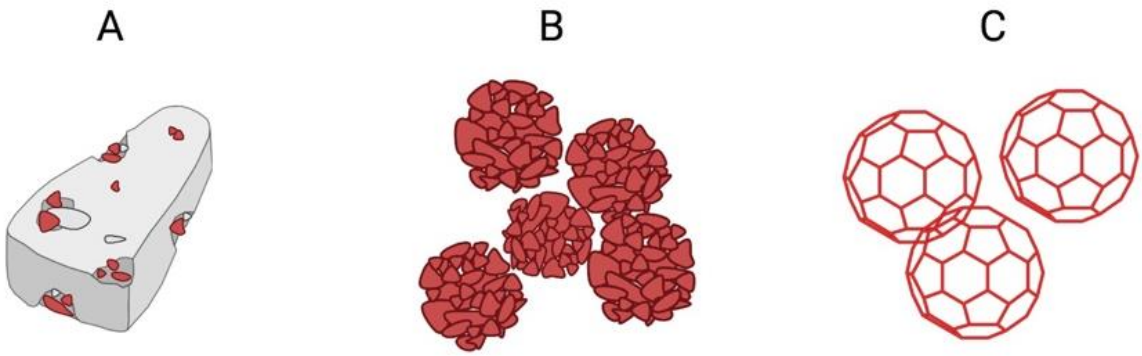

Figure 2: Illustration of formulation strategies for dry powders for inhalation. A) interactive blends B) spheronised powders and C) engineered powders.

3. Fundamentals of particle-particle adhesion

The following sections will provide some fundamental knowledge of adhesion in general and how it can be transferred to DPI formulation development.
Adhesion is a collective term for multifactorial phenomena. Different adhesion theories were proposed, trying to explain the versatile facets of adhesive interactions.

The first distinction to be made is between fundamental and practical adhesion. Fundamental adhesion represents interactions associated with molecular forces on the interface, whereas practical adhesion additionally includes other energy absorbing processes during fracture (e.g., plastic, and viscoelastic deformations). Fundamental adhesion is mainly expressed by the surface energy interaction of the respective interacting materials.

Practical adhesion is typically magnitudes larger than just the surface energy derived (i.e., thermodynamic) work of adhesion and cohesion, respectively. Since it considers many interdepending factors, practical adhesion is hard to predict. It can be directly measured by assessing the force, which is required to produce failure of the adhesive bond. The colloidal probe technique of the atomic force microscope (AFM) for instance allows for direct measurement of practical adhesion between two particles. To obtain adhesion or cohesion data, one must glue one particle on the cantilever of the AFM. This particle will be placed on the surface of a second particle and the force which is necessary to overcome the adhesive interaction will be measured [24,25]. Although this straight-forward method provides real data on adhesive bonds, it lacks reproducibility and expressiveness. Real materials (particles) are irregular and behave different as soon as a single test parameter changes. Thus, measured

adhesion forces are just snapshots of practical adhesion which may provide an indication, but which are not necessarily transferrable to the whole powder bulk.

A different approach to obtain adhesion data is the simulation of particles in contact. At the moment, a range of different models is available to simulate particle interaction: The Hertz model [17], the Johnson-Kendall-Roberts model [27] and the Derjaguin-Muller-Toporov model [28] should be mentioned in this context, without being further evaluated in this thesis. In summary, assumptions need to be made to enable calculable (simulatable) situations. These assumptions usually lead to ignoring of characteristics which influence real particles in contact (morphologies, roughness, physical parameters).

Further developed simulation attempts for practical adhesion, like multi-asperity models, provide increasingly precise approximations of surface interactions. But the irregularity of real surfaces is hard to simplify [29,30]. Additionally, the more characteristics are considered within a simulation, the more computational power and time is needed. Thus, the more realistic, the less suitable is the simulation for rapid formulation development.

Fundamental adhesion properties (surface energy of solids or surface tension of liquids) in turn can be measured as a bulk property using wetting or gas sorption techniques. The surface energy of solids mainly occurs since molecules on the surface are capable of more interaction than they actually engage [31]. These techniques provide information on the average adhesion (physisorption) behaviour of the investigated surface. Wetting techniques (contact angle measurements) usually require a flat sample surface on which the contact angle to known liquids is assessed. This is mostly feasible for large surfaces like films, polymer coatings etc. and just partly suitable for compressed powders. The main disadvantages of contact angle measurements of powder samples are the liquid absorbing properties of powders (in dependence of the liquid) as well as the sample surface morphology after compressing (flatness of surface sample). Therefore, gas sorption techniques seem more suitable for powdered samples.
Inverse gas chromatography (iGC) allows the determination of surface energies (SE) without the need for special sample preparation like compression (which also could alter the sample habit). A valid measurement requires an adequate available sample surface (typically > 0.5 m^2). As the name inverse gas chromatography suggests, this method bases on an inversion of “known“ and “unknown“ from a gas chromatography (GC). The sample (unknown) will be placed in the column (silanised glass tubes with selectable inner diameters between 2 and 4 mm), while the gas phase represents the “known“ component. As soon as the probe gases leave the sample column, a flame ionisation detector will transfer the gas pulse into a

measurable signal. Based on the retention behaviour of the probe gases, surface energy parameters can be derived. The retention of probe gases is dependent on the principles of fundamental adhesion. Fundamental adhesion is described by a range of different theories. All theories cover different aspects of interface interactions, whereas just some of them are important for iGC analysis, or particle-particle adhesion in general [32].
The adsorption theory covers physisorption and chemisorption. As soon as two materials get in contact on a molecular level, there will be a kind of interaction. Chemisorption describes covalent and ionic bonds, which are both high energy interactions. These kinds of interactions are hardly reversible and would result in non-separable particles (or sample and probe, respectively). Usually covalent bonds result from chemical reactions. Although this could occur between two surfaces, this work focuses on secondary interactions (physisorption).
The essential idea of the adsorption theory is that at least London dispersion forces will be present at all interfaces. London dispersion forces are intermolecular forces, based on the varying positions of electrons in their electron cloud (instantaneous dipoles). Furthermore, interactions between permanent dipoles (Keesom forces) or induced dipole and permanent dipole (Debye forces) may be present at the interface. These three are usually summarised as van-der-Waals forces and build the fundament of non-polar interactions [33].
Within this thesis I am referring to van der Waals forces according to the Lifshitz theory [34]. Lifshitz defined attractive forces between substances as bulk properties (macroscopic approach), so to be dependent on the media as well, instead of just taking the interaction partners into account (i.e., pairwise additivity as assumed by Hamaker [35]).

Van-der-Waals forces are complemented by polar interactions. Whenever a Lewis-acid (electron acceptor) and a Lewis-base (electron donor) are brought close to each other's interface, it will result in an acid-base complex (acid-base adhesion theory). Such interactions are short range interactions (0.2 to 0.3 nm) due to their energy origin in coulombic forces. Strength-wise they are comparable to London dispersion forces, although London forces can operate at distances exceeding 10 nm [36].

This work also categorises hydrogen bonds together with acid-base interactions as polar interactions, whereas according to the definition of Keesom and Debye forces, it could also be mentioned within the context of dispersive forces (i.e., dipole - dipole interactions) [37].

Whenever a probe gas molecule is injected into the iGC column it starts interacting with the sample surface. In iGC theory there is a strict distinction between dispersive (non-polar) and polar interactions. The former is determined by injecting a series of different alkanes. To calculate the dispersive surface energy from alkane retention data, two calculation theories

were proposed. Schultz et al. [38] used injections of n-alkanes in the Henry ‘s Law region (infinite dilution, no probe-probe interactions) to calculate the dispersive SE of the sample material. They assumed that the n-alkanes are solely capable of dispersive interactions. Therefore, the resulting Gibbs free energy of ad- and desorption is just based on non-polar interactions and only dependent on the carbon number (or cross-sectional area of the probe molecule, respectively) and on the work of adhesion between probe and sample. The work of adhesion in turn composes of the SE of both interacting surfaces, of which one is known (namely SE of the probe molecule). Combining these thermodynamic equations results in a function that provides a linear graph. The slope of that graph gives the dispersive SE of the sample. Polar probes will result in data points above that “alkane line”. The vertical distance between the polar probe and the alkane line gives the specific (acid-base) part of the Gibbs free energy [39].

The second approach is by Dorris and Gray [40]. They considered just the methylene groups of the injected n-alkanes to affect the free energy of adsorption. Furthermore, they stated that the Gibbs free energy of adsorption per mole methylene is equal to the work of adhesion between stationary and mobile phase. Using the given SE value per methylene group, one can derive the dispersive SE of the sample (Equation 2, Figure 3). Since that methylene-approach is not transferable to polar samples like chloroform, the Dorris and Gray approach just provides information on dispersive SE properties. In contrast to the Schultz-approach an additional method is necessary to obtain data regarding polar interactions, e.g., the polarisation method (Figure 4) [41]. By plotting RTlnVN (with V being the retention volume of the probe gas) against the molar deformation polarisation of the respective probes (P_D), we obtain an alkane line with polar samples being above that line. The vertical distance between the alkane line and the respective polar data points provides the specific free energy (ΔG_{SP}) per polar probe. Calculated values of polar SE properties crucially depend on the used probe gas, regardless of the methods. Thus, by changing the polar probes, the specific SE (and hence the total surface energy) will change significantly. In consequence, the specific (and the derived total SE) is just comparable, if always the same probes were used. Also, the magnitude of the specific SE in contrast to the dispersive is not necessarily comparable. Some polar probes are very sensitive to changes in the polar surface properties, so even small changes in polarity result in big changes in the specific surface energy. Contrarily, the dispersive surface energy is always measured the same way and thus comparable (when using the same calculation method). Even if Schultz et al. stated that their results are similar to the ones from Dorris and Gray [42], a comparative study by Shi et al. found that the latter results in higher dispersive surface energies [43]. Another study also attributed a higher measurement precision to the Dorris-Gray method [44].

$$\gamma_S^D = \frac{slope^2}{4 \times N^2 \times \left(a_{CH_2}\right)^2 \gamma_{CH_2}} \quad (2)$$

$\gamma_S^D = Dispersive\ surface\ energy\ of\ the\ stationary\ phase\ (sample)$

$N = Avogadro's\ number$

$a_{CH_2} = Cross-sectional\ area\ of\ a\ methylene\ group$

$\gamma_{CH_2} = Dispersive\ surface\ energy\ of\ a\ methylene\ group$

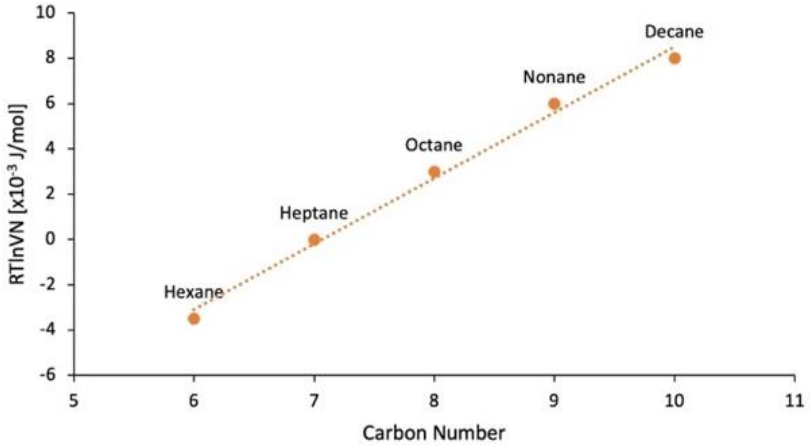

Figure 3: Dorris and Gray approach to calculate the dispersive surface energy of solids.

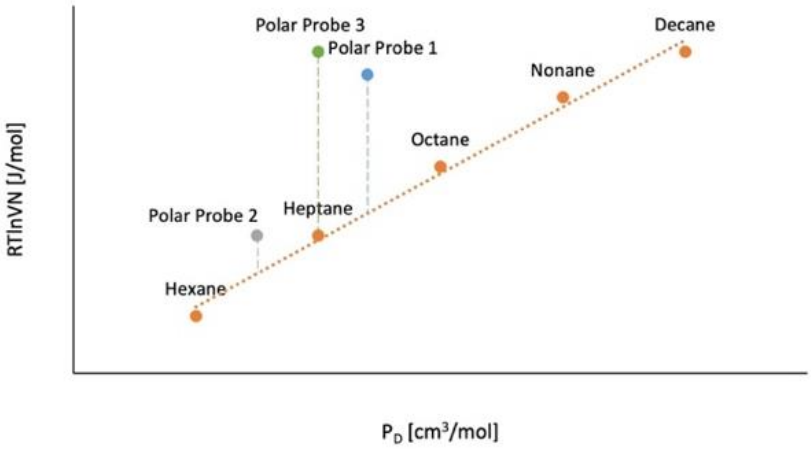

Figure 4: The Polarisation method enables the calculation of polar surface energies.

To conclude, a change in dispersive SE is not to be equated with a change in the specific SE, due to the strong probe dependency of the latter.

In addition, the absolute value for specific SEs is dependent on the scale which provides Lewis-acid and -base properties of probe gases for calculation. In 1991 van Oss et al. published an equation which allows for the calculation of acid-base properties based on contact angle measurements [45]. A few years later DellaVolpe et al. re-evaluated this method and modified it to be more accurate and realistic [46]. The weakness of the original theory was

that surfaces will always be calculated as being very basic, due to the usage of a specific SE reference value for water. The latter fixed this “inaccuracy” by recalculating the dispersive surface free energy of water and recalculated SE values for various surfaces, which led to more realistic acid-base values (in alignment with chemical properties and other measurement techniques as iGC).

Although, the adsorption of probe gases in iGC represents fundamentally transferrable adhesion mechanisms, adhesion has many more aspects. The electrostatic, as well as the mechanical adhesion theories cover essential interaction types, which occur between particles in contact.

The electrostatic adhesion theory derives the hypothesis of an electrochemical potential difference between two materials in contact. Even without any charge transfer, an electric double layer will be established, which results in attraction forces between the surfaces. According to Coulomb ‘s law the attraction or repulsion force mainly depends on the particle charges (q) and their distance (d).

$$F_{el} = \frac{q_1 \times q_2}{4 \times \pi \times \varepsilon \times d^2} \quad (3)$$

Depending on the reference, some of the above-mentioned theories were categorised differently. This list of underlying principles has no claim of completeness. It highlights some distinguishable reasons for attractive forces between solid particles. Additional theories like the diffusion theory (entanglement of movable polymer chains) or wetting theory (establishment of continuous contact) were excluded since they lack transferability to interactive blends. Although the term “wetting” is not directly transferrable to a solid - solid interface, a strong correlation of area in contact and interaction strength has been reported [47].

In addition to surface chemistry related interactions, the mechanical adhesion theory covers effects which are solely based on morphological interactions. Real surfaces are usually rough. They contain asperities, protuberances, cavities, or buckles. The mechanical (interlock) theory attributes adhesion forces to the mechanical interlocking between these asperities.

Even if it is no fundamental adhesion theory, especially important for dry formulations is the induction of electric charges due to particle-particle friction. This triboelectricity occurs when powders flow and are therefore ubiquitous in dry powders for inhalation.

Triboelectricity or electric charge build-up is strongly depending on the surrounding relative humidity. While increasing humidity decreases surface conductivity [48] and hence

electrostatic interactions, the condensation of humidity on the particle surface may lead to liquid bridges and thus capillary forces [49]. Both are considerable attraction forces, which can exceed the above-mentioned van der Waals forces [50]. Notwithstanding, triboelectric charging is also affected by surface chemistry, which means it has an indirect dependence on iGC data [51].

It can be concluded that iGC characterisation covers physisorption but neglects mechanical interactions. Particle property changes, which occur during handling and processing (e.g., triboelectricity) are also not directly considered.

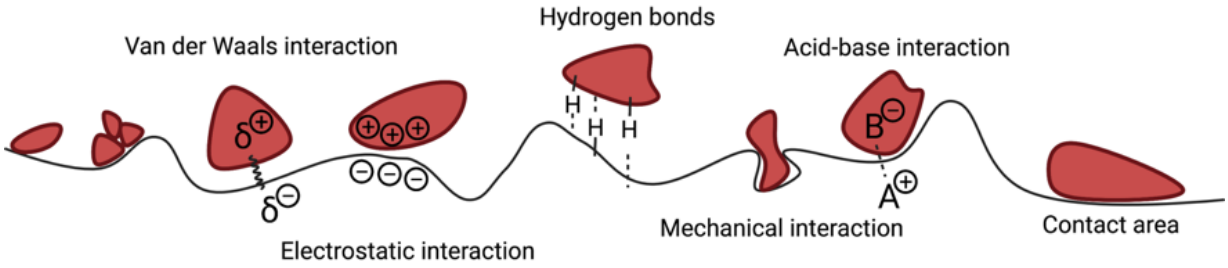

Figure 5: Different interaction types between particles. All interactions occur simultaneously to varying extents; figure adapted from Hickey et al [52].

4. How to overcome particle-particle interactions

During inhalation of dry powders, all the described adhesion mechanisms are present, influencing and complementing each other. Fundamental understanding of the interaction possibilities is crucial to tailor these and thus to achieve a sufficient drug detachment and hence drug delivery. Powder dispersion during inhalation bases on different dispersion mechanisms. It starts with the fluidisation of the static powder bed. Hereby drag and lift forces can already separate drug particles from the carriers. The fluidised powder will then be exposed to shear (particle - particle and particle - wall), friction (particle - particle, particle - wall and particle - airstream) and inertial forces (particle - particle and particle - wall collisions) [53].These forces need to exceed the cohesive and adhesive forces within the powder bed. A unique possibility in respiratory drug delivery is to increase dispersion forces by device design. In dependence of the device structure and the resulting flow pattern within the device, the dispersion forces change and hence the aerodynamic performance [4]. The device design itself is a complex science, which needs to be mentioned, but will not be part of this thesis. Apart from increasing the dispersion forces, another well-established approach is to weaken the adhesion.

As mentioned before, adhesion strength always depends on both interacting material surfaces. Thus, all strategies to weaken the interaction can basically be applied either on the

carrier or on the drug particle. Influencing factors are I) the area of contact, II) morphological opportunities for mechanical interlocking and III) the physico-chemical interaction capabilities. Each of them is modifiable.

Particle morphology influences both, the area of contact and the extent of mechanical interlocking, albeit in different size ranges, respectively. Particle roughness (morphology on a micro- to nanoscale) defines the extent of interfacial area, although it depends on the combination of both surfaces. Consequently, it should not be surprising that different working groups came to different conclusions. Iida et al. and Young et al. reported surface smoothening led to decreased adhesion, whereas Chan et al. concluded that increasing carrier roughness also decreased the respective adhesion [54–56]. Renner et al. gradually increased roughness of a model carrier and showed that nano roughness resulted in decreased adhesion, whereas micro scale roughness increased adhesion strength (mechanical interlocking) [57].

If morphology is considered in a larger size range, irregular shaped particles offer in general more opportunities for interlocking than uniform ones.

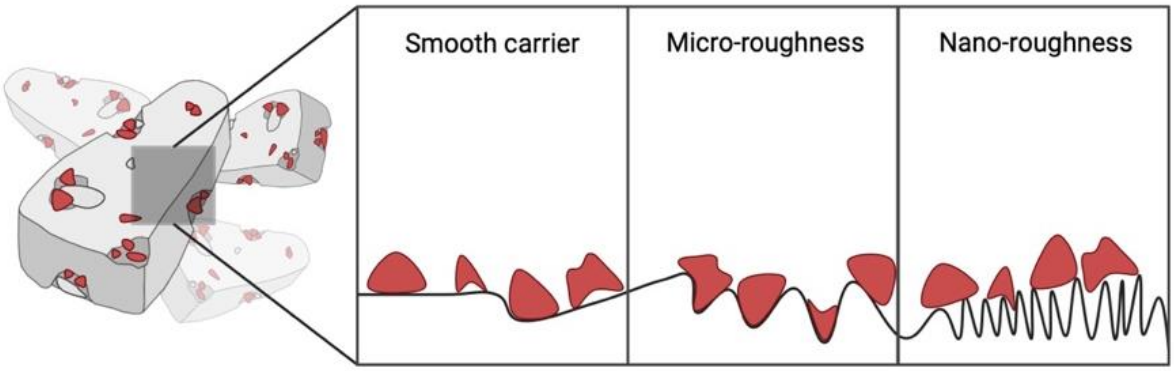

Figure 6: Contact area between coarse and fine particles strongly depend on roughness and morphologies. It has been shown that a micro-scale roughness increases interactions, whereas a nano-scale roughness lessens the area of interaction.

Physico-chemical properties can be modified by altering the chemical composition of the particle surface or the crystal behaviour of the respective surface. Coating techniques, either wet or dry, can add thin layers of an additive substrate onto the surface. Depending on the technique and additive, one will have a continuous or non-continuous coating, forcing the adhesion partner to interact with a new chemical composition. Similar effects are achievable using co-processing, even though most co-processing techniques result in completely new particles (particle size distribution and morphology), which complicates the comparison with the raw material. In dependence of the additive either strengthening or weakening of the adhesion occurs. The inverse gas chromatography offers an opportunity to evaluate the resulting changes in surface chemistry and hence adhesion behaviour.

Generally, all modifications of the surface will result in changes of the surface energy and adhesion capabilities, respectively. So apart from specific surface chemistry alteration using coating techniques [58] also amorphous content [59], different crystal facets [60] or adsorbed moisture [61] lead to changes in the SE. Hence, inverse gas chromatography is suitable to track process induced changes, storage related effects or batch-to-batch variations, as soon as the respective process affects the samples surface.

To exploit the full potential of SE assessments, the obtained data needs to be combined with already established solid-state characterisation tools [62].

References Chapter 1

[1] A. della Bella, E. Salomi, F. Buttini, R. Bettini, The role of the solid state and physical properties of the carrier in adhesive mixtures for lung delivery, Expert Opinion on Drug Delivery. 15 (2018) 665–674. https://doi.org/10.1080/17425247.2017.1371132.

[2] T. Peng, S. Lin, B. Niu, X. Wang, Y. Huang, X. Zhang, G. Li, X. Pan, C. Wu, Influence of physical properties of carrier on the performance of dry powder inhalers, Acta Pharmaceutica Sinica B. 6 (2016) 308–318. https://doi.org/10.1016/j.apsb.2016.03.011.

[3] H. Adi, D. Traini, H.-K. Chan, P.M. Young, The Influence of Drug Morphology on Aerosolisation Efficiency of Dry Powder Inhaler Formulations, Journal of Pharmaceutical Sciences. 97 (2008) 2780–2788. https://doi.org/10.1002/jps.21195.

[4] Friebel C, Rationale Entwicklung eines Inhalationssystems, 2010.

[5] S.W. Stein, C.G. Thiel, The History of Therapeutic Aerosols: A Chronological Review, Journal of Aerosol Medicine and Pulmonary Drug Delivery. 30 (2017) 20–41. https://doi.org/10.1089/jamp.2016.1297.

[6] J. Soriano, P.J. Kendrick, K.R. Paulson, R.A. Adedoyin, T.B. Adhikari, Prevalence and attributable health burden of chronic respiratory diseases, 1990–2017: a systematic analysis for the Global Burden of Disease Study 2017, The Lancet Respiratory Medicine. 8 (2020) 585–596. https://doi.org/10.1016/S2213-2600(20)30105-3.

[7] WHO Fact sheet COPD, (2021). Last accessed: 14.02.2022.

[8] WHO Fact sheet Asthma, (2021). Last accessed: 14.02.2022.

[9] Bundesärztekammer (BÄK), Kassenärztliche Bundesvereinigung (KBV), Arbeitsgemeinschaft der Wissenschaftlichen Medizinischen Fachgesellschaften (AWMF), Nationale VersorgungsLeitlinie Asthma, (2020).

[10] S.P. Newman, W.W. Busse, Evolution of dry powder inhaler design, formulation, and performance, Respiratory Medicine. 96 (2002) 293–304. https://doi.org/10.1053/rmed.2001.1276.

[11] D.A. Groneberg, C. Witt, U. Wagner, K.F. Chung, A. Fischer, Fundamentals of pulmonary drug delivery, Respiratory Medicine. 97 (2003) 382–387. https://doi.org/10.1053/rmed.2002.1457.

[12] Y. Ye, Y. Ma, J. Zhu, The future of dry powder inhaled therapy: Promising or discouraging for systemic disorders?, International Journal of Pharmaceutics. 614 (2022) 121457. https://doi.org/10.1016/j.ijpharm.2022.121457.

[13] Hellfritzsch, Scherließ, Mucosal Vaccination via the Respiratory Tract, Pharmaceutics. 11 (2019) 375. https://doi.org/10.3390/pharmaceutics11080375.

[14] Y. Ye, Y. Ma, J. Zhu, The future of dry powder inhaled therapy: Promising or discouraging for systemic disorders?, International Journal of Pharmaceutics. 614 (2022) 121457. https://doi.org/10.1016/j.ijpharm.2022.121457.

[15] FDA Approval Letter Bronchitol, https://www.Accessdata.Fda.Gov/Drugsatfda_docs/Nda/2021/202049Orig1s000Approv.Pdf. (2020). Last accessed: 14.02.2022

[16] N. Hertel, Mannitol als alternativer Träger in interaktiven Pulvermischungen zur Inhalation, 2020. Dissertation, Kiel University.

[17] J. Ooi, D. Traini, S. Hoe, W. Wong, P.M. Young, Does carrier size matter? A fundamental study of drug aerosolisation from carrier based dry powder inhalation systems, International Journal of Pharmaceutics. 413 (2011) 1–9. https://doi.org/10.1016/j.ijpharm.2011.04.002.

[18] P. Demoly, P. Hagedoorn, A.H. de Boer, H.W. Frijlink, The clinical relevance of dry powder inhaler performance for drug delivery, Respiratory Medicine. 108 (2014) 1195–1203. https://doi.org/10.1016/j.rmed.2014.05.009.

[19] A. Benassi, I. Perazzi, R. Bosi, C. Cottini, R. Bettini, Quantifying the loading capacity of a carrier-based DPI formulation and its dependence on the blending process, Powder Technology. 356 (2019) 607–617. https://doi.org/10.1016/j.powtec.2019.08.109.

[20] Etschmann C, Development of a Softpellet Formulation for Inhaled High-Dose Therapy, 2021.

[21] J. Weers, T. Tarara, The PulmoSphere™ platform for pulmonary drug delivery, Therapeutic Delivery. 5 (2014) 277–295. https://doi.org/10.4155/tde.14.3.

[22] R. Vehring, Pharmaceutical Particle Engineering via Spray Drying, Pharmaceutical Research. 25 (2008) 999–1022. https://doi.org/10.1007/s11095-007-9475-1.

[23] R. Scherließ, S. Bock, N. Bungert, A. Neustock, L. Valentin, Particle engineering in dry powders for inhalation, European Journal of Pharmaceutical Sciences. 172 (2022) 106158. https://doi.org/10.1016/j.ejps.2022.106158.

[24] N. Islam, R.A. Tuli, G.A. George, T.R. Dargaville, Colloidal drug probe: Method development and validation for adhesion force measurement using Atomic Force Microscopy, Advanced Powder Technology. 25 (2014) 1240–1248. https://doi.org/10.1016/j.apt.2014.06.021.

[25] H. Adi, D. Traini, H.-K. Chan, P.M. Young, The Influence of Drug Morphology on Aerosolisation Efficiency of Dry Powder Inhaler Formulations, Journal of Pharmaceutical Sciences. 97 (2008) 2780–2788. https://doi.org/10.1002/jps.21195.

[26] H. Hertz, Ueber die Berührung fester elastischer Körper, in: Journal Für Die Reine Und Angewandte Mathematik Band 92, De Gruyter, 1882: pp. 156–171. https://doi.org/10.1515/9783112342404-004.

[27] Johnson K L, Kendall K, Roberts A D, Surface energy and the contact of elastic solids, Proceedings of the Royal Society of London. A. Mathematical and Physical Sciences. 324 (1971) 301–313. https://doi.org/10.1098/rspa.1971.0141.

[28] B.V. Derjaguin, V.M. Muller, Yu.P. Toporov, Effect of contact deformations on the adhesion of particles, Journal of Colloid and Interface Science. 53 (1975) 314–326. https://doi.org/10.1016/0021-9797(75)90018-1.

[29] P. Prokopovich, S. Perni, Comparison of JKR- and DMT-based multi-asperity adhesion model: Theory and experiment, Colloids and Surfaces A: Physicochemical and Engineering Aspects. 383 (2011) 95–101. https://doi.org/10.1016/j.colsurfa.2011.01.011.

[30] Y.I. Rabinovich, J.J. Adler, A. Ata, R.K. Singh, B.M. Moudgil, Adhesion between Nanoscale Rough Surfaces, Journal of Colloid and Interface Science. 232 (2000) 17–24. https://doi.org/10.1006/jcis.2000.7168.

[31] Zeng X M, Martin G P, Marriot C, Particulate Interactions in Dry Powder Formulation for Inhalation, CRC Press, 2000.

[32] D.E. Packham, Theories of Fundamental Adhesion, in: Handbook of Adhesion Technology, Springer International Publishing, Cham, 2017: pp. 1–31. https://doi.org/10.1007/978-3-319-42087-5_2-2.

[33] Introduction and Adhesion Theories, in: Adhesives Technology Handbook, Elsevier, 2009: pp. 1–19. https://doi.org/10.1016/B978-0-8155-1533-3.50004-9.

[34] E.M. Lifshitz, M. Hamermesh, The theory of molecular attractive forces between solids, in: Perspectives in Theoretical Physics, Elsevier, 1992: pp. 329–349. https://doi.org/10.1016/B978-0-08-036364-6.50031-4.

[35] H.C. Hamaker, The London—van der Waals attraction between spherical particles, Physica. 4 (1937) 1058–1072. https://doi.org/10.1016/S0031-8914(37)80203-7.

[36] Frederick M. Fowkes, Acid-Base Interactions: Relevance to Adhesion Science and Technology , 1st ed., CRC Press, 1991.

[37] F.M. Fowkes, Role of acid-base interfacial bonding in adhesion, Journal of Adhesion Science and Technology. 1 (1987) 7–27. https://doi.org/10.1163/156856187X00049.

[38] J. Schultz, L. Lavielle, C. Martin, The Role of the Interface in Carbon Fibre-Epoxy Composites, The Journal of Adhesion. 23 (1987) 45–60. https://doi.org/10.1080/00218468708080469.

[39] S. Mohammadi-Jam, K.E. Waters, Inverse gas chromatography applications: A review, Advances in Colloid and Interface Science. 212 (2014) 21–44. https://doi.org/10.1016/j.cis.2014.07.002.

[40] G.M. Dorris, D.G. Gray, Adsorption of n-alkanes at zero surface coverage on cellulose paper and wood fibers, Journal of Colloid and Interface Science. 77 (1980) 353–362. https://doi.org/10.1016/0021-9797(80)90304-5.

[41] S. Dong, M. Brendlé, J.B. Donnet, Study of solid surface polarity by inverse gas chromatography at infinite dilution, Chromatographia. 28 (1989) 469–472. https://doi.org/10.1007/BF02261062.

[42] J. Schultz, L. Lavielle, Interfacial Properties of Carbon Fiber—Epoxy Matrix Composites, in: 1989: pp. 185–202. https://doi.org/10.1021/bk-1989-0391.ch014.

[43] B. Shi, Y. Wang, L. Jia, Comparison of Dorris–Gray and Schultz methods for the calculation of surface dispersive free energy by inverse gas chromatography, Journal of Chromatography A. 1218 (2011) 860–862. https://doi.org/10.1016/j.chroma.2010.12.050.

[44] P.P. Ylä-Mäihäniemi, J.Y.Y. Heng, F. Thielmann, D.R. Williams, Inverse Gas Chromatographic Method for Measuring the Dispersive Surface Energy Distribution for Particulates, Langmuir. 24 (2008) 9551–9557. https://doi.org/10.1021/la801676n.

[45] R.J. Good, M.K. Chaudhury, C.J. van Oss, Theory of Adhesive Forces Across Interfaces, in: Fundamentals of Adhesion, Springer US, Boston, MA, 1991: pp. 153–172. https://doi.org/10.1007/978-1-4899-2073-7_4.

[46] C. della Volpe, S. Siboni, Acid–base surface free energies of solids and the definition of scales in the Good–van Oss–Chaudhury theory, Journal of Adhesion Science and Technology. 14 (2000) 235–272. https://doi.org/10.1163/156856100742546.

[47] K. Meine, K. Kloß, T. Schneider, D. Spaltmann, The influence of surface roughness on the adhesion force, Surface and Interface Analysis. 36 (2004) 694–697. https://doi.org/10.1002/sia.1738.

[48] G. Buckton, A. Choularton, A.E. Beezer, S.M. Chatham, The effect of the comminution technique on the surface energy of a powder, International Journal of Pharmaceutics. 47 (1988) 121–128. https://doi.org/10.1016/0378-5173(88)90222-0.

[49] Y.I. Rabinovich, M.S. Esayanur, B.M. Moudgil, Capillary Forces between Two Spheres with a Fixed Volume Liquid Bridge: Theory and Experiment, Langmuir. 21 (2005) 10992–10997. https://doi.org/10.1021/la0517639.

[50] J.P.K. Seville, C.D. Willett, P.C. Knight, Interparticle forces in fluidisation: a review, Powder Technology. 113 (2000) 261–268. https://doi.org/10.1016/S0032-5910(00)00309-0.

[51] N.M. Ahfat, G. Buckton, R. Burrows, M.D. Ticehurst, An exploration of inter-relationships between contact angle, inverse phase gas chromatography and triboelectric charging data, European Journal of Pharmaceutical Sciences. 9 (2000) 271–276. https://doi.org/10.1016/S0928-0987(99)00063-9.

[52] A.J. Hickey, H.M. Mansour, M.J. Telko, Z. Xu, H.D.C. Smyth, T. Mulder, R. McLean, J. Langridge, D. Papadopoulos, Physical Characterization of Component Particles Included in Dry Powder Inhalers. I. Strategy Review and Static Characteristics, Journal of Pharmaceutical Sciences. 96 (2007) 1282–1301. https://doi.org/10.1002/jps.20916.

[53] G. Pilcer, N. Wauthoz, K. Amighi, Lactose characteristics and the generation of the aerosol, Advanced Drug Delivery Reviews. 64 (2012) 233–256. https://doi.org/10.1016/j.addr.2011.05.003.

[54] K. Iida, Y. Hayakawa, H. Okamoto, K. Danjo, H. Leuenberger, Preparation of Dry Powder Inhalation by Surface Treatment of Lactose Carrier Particles., Chemical and Pharmaceutical Bulletin. 51 (2003) 1–5. https://doi.org/10.1248/cpb.51.1.

[55] P.M. Young, D. Cocconi, P. Colombo, R. Bettini, R. Price, D.F. Steele, M.J. Tobyn, Characterization of a surface modified dry powder inhalation carrier prepared by "particle smoothing," Journal of Pharmacy and Pharmacology. 54 (2010) 1339–1344. https://doi.org/10.1211/002235702760345400.

[56] L.W. Chan, L.T. Lim, P.W.S. Heng, Immobilization of fine particles on lactose carrier by precision coating and its effect on the performance of dry powder formulations, Journal of Pharmaceutical Sciences. 92 (2003) 975–984. https://doi.org/10.1002/jps.10372.

[57] N. Renner, H. Steckel, N. Urbanetz, R. Scherließ, Nano- and Microstructured model carrier surfaces to alter dry powder inhaler performance, International Journal of Pharmaceutics. 518 (2017) 20–28. https://doi.org/10.1016/j.ijpharm.2016.12.052.

[58] S.C. Das, Q. Zhou, D.A.V. Morton, I. Larson, P.J. Stewart, Use of surface energy distributions by inverse gas chromatography to understand mechanofusion processing and functionality of lactose coated with magnesium stearate, European Journal of Pharmaceutical Sciences. 43 (2011) 325–333. https://doi.org/10.1016/j.ejps.2011.05.012.

[59] H.E. Newell, G. Buckton, D.A. Butler, F. Thielmann, D.R. Williams, The Use of Inverse Phase Gas Chromatography to Measure the Surface Energy of Crystalline, Amorphous, and Recently Milled Lactose, Pharmaceutical Research. 18 (2001) 662–666. https://doi.org/10.1023/A:1011089511959.

[60] R. Ho, M. Naderi, J.Y.Y. Heng, D.R. Williams, F. Thielmann, P. Bouza, A.R. Keith, G. Thiele, D.J. Burnett, Effect of Milling on Particle Shape and Surface Energy Heterogeneity of Needle-Shaped Crystals, Pharmaceutical Research. 29 (2012) 2806–2816. https://doi.org/10.1007/s11095-012-0842-1.

[61] Naderi M, Acharya M, Dienstmaier J, Kondor A, Lozano E, Burnett D, Characterization of Structural and Stereo Isomeric Amino Acids Using Raman Spectroscopy and Vapour Sorption Techniques, London, 2015.

[62] X. Kou, L.W. Chan, H. Steckel, P.W.S. Heng, Physico-chemical aspects of lactose for inhalation, Advanced Drug Delivery Reviews. 64 (2012) 220–232. https://doi.org/10.1016/j.addr.2011.11.004.

Chapter 2: In-Depth Comparison of Dry Particle Coating Processes Used in DPI Particle Engineering

This chapter is published as:
Bungert, N., Kobler, M., Scherließ, R.: In-Depth Comparison of Dry Particle Coating Processes Used in DPI Particle Engineering.
Pharmaceutics **2021**, 13, 580.
https://doi.org/10.3390/pharmaceutics13040580

Abstract:

High-shear mixer coatings as well as mechanofusion processes are used in the particle-engineering of dry powder inhalation carrier systems. The aim of coating the carrier particle is usually to decrease carrier–drug adhesion. This study comprises the in-depth comparison of two established dry particle coating options. Both processes were conducted with and without a model additive (magnesium stearate). In doing so, changes in the behaviour of the processed particles can be traced back to either the process or the additive. It can be stated that the coarse model carrier showed no significant changes when processed without additives. By coating the particles with magnesium stearate, the surface energy decreased significantly. This leads to a significant enhancement of the aerodynamic performance of the respective carrier-based blends. Comparing the engineered carriers with each other, the high-shear mixer coating shows significant benefits, namely, lower drug–carrier adhesion and the higher efficiency of the coating process.

1. Introduction

The increasing prevalence of respiratory diseases has been reported frequently [1]. Due to numerous advantages of dry powder inhalation (DPI) formulations, their importance has increased in the past decades. Out of several formulation options, the interactive blend is the most important one when it comes to frequency of use [2]. To reach processability of higher cohesiveness, micronised drug particles are mixed with a coarse carrier. While mixing, the drug attaches to the carrier but just so strong that it can detach in the inhalation airstream. Commercially available respiratory medicines show insufficient drug delivery to the lungs [3,4], usually significantly below 50%. The share of the active pharmaceutical ingredient (API), which is not able to detach and disperse, will impact with the carrier in the throat or in the upper airways. This can lead to side effects and decreased API concentrations in the deeper lung tissues. There are numerous strategies of using additives for the improvement of aerodynamic performance of carrier-based blends. Beside the addition of lactose fines [5], magnesium stearate [6] is a well-established additive as a force control agent (FCA). Several scientific articles report about the beneficial effect of the addition of the well-known lubricant [6,7]. Nearly as many articles try to explain the underlying principle of the enhanced aerodynamic performance [8,9]. To date, the operating principle is not completely clarified. It is most likely a combination of smoothening and weakening of binding energy. Since Hertel et al. (2020) found that force control agents combined with additional extrinsic fines do not lead to the addition of beneficial effects, the decrease in binding energy using FCAs is further substantiated. This is due to the fact that additional fines work, amongst other interactions, through the occupation of higher energy sites on the carrier. Weakening those makes additional fines superfluous, as also observed by Hertel et al. In the past, different approaches were published describing how magnesium stearate is added and the corresponding impact of it. The most common attempt is just by blending the carrier and additive in a high-shear mixer. Recent work showed an evenly distributed lubricant coating for high-shear mixing with magnesium stearate using TOF- SIMS (time-of-flight secondary-ion mass spectrometry) [10]. Another strategy is to make use of the so-called mechanofusion [11], an approach that merges substances with high mechanical energy input. The claimed benefit is a mechano-chemical reaction in the contact area of two solid substances leading to new compositions [12]. While being processed, the sample in the mechanofusion reactor is compressed and simultaneously stressed by intense shear. Both dry particle coating strategies are dependent on rotor speed and pro- cessing time. The parameters in this work are based on already published data using these methods [7,11,13]. The comparison between the high-shear and low-shear addition of the lubricant has already been investigated in the past, showing no significant increase in

aerodynamic performance after low-shear mixing [14]. In general, numerous methods can be used for dry particle coatings, even though not all of them are suitable for coating DPI carrier particles without fundamental changes in particle morphology. A wide range of applications had been extensively reviewed recently by Sharma et al. [15]. It is reported that mechanofusion with FCAs leads to enhanced flowability and powder de-agglomeration combined with an overall decreased and more homogeneous surface energy of the created compound particles [13,16,17]. The surface energy of solids is undoubtedly a powerful parameter to characterise a particles' interaction behaviour. However, since it is able to detect even small changes in particle properties introduced by processing (e.g., milling, amorphisation, recrystallisation), how much of the resulting changes observable after the dry particle coating are either additive or solely process induced is a justified question.

In this study, an assessment of additive-free and additive-containing processed powders was conducted. This enables the comparison of both approaches on different levels, allowing conclusions on whether changes can be attributed to the additive or the process itself. Since both methods are already established and lead to distinct increases in fine particle fraction (FPF), it is important to investigate the differences. Moreover, this study can help in deciding which particle coating process shall be preferred for adding magnesium stearate or similar additives.

2. Materials and Methods

2.1. Materials

As the model carrier in the coating processes, InhaLac® 230 (Meggle, Wasserburg, Germany) a crystalline, sieved inhalation grade lactose monohydrate was used. Magnesium stearate (Parteck® LUB MST, Merck, Darmstadt, Germany) served as the model coating material. For the sake of simplicity, the materials are shortened to the following: InhaLac 230 (IH230), magnesium stearate (MgSt), InhaLac 230 processed in the mechanofusion reactor (IH230AMS, suffix "+" or "−" indicating if processed with the additive or without), InhaLac 230 processed in the high-shear mixer (IH230HSM, suffix "+" or "−" indicating if processed with the additive or without). Micronised ipratropium bromide served as the model drug (d_{90} < 5 µm, Boehringer Ingelheim Pharma AG & Co. KG, Ingelheim, Germany).

2.2. Dry Particle Coating

The mechanofusion process was conducted with the Angmill Mechanofusion System (AMS) unit of the Picobond® using the Picoline® platform (Hosokawa Alpine, Augsburg, Germany).

The carrier and coating materials (2% w/w MgSt) were premixed in a Turbula® blender (Willy A. Bachofen Maschinenfabrik, Basel, Switzerland) at 42 rpm for 5 min. Pre- blends were then transferred to the AMS. The AMS coating started by increasing the rotor speed up to 4000 rpm within one minute and keeping it constant at 4000 rpm over 10 min.

The high-shear mixer (HSM) coating was conducted using the Picomix® unit of the Picoline platform. A rotor speed of 500 rpm was kept constant for 15 min.

All raw materials were sieved before processing (mesh size: 250 µm), as well as the coated samples after processing. To assess the energy input to the powder, the data transfer

tool of the Picoline was used. The instrument performance over the whole processes using the same powder mass was averaged and then multiplied with the respective process duration to obtain the total energy input. The procedure was then repeated without powder. The idle running energy was subtracted from the total energy input to calculate the energy input into the powder sample. All coatings were conducted at monitored relative humidity (RH) of 45% ± 15% and room temperature (20 °C to 25 °C).

2.3. Determination of Thermal Properties—Differential Scanning Calorimetry (DSC)

A power compensation DSC (PerkinElmer DSC 7, PerkinElmer Inc., Waltham, MA, USA) was used for each measurement, and data were evaluated with the PYRISTM Software (PerkinElmer Inc.). Approximately 5 mg of the respective sample was weighed into an aluminium pan, which was sealed and pierced afterwards to allow gas to escape. A pierced, empty aluminium pan was used as reference. During analysis, the sample was flushed with nitrogen to avoid any oxidation processes. All samples were heated at a rate of 10 °C/min up to 240 °C. Results are plotted as the heat flow (mW) over temperature. Furthermore, the thermogravimetric properties of the sample were analysed (Simultaneous Thermic Analyzer 6000, STA), using the same heating rate and heating range as that of the DSC. This provides additional information on what happens at the events observable in the DSC (e.g., loss of crystal water).

2.4. Determination of Crystal Properties—Vapour Sorption Technique

Dynamic vapour sorption (DVS) was carried out using the DVS Resolution (Surface Measurement Systems Ltd., London, UK). For these experiments, approximately 70 mg of the respective sample was weighed into the sample pan. Measurements were carried out at 25 °C. The method consisted of two cycles of increasing the partial pressure of bidistilled water (aq.

bidest.) from 0% – 90% in 10% steps and returning to 0%. At the beginning of every measurement, the sample was conditioned for 180 min at 0% RH. Every step of the method was not limited by time but by a change in mass of below 0.005%/min.

2.5. Particle Size Distributions (PSD)

Laser diffraction was applied to determine the particle size distribution (PSD) of the initial and processed material. For this, a Helium Neon Laser Optical System (HELOS®, Sympatec GmbH, Clausthal-Zellerfeld, Germany) was equipped with a RODOS® dispersion module and a R4 lens with a measuring range of 0.5 to 350 µm. With compressed air (2 bar), the automatically fed (VIBRI® dry dosing system, Sympatec GmbH) material was dispersed in an aerosol jet towards the measuring zone.

Evaluation of the size distribution was performed with the Windox 5 software (Sympatec GmbH) based on the Fraunhofer enhanced equation.

2.6. Specific Surface Area (SSA) and Surface Energy (SE)

The assessment of specific surface area (SSA) using the BET method and the surface energy of solids (SE) was carried out using the surface energy analyser (SEA, Surface Measurement Systems Ltd., London, UK). The powder samples were weighed into silanised glass columns (4 mm inner diameter) and fixed with silanised glass wool on both ends. To avoid hollows and cracks in the powder bed, the filled columns were compressed by tapping for 10 min using the SMS column packer accessory. Prior to every measurement, all columns were conditioned at 0% RH and 10 cm^3/min carrier gas flow (nitrogen) for one hour to get rid of any volatile contamination. For SSA measurements, a series of octane injections was performed, providing an adsorption isotherm. The calculation of the SSA was based on the linear section of the adsorption isotherm (p/p^0 0.05 – 0.35).

The measurement of SE distributions was conducted by injecting a series of alkanes (octane – undecane) for dispersive SE as well as chloroform and toluene for determination of acid-base surface properties. All injected concentrations were based on the respective monolayer capacity, leading to surface coverages from 0.5% up to 10%. For the determination of the dead volume, a double injection of methane was performed at the beginning and at the end of every experiment. All experiments were carried out at 0% RH and 30 °C with a carrier gas flow of 10 cm^3/min.

The raw data were analysed using the SEA Analysis Software (Surface Measurement Systems Ltd., London, UK). Calculations were based on the DellaVolpe scale in combination with the Dorris and Gray approach and the polarisation method [18,19]. For SSA calculations, peak maxima were used, for SE calculations served the peak centre of mass.

2.7. Particle Imaging

The imaging of particle morphology was conducted with scanning electron microscopy (SEM) using Phenom XL (Phenom-World BV, Eindhoven, The Netherlands). To guarantee sample grounding and to minimise charging effects, samples were fixed onto carbon stickers and gold-sputtered with BAL-Tec SCP 050 Sputter Coater (Leica Instruments, Wetzlar, Germany). All images were taken at 1000x or 2500x magnitude with an acceleration voltage of 10 kV and with the use of a backscatter detector.

2.8. High-Performance Liquid Chromatography

The quantification of drug content was carried out using high-performance liquid chromatography (Waters Corporation, Milford, MA, USA). The analytical procedure was based on a cyanopropyl-substituted stationary phase (LiChrospher® 100 CN, Merck), using a solvent mixture (71% aq. bidest., 29% acetonitrile, 1.42 g/L heptane sulfonic acid) adjusted to pH 3.2 as mobile phase. The method was validated in terms of system suitability, specificity, precision, repeatability and linearity. The limit of quantification was calculated based on the corresponding ICH guideline (CPMP/ICH/381/95) as 0.08 µg/mL. The quantification calculations were based on an external standard calibration curve ($R2 > 0.99$) covering a concentration range from 0.21 µg/mL to 104.8 µg/mL. All values used were within the calibrated range. All solvents used were chromatographic grade and supplied by Honeywell Riedel-de Haën (Chromasolv, Seelze, Germany).

2.9. Preparation of Interactive Blends

All adhesive mixtures were prepared (1% w/w*)* active ingredient) using the Picomix high-shear mixer module with two mixing steps at 500 rpm and one sieving step (mesh size: 250 µm) in between. All mixing steps were conducted at a monitored RH of 45% ± 15% and room temperature (20 °C to 25 °C). Every mixture comprised a batch size of 30 g and was tested for homogeneity by analysing 10 randomly picked samples via high performance liquid chromatography. A blend was considered homogeneous at a relative standard deviation below 5% and a recovery of 90 – 110%.

2.10. Aerodynamic Assessment

The aerodynamic assessment was carried out using the Novolizer® (MEDA Pharma GmbH & Co. KG, Bad Homburg, Germany) with the fast-screening impactor (FSI, Copley Scientific, Nottingham, United Kingdom). The FSI allows rapid determination of fine particle dose < 5 µm (FPD) and fine particle fraction (FPF). All experiments were operated at a flow rate corresponding to a 4 kPa pressure drop over the inhaler (78.3 L/min). All results are shown as an average of five measurements with five doses per measurement. All FSI experiments took place in a climate chamber with constant environmental conditions of 21 °C and 45% RH. High performance liquid chromatography (Waters Corporation, Milford, MA, USA) was used for drug quantification.

2.11. Carrier–Drug Adhesion Screening

For the adhesion strength screening, an e200LS air-jet sieve (AJS; Hosokawa Alpine, Augsburg, Germany) was used. A specified mesh-sized analytical sieve was inserted (20 µm for adhesion strength screening). For every repetition, 5 g of sample was placed on the sieve, covered with a lid and then dispersed via a rotating pressurised air nozzle. A negative pressure of 4 kPa was created by a pump, sucking particles below 20 µm through the sieve. The process was stopped at 6 s, 30 s, 1 min, 2 min, 5 min and 10 min for sampling. Per sampling time, 10 randomised powder samples were picked from above the sieve. From each of the resulting 60 samples, a specific mass of 7 mg (±0.5 mg) was weighed into an Eppendorf tube, dissolved in 2 mL of solvent (aq. bidest.) and analysed in the high-performance liquid chromatography. The resulting drug content was put in in relation to the nominal drug content of the adhesive mixture (namely 1% w/w). All results are displayed as the average of three measurements at a monitored temperature of 20 ◦C (±5 ◦C) and 45% (±15%) RH.

2.12. Removal of Residual Excipient Particles

For the removal of residual MgSt particles from the carrier, the e200LS air-jet sieve with a mesh size of 32 µm was utilised. The sieve step was conducted for 15 min with a negative pressure of 4 kPa.

2.13. Quantification of Magnesium Stearate

The content of MgSt was measured using atomic absorption spectroscopy (AAS). All samples were dissolved using diluted nitric acid in combination with sonication (20 min) and shaking (15 min). After centrifugation (10 min, 7000 rpm), the samples were diluted and measured

using a flame atomisation (air–acetylene flame) AAS system (AAS 3030, PerkinElmer Inc., Waltham, MA, USA). The calculation of the content was based on a six-point calibration curve from zero up to 1 ppm magnesium concentration.

2.14. Statistical Evaluation

All statistical calculations were carried out with Microsoft Excel 2016 (Microsoft Corporation, Redmond, WA, USA).

3. Results and Discussion

The in-depth investigation of two established dry particle coating processes was conducted with a broad spectrum of physico-chemical analysis tools. Since those particle coating processes are used for formulation optimisation attempts [7,11] in the dry powder inhalation area, an aerodynamic assessment of the respective interactive blends was also part of this study. Both coating mechanisms (AMS, HSM) are based on the introduction of mechanical stress: on the one hand, utilising a rotating stirring tool, on the other hand, forcing the powder through a tight gap.

The energy input in both preparation procedures was determined by recording the performance data of the instrument for both conducted processes using the same sample mass. The energy input into the powder was calculated to be 1234 J for the AMS and 1318 J for the HSM process. This corresponds to approximately 6% higher energy input in the HSM coating attempt. Even though both processes show no major differences in energy input, both methods introduce considerable amounts of mechanical energy into the sample. As a comparison: preparing an interactive blend as described introduces approximately 250 J of mechanical energy. Since the mechanical stress during dry particle coating could already cause fundamental changes in the particle properties, such as amorphisation or fragmentation, both processes were conducted with and without additives. This allows the evaluation of whether changes in powder behaviour can be attributed to processing or to the additive itself.

3.1. Process-Induced Particle Alteration

When applying mechanical stress to a powder sample, an expectable change is in particle size distribution. To make sure no particle fragmentation occurs, particle size distributions were measured via laser diffraction. The results are displayed in Table 1 and Figure 1.

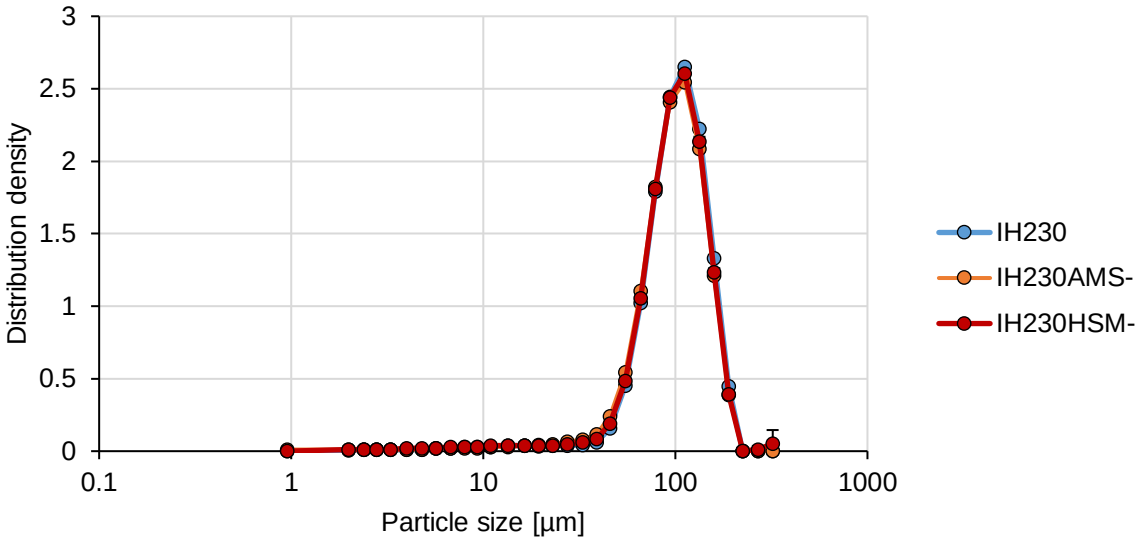

Figure 1: Particle size distribution density of the raw material in comparison to processed powders without additive. n=3, error bars show SD.

The results demonstrate that even though considerable mechanical stress was applied during both processes, the particle size distribution is unchanged, which indicates that particles were not fragmented significantly when processed without the additive.

Table 1: Particle size distributions of all investigated materials. n=3, SD in parentheses.

	IH230		IH230AMS-		IH230HSM-		IH230AMS+		IH230HSM+	
d_{10} [µm]	62.1	(0.1)	57.3	(0.5)	60.2	(0.1)	47.8	(1.7)	58.8	(0.7)
d_{50} [µm]	103.4	(0.1)	100.4	(0.4)	101.8	(0.2)	96.7	(0.6)	101.8	(0.2)
d_{90} [µm]	155.4	(0.1)	152.3	(0.5)	154.4	(2.0)	147.5	(0.9)	153.2	(0.2)
Span	0.9		1.0		0.9		1.2		0.9	

Since particle size distributions have a huge impact on the performance as a carrier platform in dry powder inhalation formulations [20], not decreasing particle sizes is very important for a meaningful comparison. In addition to particle size distribution measurements, octane adsorption isotherms were determined to calculate the specific surface area. The BET data confirmed that no particle fragmentation occurred (Table 2).

Otherwise, one would observe increasing surface areas after processing due to decreased particle sizes.

Table 2: SSA of the raw material and processed with and without additives. Data marked with "AJS" displays results after removal of residual particles via air-jet sieving n=3, SD in parentheses.

Octane BET SSA [m^2/g]	IH230		IH230AMS		IH230HSM	
Processed without additive			0.110	(0.001)	0.106	(0.003)
Processed with additive	0.105	(0.011)	0.432	(0.020)	0.809	(0.102)
Processed with additive (AJS)			0.292	(0.010)	0.561	(0.010)

Another alteration, which could have been introduced even without particle fragmentation, is the formation of crystal defects, leading to partial amorphisation. Since the starting material, InhaLac 230, is a highly crystalline lactose, even small amounts of process-induced amorphous content are detectable. As analytical tools, two different methods were used: differential scanning calorimetry (DSC) in combination with thermogravimetric analysis (TGA) and dynamic vapour sorption (DVS). Both techniques were applied to the additive-free samples. Thus, solely the process-induced changes in solid state properties can be tracked.

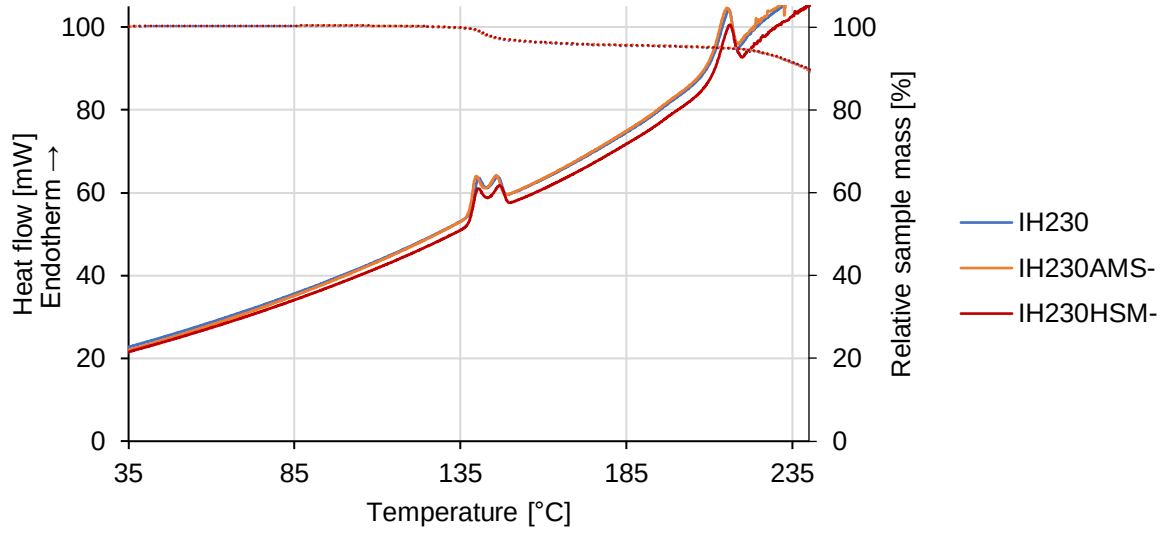

Figure 2: Results of DSC analysis of the raw material in comparison to processed powders without additive. The secondary y-axis shows the relative mass decrease (dotted lines). n=3. Negligible variation between the compared data series results in overlapping curves.

All DSC graphs (Figure 2) show essentially the same peaks: one endotherm double peak starting at almost 140 °C represents the dehydration of the lactose monohydrate, the other endotherm peak, beginning at 200 °C, indicates the decomposition and charring of the anhydrous lactose samples. Neither a glass transition step nor a recrystallisation peak indicating amorphous content was observed in any plot. A combination of DSC and

thermogravimetric measurements allows for further insights into thermal events by analysing temperature-related mass changes. The step at 140 °C was aligned with a relative mass decrease of approximately 5%, which represents the loss of crystal water of the lactose monohydrate. The melting and charring at 200 °C led to an unspecific mass decrease.

DVS was chosen as an orthogonal method to verify the conclusion made based on the DSC experiments. For comparability, only additive-free, processed lactose samples were investigated. Figure 3 displays mass changes of all samples. The maximum mass change was approximately 0.05% for all samples unrelated to processing. If recrystallisation of amorphous parts would have occurred, the mass change in the second half of the double cycle would show decreased mass changes. This would be due to less amorphous content (recrystallised in the first half of the cycle), which is able to absorb water and leads to a distinct increase in sample mass. For the investigated samples, this cannot be deduced from the measured values. Furthermore, the relative mass change in general was extremely small, indicating (for a hydrophilic substance, such as lactose) a highly crystalline and non-hygroscopic material.

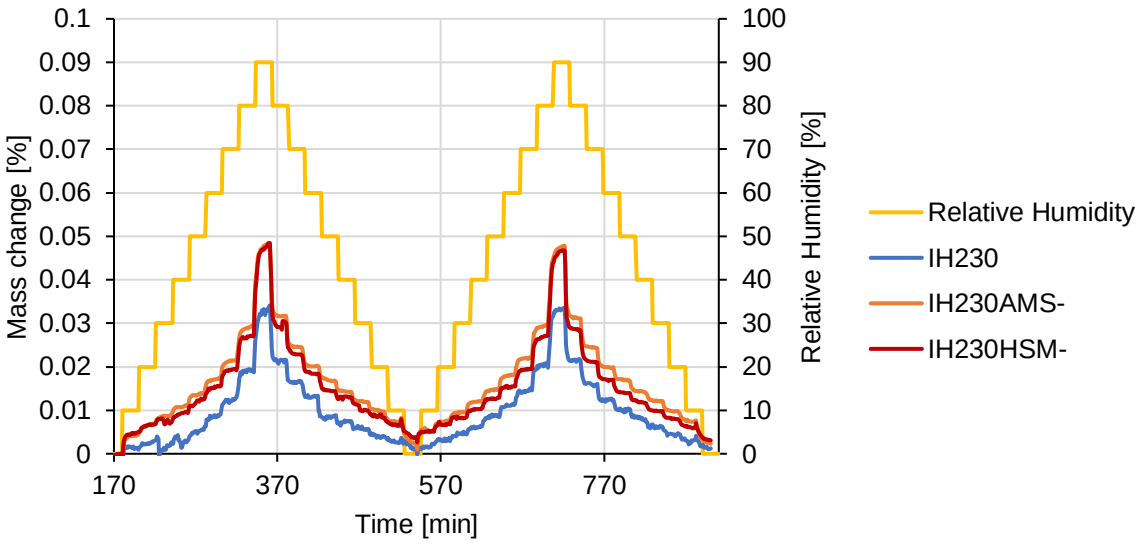

Figure 3: DVS plot showing relative mass change related to the reference mass in dependence of the relative humidity. Sample conditioning data (0-170 min) is not shown.

A slight difference between processed and non-processed samples can be seen. The processed samples reproducibly gained more mass than the non-processed, which can be explained by little differences in surface appearance or the creation of non-recrystallisable defects, which is substantiated by no identifiable differences between both cycles. This combination of methods showed that in both used dry particle coating methods, no introduction

of major changes in the solid state of the particles had occurred. This is important not only for stability issues but also for tracing back new particle properties after the process with the additive - not to the process itself, but to the additive.

3.2. Additive-Induced Particle Alteration

Following the investigation of the addition of mechanical stress, the determination of particle specifications, namely PSD (Figure 4 and Table 1) and BET (Table 2), after processing with the additive was conducted.

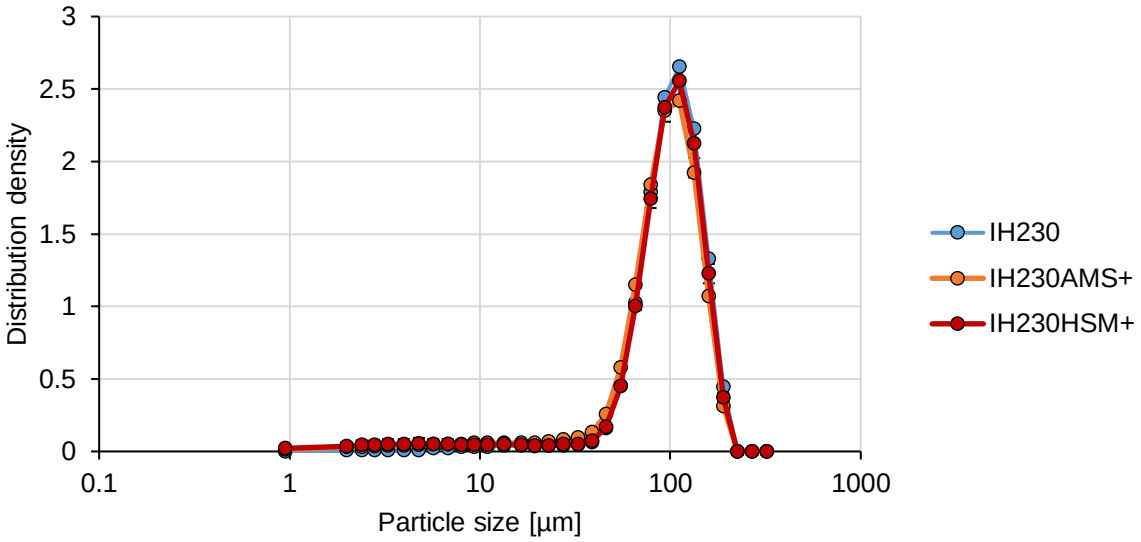

Figure 4: Particle size distribution density of the raw material in comparison to processed powders with additive. n=3, error bars show SD.

Since fragmentation or milling of the lactose carrier can be excluded as discussed above, the PSD shift to slightly lower particle sizes (Table 1) can be explained by residual particles of MgSt, which are the size of approximately 6 µm. When the total amount of coating material had not been coated successfully, some loose particles were left in the powder bed and caused significant shifts towards lower PSDs (p-value < 0.05 when comparing d_{10}, d_{50} and d_{90} values).

This observation was supported with the specific surface area results. Both processed samples showed a difference between the BET-specific surface area depending on if processed with or without the additive. The specific surface area of the HSM sample increased to 0.8 m^2/g while the AMS sample only increased to 0.4 m^2/g. A general increase in surface can be substantiated by the SEM images (A and B) in Figure 5 and Figure 6. Figure 5A,B

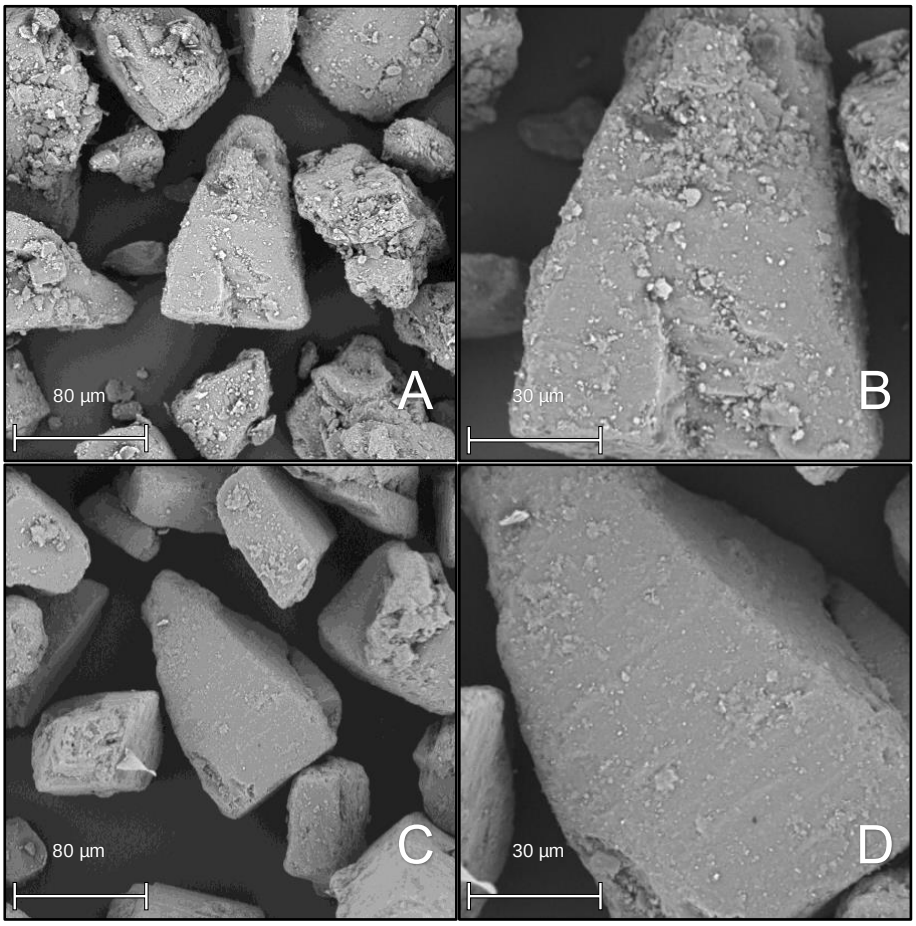

Figure 5: SEM images showing IH230AMS+. A and B before and C and D after removing residual particles via air-jet sieving. A and C in 1000x magnification, B and D in 2500x magnification.

show the surface of the AMS sample and Figure 6A,B the surface of the HSM sample. Based on the SEM images, one would assume that the AMS sample should exhibit a larger surface area due to a higher number of small particles (Figure 5B). On the other hand, in Figure 6B, the merging process of the additive and the carrier seemed further developed, with less individual particles on the surface. For further investigation of the coating uniformity, residual fine MgSt particles were removed using the air-jet sieve (mesh size: 32 µm). The resulting particle surfaces are shown in Figure 5C,D and Figure 6C,D, respectively. Comparing the surfaces after removing residual MgSt particles, the high-shear mixed sample looked more similar to the surface before air-jet sieving. For the mechanofused surface, a significant decrease in the number of small particles was observable.

To gain further insight into the coating effectivity, the amount of successfully attached and non-removable MgSt was determined using AAS. In order to assess the share of the strongly

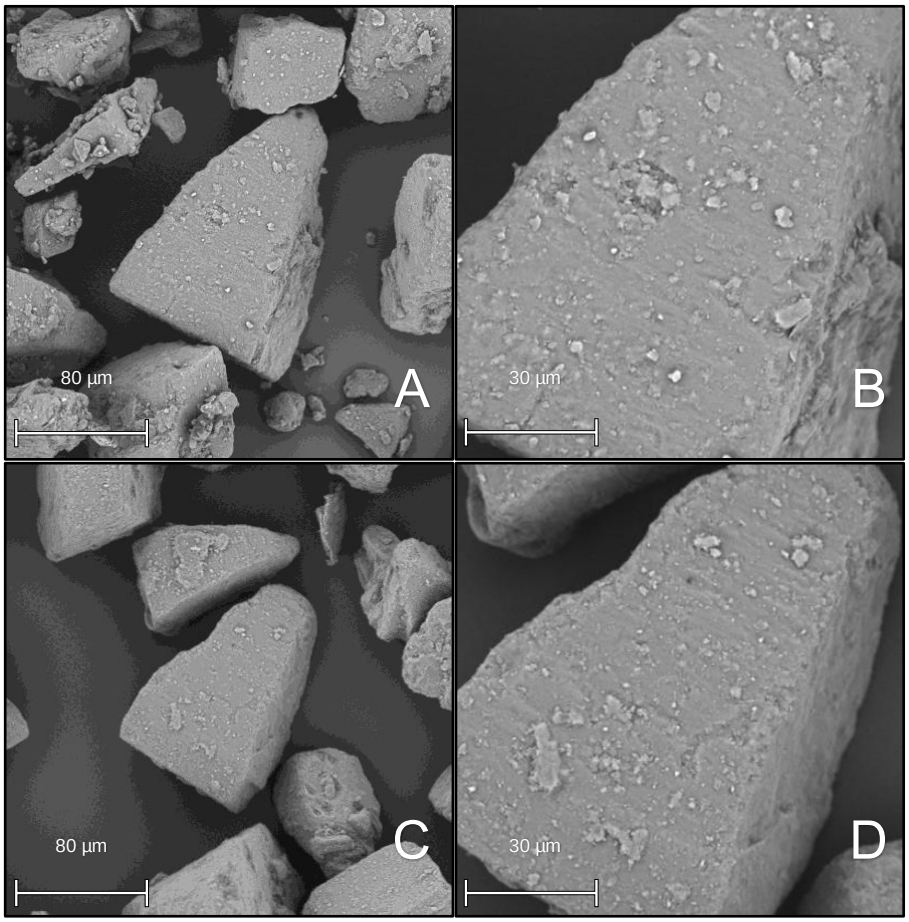

Figure 6: SEM images showing IH230HSM+. A and B before and C and D after removing residual particles via air-jet sieving. A and C in 1000x magnification, B and D in 2500x magnification.

bonded additive, the MgSt content in the blend before and after the removal of residual particles was measured. The decrease in percent provides information about the share of the additive, which was not merged but only adhered to the surface after processing. Initially, 2% (w/w) MgSt was added in both coating strategies. The measured MgSt content of 1.31% and

1.23% before air-jet sieving indicates a loss of more than 30% due to processing. After air-jet sieving, the additive content of the HSM sample decreased by 18.0%, while the content of the AMS sample decreased by over 60% (Table 3)

Table 3: Additive content before and after the removal of residual particles (AJS). n=1.

	IH230AMS+	IH230AMS+AJS	IH230HSM+	IH230HSM+AJS
MgSt content [%]	1.31	0.52	1.23	1.01

This substantiates the observations of the SEM images. Based on these experiments, it can be stated that the merging process was further advanced in the HSM sample, resulting in a more firmly bound lubricant. The structure of the stirring tool and mixing vessel of the Picomix,

as well as the longer processing time could be the reason. There might be less concentrated mechanical stress in the Picomix compared to the Picobond, but more particle–particle friction with the additive in the contact area could occur due to the more effective mixing. This suggests that the merging process was not yet complete in the Angmill Mechanofusion System, leading to a greater loss of residual, not firmly bound MgSt.

All samples were then also assessed in the SEA to enable an expressive comparison of BET surfaces after the coating process. The resulting BET surface areas are presented in Table 2. The AMS sample appeared very smooth after removal of residual MgSt, resulting in lower SSA. Even though no big changes were observable in SEM images for the HSM sample, the SSA had also decreased. Only the order of the SSA values was contradictory to the surface appearance, being lower for the sample with more visible small residual particles (Table 2). This could be due to a more irregular surface after the HSM coating, resulting in higher SSA, while the AMS sample surface area was more similar to the raw material IH230 SSA because of the insufficient coating mechanism.

Another technique, which was used to investigate the processing and coating process impact, was inverse gas chromatography. The measured surface energy can be plotted over the surface coverage. Since the surface energy is derived from chemical composition and physical properties, such as crystal habit, it is perfectly suitable for the investigation of particle coating processes. Prior to every measurement of surface energy, an octane adsorption isotherm was performed to calculate BET surface area (Table 2), which was then used to determine monolayer capacity. With known monolayer capacity, all injections of probe gases are comparable since specific surface coverages are injected instead of injecting fixed concentrations (leading to different surface coverages). In Table 4, the range of the different components of the surface energy of solids (i.e., dispersive and acid-base part) of the starting material IH230 and all processed materials are displayed. The total surface energy of solids (right column) is calculated as the sum of both parts. The surface energy is dependent on the surface coverage because at low surface coverages, the probe gases will primarily interact with high energy sites on the sample. With increasing surface coverage, more sites are taken into account. Usually, measurements would not be performed above 20% of the monolayer capacity because probe gas molecules start to interact with each other at higher concentrations [21].

Table 4: Results of the SE determination of the raw material in comparison to processed powders with and without additive. n=3, SD in parentheses.

	γ^D [mJ/m^2]				γ^{AB} [mJ/m^2]				γ^{Total} [mJ/m^2]			
	Min		Max		Min		Max		Min		Max	
IH230	40.4	(0.8)	43.9	(1.3)	29.0	(3.7)	33.8	(2.3)	69.8	(4.2)	77.8	(3.6)
IH230AMS-	38.4	(0.7)	44.5	(0.5)	27.3	(1.1)	29.6	(2.6)	65.6	(1.0)	73.6	(3.0)
IH230HSM-	40.8	(1.2)	45.1	(0.2)	28.3	(1.8)	30.3	(1.7)	70.8	(2.1)	75.5	(1.0)
IH230AMS+	42.1	(0.7)	43.2	(0.6)	25.9	(1.3)	29.3	(0.9)	69.0	(1.3)	71.9	(0.7)
IH230HSM+	44.8	(0.9)	45.7	(0.9)	20.7	(0.4)	23.7	(0.3)	65.9	(0.7)	69.4	(0.7)

Comparing the surface energy distribution of the starting material with the material after processing without the additive, the dispersive part of the surface energy showed no significant changes. The acid-base (polar) part, however, decreased after processing. Considering the standard deviations, there was no significant change (*p*-values > 0.05 when comparing min. and max. values of the SE distribution). Figure 7 shows the SE distribution of the total surface energy measured for the starting material as well as the AMS and HSM samples without the additive. In combination with the measured BET surface area, it can be concluded that no significant surface alterations were caused solely by processing because these two methods cover the morphology part (surface roughness alteration would cause changes in BET SSA) as well as the crystal habit part (crystal habit alterations would lead to SE changes due to different adsorption behaviour in inverse gas chromatography). Processing with the model additive MgSt caused significant changes in surface area and surface energy (*p*-values < 0.05 when comparing surface area and surface energy maxima). At low surface coverages of the probe gases, the total surface energy decreased by up to 15.3% (HSM). Comparing both coating processes, it can be observed that coating in a high-shear mixer led to lower surface energies at low surface coverages (Figure 8), which could be linked to the levelling of higher energy sites. Measuring at higher surface coverages, the surface energies resemble one another (Table 4 and Figure 8). While the dispersive maximum of the SE shows no significant changes when comparing raw and processed materials, the polar part does. The maximum of the polar SE decreased by 13.3% (AMS) and 30.0% (HSM). This is a significant decrease (*p*-value < 0.05) as well as a significant difference between both processes (*p*-value < 0.005). Such decreases in surface energy can be linked to the decreased tendency of the surface to interact with surroundings (e.g., during adhesion) [22].

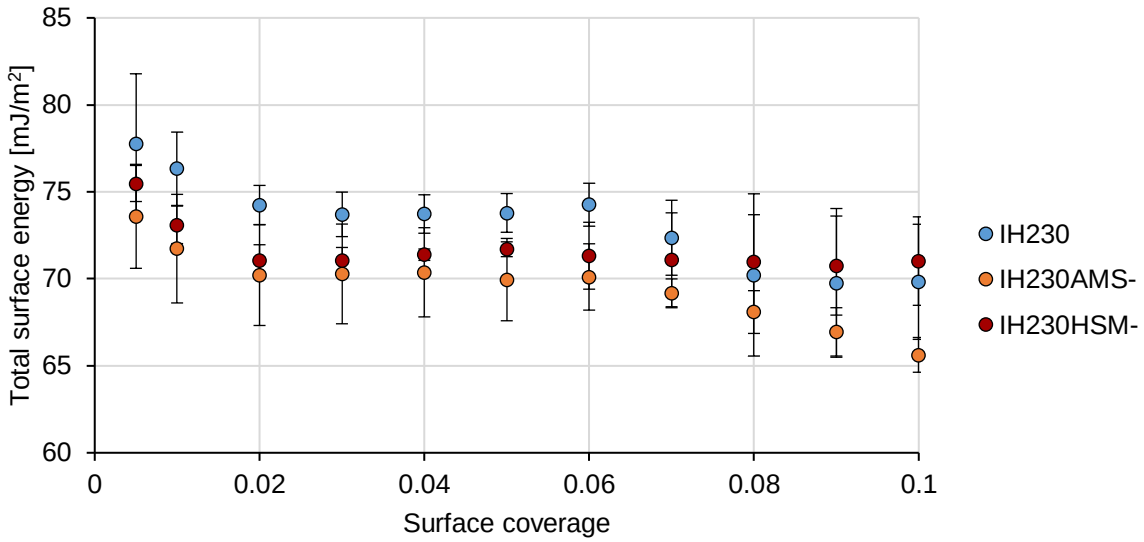

Figure 7: Total surface energy of the raw material in comparison to processed powders without additive. n=3, error bars show SD.

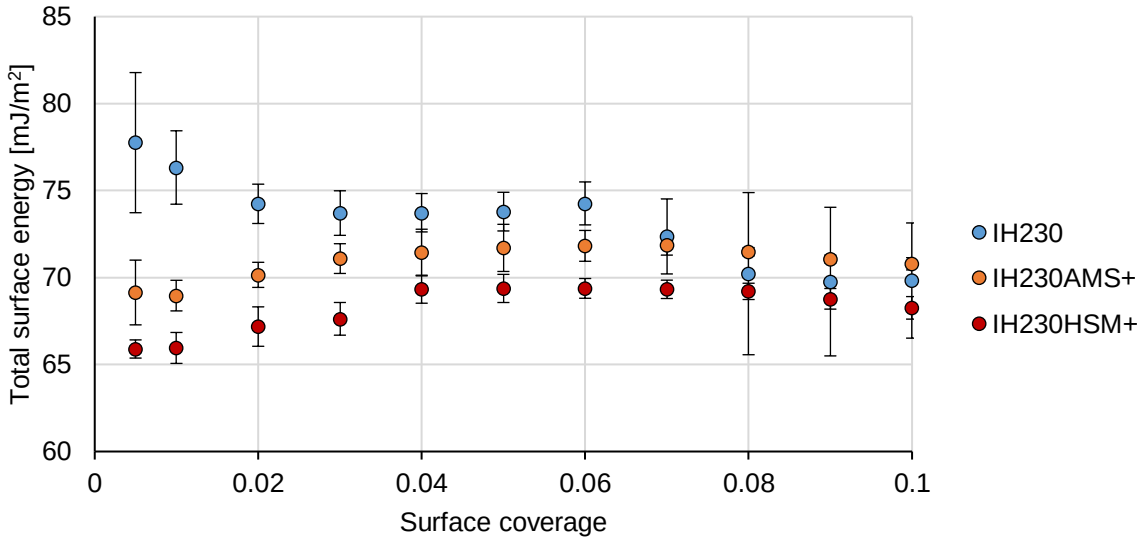

Figure 8: Total surface energy of the raw material in comparison to processed powders with additive. n=3, error bars show SD.

3.3. Assessment of Processed Powders as DPI Carriers

Decreases in interaction strength can therefore lead to significant changes in aerodynamic performance, as attachment and detachment of micronised drug particles will be altered. The impact of processing with the additive on resulting fine particle fractions (FPF) of the respective interactive blends assessed in the FSI is displayed in Table 5. The FPF increased after

processing the carrier with MgSt by 128.2% (AMS) and 120.0% (HSM). The increases in comparison to the non-processed carrier were statistically significant (p-value < 0.001), but the difference between both processed carriers was not (p-value > 0.05).

Table 5: FPF and FPD of interactive blends of all prepared adhesive mixtures. n=5, SD in parentheses.

	IH230		IH230AMS+		IH230HSM+	
Fine Particle Fraction [%]	25.8	(1.4)	58.9	(1.4)	56.8	(2.5)
Fine Particle Dose [µg]	33.8	(1.5)	73.5	(2.0)	72.8	(5.0)

To gain further insight into the adhesion of drug particles on either non-processed or processed carriers, an adhesion force screening of the blends was carried out. The air-jet sieve (AJS) allows the simulation of a situation that is exemplary of a blend that is intended to be dispersed in the airstream. With a mesh size of 20 µm and a negative pressure of 4 kPa, mainly drug particles are sucked through the sieve and therefore eliminated from the dispersed (using pressurised air) system. Sampling at defined times and quantification of residual API in the blend allow conclusions of adhesion strength; the higher the adhesion strength, the less API will detach from the lactose particles. All prepared interactive blends were assessed with this method. The gathered data (Figure 9) were described with a power regression model (R^2 > 0.95).

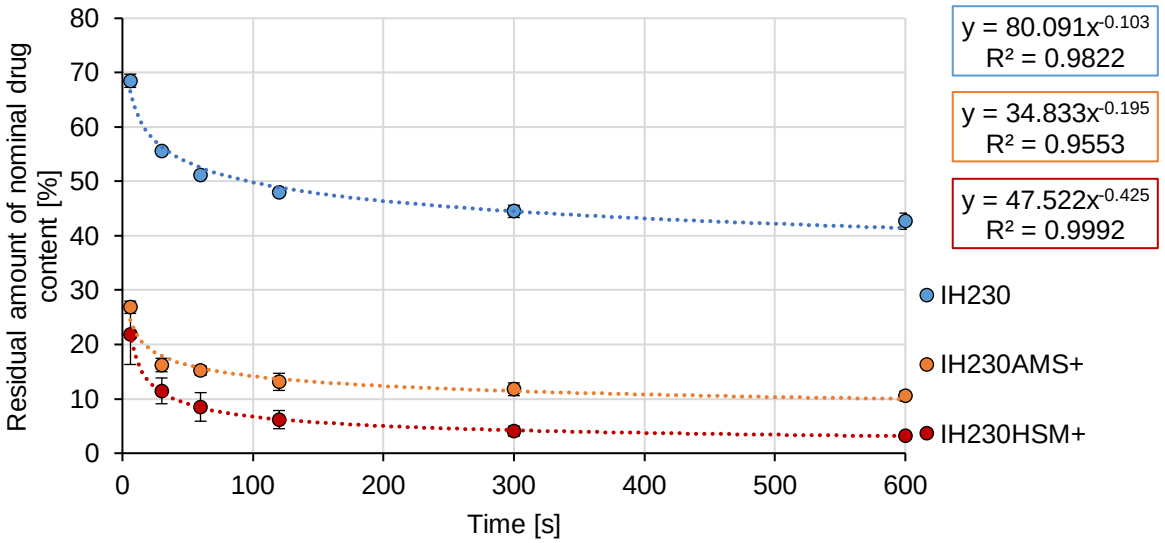

Figure 9: Residual amount of nominal drug content of respective interactive blends (percentage of nominal drug content) in dependence of the time dispersed by the AJS. n=3, error bars show SD.

The mean residual drug concentration (starting concentration defined as 100%) after 10 min of dispersing and removing particles below 20 µm is defined as carrier residue (CR). The slope of the linearised function describes the speed of decrease (SOD) of drug content in the dispersed system. In a real setting, the drug has to be detached in a split second [23] during inhalation. Thus, the SOD is a parameter allowing quantification of a formulation property with crucial influence on the performance. The CR however serves as a blend characteristic for comparing the share of the strongly bonded drug. The results are displayed in Table 6.

Table 6: Results of the AJS adhesion strength screening of all prepared adhesive mixtures. n=3, SD in parentheses.

	IH230		IH230AMS+		IH230HSM+	
Carrier residue [%]	42.7	(1.5)	10.5	(0.9)	3.2	(0.2)
Speed of decrease	0.1	(0.01)	0.2	(0.02)	0.4	(0.07)

All blends fulfilled the mentioned requirements to be considered homogenous before the testing, so the data point at zero seconds is 100% ± 10% (data point excluded to allow power regression). It can be observed that the HSM blend showed less adhesion forces between carrier and API, leading to higher detachment and drug content decreases in the dispersed system. The resulting CR and SOD values of all investigated blends differ in statistical significance (CR: *p*-values < 0.001; SOD: *p*-values < 0.05). This was confirmed by the results of the SEA analysis. Another indication for reduced adhesion between the carrier and drug was the share of drug deposited in the pre-separator of the FSI. It also represents an approximation of the amount of drug, which did not detach and, hence, impacted the lactose carrier in the pre-separator. The shares are shown in Table 7. They showed essentially the same trend as the AJS results, confirming higher drug detachment for the HSM blend. All differences were statistically significant (*p*-value < 0.001).

Table 7: Share of the recovered dose, which impacted in the pre-separator of the FSI. n=5, SD in parentheses.

	IH230		IH230AMS+		IH230HSM+	
Pre-separator impaction [%]	48.2	(2.9)	19.6	(0.9)	15.3	(1.2)

4. Conclusions

Both high-shear mixing and mechanofusion were suitable for DPI carrier engineering. This study proves that dry particle coatings with specific additives (e.g., lubricants) lead to

substantial alterations in particle behaviour. The investigation of coating attempts with and without coating materials allowed conclusions on the origin of the introduced changes. Using additive-free processes, the alterations in particle appearance, aerodynamic performance or adhesive properties were traced back to the additive, not the process. Even if AMS and HSM coatings both led to significant increases in FPF, the HSM coating showed superiority in terms of carrier residues and speed of detachment (of drug content). In addition, the SEM images before and after air-jet sieving showed a more complete coating for the HSM process. This was substantiated by the determination of firmly bound additive content. Even though SE decrease and therefore the decrease in the work of adhesion were superior for the HSM surface, the aerodynamic performance showed no significant difference between both options. This supports the theory of energetic levelling of higher energy binding sites on the DPI carrier surface. Although the AMS coating showed inferior coating efficacy, the high-energy sites on the lactose surface decreased for both coating strategies, which therefore substantiates the positive effect of using dry particle coatings in DPI formulation development. Furthermore, this work supports the hypothesis that adhesion strength between drug and carrier may be crucial but not solely decisive for the aerodynamic performance of the respective interactive blend. In conclusion, the HSM strategy should be preferred in a comparable experimental setup due to its reported benefits combined with less processing time.

References Chapter 2

[1] W.W. Labaki, M.K. Han, Chronic respiratory diseases: A global view, The Lancet Respiratory Medicine. 8 (2020) 531–533. https://doi.org/10.1016/S2213-2600(20)30157-0.

[2] J. Shur, R. Price, D. Lewis, P.M. Young, G. Woollam, D. Singh, S. Edge, From single excipients to dual excipient platforms in dry powder inhaler products, International Journal of Pharmaceutics. 514 (2016) 374–383. https://doi.org/10.1016/j.ijpharm.2016.05.057.

[3] A.H. de Boer, P. Hagedoorn, M. Hoppentocht, F. Buttini, F. Grasmeijer, H.W. Frijlink, Dry powder inhalation: Past, present and future, Expert Opinion on Drug Delivery. 14 (2017) 499–512. https://doi.org/10.1080/17425247.2016.1224846.

[4] H. Steckel, B.W. Müller, In vitro evaluation of dry powder inhalers I: Drug deposition of commonly used devices, International Journal of Pharmaceutics. 154 (1997) 19–29. https://doi.org/10.1016/S0378-5173(97)00113-0.

[5] M.D. Jones, R. Price, The influence of fine excipient particles on the performance of carrier-based dry powder inhalation formulations, Pharmaceutical Research. 23 (2006) 1665–1674. https://doi.org/10.1007/s11095-006-9012-7.

[6] R. Guchardi, M. Frei, E. John, J.S. Kaerger, Influence of fine lactose and magnesium stearate on low dose dry powder inhaler formulations, International Journal of Pharmaceutics. 348 (2008) 10–17. https://doi.org/10.1016/j.ijpharm.2007.06.041.

[7] N. Hertel, G. Birk, R. Scherließ, Performance tuning of particle engineered mannitol in dry powder inhalation formulations, International Journal of Pharmaceutics. 586 (2020) 119592. https://doi.org/10.1016/j.ijpharm.2020.119592.

[8] M.W. Jetzer, M. Schneider, B.D. Morrical, G. Imanidis, Investigations on the Mechanism of Magnesium Stearate to Modify Aerosol Performance in Dry Powder Inhaled Formulations, Journal of Pharmaceutical Sciences. 107 (2018) 984–998. https://doi.org/10.1016/j.xphs.2017.12.006.

[9] T. Tay, S. Das, P. Stewart, Magnesium stearate increases salbutamol sulphate dispersion: What is the mechanism?, International Journal of Pharmaceutics. 383 (2010) 62–69. https://doi.org/10.1016/j.ijpharm.2009.09.006.

[10] M. Nicholas, M. Josefson, M. Fransson, J. Wilbs, C. Roos, C. Boissier, K. Thalberg, Quantification of surface composition and surface structure of inhalation powders using TOF-SIMS, International Journal of Pharmaceutics. 587 (2020) 119666. https://doi.org/10.1016/j.ijpharm.2020.119666.

[11] M. Kumon, M. Suzuki, A. Kusai, E. Yonemochi, K. Terada, Novel approach to DPI carrier lactose with mechanofusion process with additives and evaluation by IGC, Chemical & Pharmaceutical Bulletin. 54 (2006) 1508–1514. https://doi.org/10.1248/cpb.54.1508.

[12] Hosokawa Micron Ltd., Picobond Product description, (n.d.). https://www.hosokawa.co.uk/products/picobond/. Last accessed: 10.11.2021.

[13] S.C. Das, Q. Zhou, D.A.V. Morton, I. Larson, P.J. Stewart, Use of surface energy distributions by inverse gas chromatography to understand mechanofusion processing and functionality of lactose coated with magnesium stearate, European Journal of Pharmaceutical Sciences. 43 (2011) 325–333. https://doi.org/10.1016/j.ejps.2011.05.012.

[14] Martin Jetzer, Bradley Morrical, Marcel Schneider, Georgios Imanidis, Investigating the Effect of the Force Control Agent Magnesium Stearate in Fluticasone Propionate Dry Powder Inhaled Formulations with Single Particle Aerosol Mass Spectrometry (SPAMS), in: Drug Delivery to the Lungs, Drug Delivery to the Lungs, Edinburgh, 2016.

[15] R. Sharma, G. Setia, Mechanical dry particle coating on cohesive pharmaceutical powders for improving flowability - A review, Powder Technology. 356 (2019) 458–479. https://doi.org/10.1016/j.powtec.2019.08.009.

[16] Q.T. Zhou, L. Qu, T. Gengenbach, I. Larson, P.J. Stewart, D.A. v Morton, Effect of surface coating with magnesium stearate via mechanical dry powder coating approach on the aerosol performance of micronized drug powders from dry powder inhalers, AAPS PharmSciTech. 14 (2013) 38–44. https://doi.org/10.1208/s12249-012-9895-z.

[17] S.C. Das, P.J. Stewart, Characterising surface energy of pharmaceutical powders by inverse gas chromatography at finite dilution, The Journal of Pharmacy and Pharmacology. 64 (2012) 1337–1348. https://doi.org/10.1111/j.2042-7158.2012.01533.x.

[18] P.P. Ylä-Mäihäniemi, J.Y.Y. Heng, F. Thielmann, D.R. Williams, Inverse Gas Chromatographic Method for Measuring the Dispersive Surface Energy Distribution for Particulates, Langmuir. 24 (2008) 9551–9557. https://doi.org/10.1021/la801676n.

[19] Anett Kondor Daryl R. Williams Daniel J. Burnett, Determination of Acid-Base Component of the Surface Energy by Inverse Gas Chromatography: iGC SEA Application Note 227, (2014). https://www.surfacemeasurementsystems.com/downloads/sea-application-notes/.

[20] W. Kaialy, A. Alhalaweh, S.P. Velaga, A. Nokhodchi, Influence of lactose carrier particle size on the aerosol performance of budesonide from a dry powder inhaler, Powder Technology. 227 (2012) 74–85. https://doi.org/10.1016/j.powtec.2012.03.006.

[21] A. Kondor, Infinite Dilution and Surface Energy Heterogeneity Profile by iGC-SEA: iGC-SEA Technical Note 807, (2020).

[22] D. R. Williams, Particle Engineering in Pharmaceutical Solids Processing: Surface Energy Considerations, Current Pharmaceutical Design. (2015) 2677–2694.

[23] S.R.B. Behara, P. Kippax, I. Larson, D.A. v Morton, P. Stewart, Kinetics of emitted mass—A study with three dry powder inhaler devices, Chemical Engineering Science. 66 (2011) 5284–5292. https://doi.org/10.1016/j.ces.2011.07.029.

Introduction to Chapter 3

Carrier modifications hold great potential towards optimised drug delivery but are additional processing steps. Thus, formulation scientists would prefer to avoid them from an economic perspective, if possible. As I pointed out in the introduction, surface energy is dependent on all properties of the respective surface. Therefore, changes in surface energies of chemically identical excipients are also induced by their manufacturing route. A high-energy manufacturing comprising a milling step for instance, may cause disorders in the crystal lattices of the excipients [1] in comparison to a slower process, like crystallisation, which would rather result in a fully ordered crystal structure - the lowest energy surface.

To benefit from surface energy dependent effects without additional processing, I recommend assessing surface energies of different commercially available excipients.

Apart from the manufacturing route, storage induced surface changes will affect the surface energy of respective materials. This could be due to rearrangement of process-induced disorders [2] or due to adsorption of surrounding substances like humidity [3].

Combining such “additive-free“ attempts it is possible to build a portfolio of varying surface energy excipients without an additional material. Hence, one can avoid introducing additive-related changes to the formulation, which could influence formulation properties without being taken into consideration (e.g. chemical reaction with drug particles or toxicological issues).

In chapter three I will focus on the fine (< 32 µm) lactose qualities in carrier-based blends. I applied the mentioned “additive-free“ strategy to investigate the effect of the surface energy of fines on their suitability to improve DPI blends.

References

[1] R. Ho, M. Naderi, J.Y.Y. Heng, D.R. Williams, F. Thielmann, P. Bouza, A.R. Keith, G. Thiele, D.J. Burnett, Effect of Milling on Particle Shape and Surface Energy Heterogeneity of Needle-Shaped Crystals, Pharmaceutical Research. 29 (2012) 2806–2816. https://doi.org/10.1007/s11095-012-0842-1.

[2] F. Thielmann, D.J. Burnett, J.Y.Y. Heng, Determination of the Surface Energy Distributions of Different Processed Lactose, Drug Development and Industrial Pharmacy. 33 (2007) 1240–1253. https://doi.org/10.1080/03639040701378035.

[3] B. Strzemiecka, J. Kołodziejek, M. Kasperkowiak, A. Voelkel, Influence of relative humidity on the properties of examined materials by means of inverse gas chromatography, Journal of Chromatography A. 1271 (2013) 201–206. https://doi.org/10.1016/j.chroma.2012.11.037.

Chapter 3: Surface energy considerations in ternary powder blends for inhalation

This chapter is published as:
Bungert, N., Kobler, M., Scherließ, R.: Surface energy considerations in ternary powder blends for inhalation.
International Journal of Pharmaceutics **2021**, Vol. 609, 121189.
https://doi.org/10.1016/j.ijpharm.2021.121189

Abstract

The need for optimisation of DPI formulations is a main research motivation in respiratory drug delivery. Well- established formulations like carrier-based blends still show a lack of efficiency. The addition of extrinsic fine excipients is extensively discussed since decades, supported by a wide range of solid-state characteristics to understand their mechanism and classify influencing parameters. The first part of this study aims at comparing the surface energies of lactose fines and their corresponding influence on the aerodynamic performance of the respective ternary blends. Five different fine lactose qualities with varying origins were used, which were distinguishable in terms of surface energy, but comparable regarding particle size, moisture content and chemical composition. It demonstrates the crucial influence of adhesion properties of fines, based on different surface energies. Secondly, one specific fine lactose quality was used on fundamentally different lactose carriers, which highlights the negligible influence of carrier properties if extrinsic fines are preferentially capable of excipient- drug interactions.

1. Introduction

Since the WHO declared SARS-CoV-2 as a global pandemic in 2020, the worldwide need to treat the corresponding disease COVID-19 remains high. Ramakrishnan et al. recently investigated the effect of inhaled budesonide, administered using dry powder inhalation (DPI), as treatment of early COVID-19 [1].

DPI applications offer direct access to the drugs target site, as well as a non-invasive entry to central blood circulation, thus they are suitable for state-of-the-art therapies. To administer medicine via the respiratory route, the drug needs to be micronised (< 5 µm) which brings many disadvantages in terms of processing and dosing. Current research has investigated numerous effective formulation strategies by particle engineering [2–4]. With the interactive blend as the traditional formulation strategy, micronised drug is blended with a coarse carrier and thus the highly cohesive drug gets processable and thereby applicable.

Nevertheless, most DPI formulations show insufficient drug release and delivery to the site of absorption [5], so that enhancement of DPI formulation efficacy is of scientific and practical interest. The adjustment of device design [6], altering the carrier [7] or even the drug [8] allows performance tuning of respiratory medicines. Another well-acknowledged approach is the addition of extrinsic fines, as reviewed by Jones and Price [9]. The operating principle of the improvement in aerodynamic performance by additional fines is not completely clarified yet. Previously published studies emphasized single theories to explain the underlying mechanism, but Grasmeijer et al. concluded, that also a combination of several principles seems realistic [10]. There are two hypotheses, which are fundamentally linked to adhesion: the saturation of active sites, as well as the formation of drug-fine agglomerates.

Various interdependent factors influence the strength of adhesion, which complicates the investigation of an isolated influencing parameter.

The aim in this study was to determine the impact of the surface energy as an adhesion predictor and its influence on aerodynamic performance in a ternary DPI blend. The study design attached importance to experiment noise reduction, so that surface energy of solids as single performance influencing factor could be investigated. Crucial parameters like particle size distribution [11], processing methods and environments [12] chemical composition [13] and moisture content [14] were kept constant. Thereby it was possible to assess the enhancement of aerodynamic performance in dependence of the surface energy of fine excipients. This also emphasises the importance of excipients storage conditions as a surface energy affecting parameter.

The second part of this study covers the diminishing importance of carrier quality in ternary blends, if fine-drug interaction is superior in terms of adhesion strength.

2. Materials and methods

2.1. Materials

The study comprised two datasets, in which micronised ipratropium bromide served as model drug (d_{90} < 5 µm, Boehringer Ingelheim Pharma AG & Co. KG, Ingelheim, Germany). Dataset one was based on InhaLac® 230 (IH230, Meggle, Wasserburg, Germany) a crystalline, inhalation grade lactose monohydrate, which was fractionated to remove intrinsic fines (> 32 µm, IH230rF). Subsequently, lactose particles with small sizes, referred to as fines, were added. This comprised sieved intrinsic fines of expired IH230 (< 32 µm, IH230Fex) or of a fresh batch (IH230F) as well as intrinsic fines of the milled lactose carrier quality InhaLac 140 (IH140F). As commercially available lactose fines InhaLac 400 (IH400) and a corresponding expired batch (IH400ex) were chosen.

Dataset two contains three types of lactose carriers. All of them are sieve fractions of commercially available lactose qualities in the size range between 60 µm and 150 µm. InhaLac 230 (IH230S) served as a sieved lactose quality, InhaLac 140 as milled lactose carrier quality (IH140S) and FlowLac 90 as spray dried carrier (FL90S). IH400 was used as extrinsic fines quality. Figure 1 shows the respective sieving steps which were performed to obtain all used excipients.

2.2. Sieving

All sieve fractions were gathered using a sieve shaker (RETSCH GmbH, Haan, Germany) with corresponding analytical sieve inserts. The mesh size for the extraction of intrinsic fines was 32 µm. The second dataset used sieve fractions caused by mesh sizes of 63 µm and 125 µm. All carrier substances were sieved additionally on an air jet sieve (e200LS, Hosokawa Alpine, Germany) with 32 µm mesh size and a negative pressure of 4 kPa to ensure complete removal of intrinsic fines.

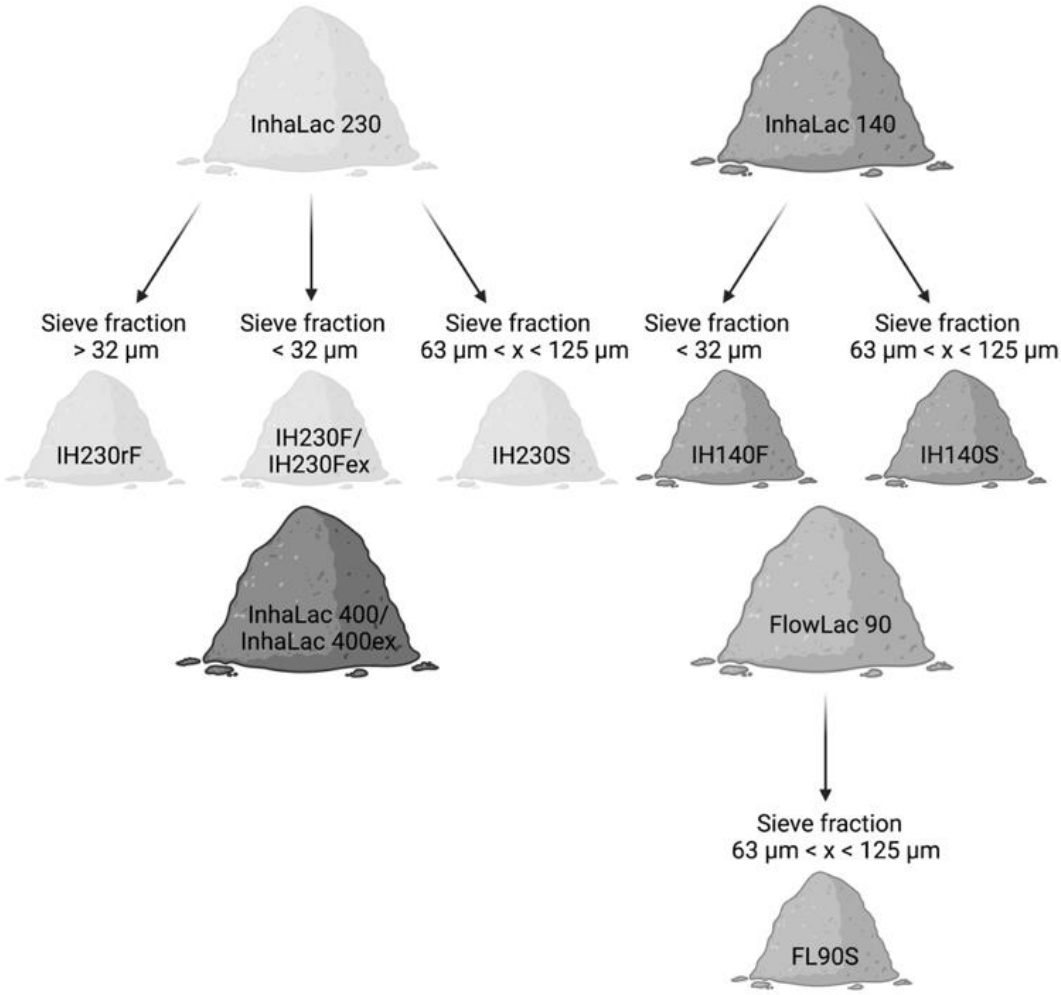

Figure 1: Preparation of lactose sieve fractions. Scheme generated with BioRender.com.

2.3. Determination of particle size distributions (PSD)

The determination of particle sizes was carried out using a Helium Neon Laser Optical System (HELOS®, Sympatec GmbH, Clausthal- Zellerfeld, Germany). The sample was dispersed using the RODOS® dispersion module in an aerosol jet with compressed air (3 bar). For the measurement of fines an R3 lens, for the measurement of carrier particles an R4 lens was used. Every measurement was carried out as triplicate.

Evaluation of size distribution was performed with the Windox 5 software (Sympatec GmbH) using the Fraunhofer enhanced equation.

2.4. Assessment of specific surface area (SSA) and surface energy (SE)

To assess the specific surface area (SSA) and the surface energy of solids (SE) the Surface Energy Analyser (SEA, Surface Measurement Systems Ltd., London, United Kingdom) was used. Sample preparation comprised weighing the powder sample into silanised glass

columns (4 mm inner diameter) and immobilising the powder with silanised glass wool on both ends. To ensure a tight and uniform packing, the prepared columns were inserted into the SMS Column Packer Accessory and tapped for 10 min. All calculated values were obtained by measuring three separately prepared sample columns. A conditioning step was performed prior to all experiments (0% RH and 10 cm^3/min nitrogen carrier gas flow for 60 min) to purge any volatile contamination, as well as the determination of the specific dead volume by a double methane injection (to ensure stable measurement conditions, methane injection was also repeated after every method). Measurement conditions were set to 0% RH and 30 °C with a carrier gas flow of 10 cm^3/min. In advance to the SE assessment, a series of octane concentrations was injected, which provided an adsorption isotherm. SSA calculations were based on the pressure range (p/p^0) from 0.05 − 0.35 (linear section of the adsorption isotherm according to BET theory).

Knowledge of the monolayer capacity in turn, enables the measurement of SE distributions. An alkane series of octane to undecane served as nonpolar probes, chloroform and toluene covered polar surface interaction properties. All probes were injected at concentrations leading to specific surface coverages (from 0.5% up to 20%), based on the monolayer capacity.

Evaluation of raw data was conducted using the SEA Analysis Soft- ware (Surface Measurement Systems Ltd.). SE calculations were based on the DellaVolpe scale in combination with the Dorris and Gray approach [15,16] and the respective peak centre of mass. For SSA calculations peak maxima were used.

2.5. Particle imaging and composition analysis

Particle morphology and composition were analysed by Scanning Electron Microscopy (SEM) and energy dispersive X-ray spectroscopy (EDS) using Phenom XL (Phenom-World BV, Eindhoven, The Netherlands). Samples were fixed onto carbon stickers to ensure sample grounding. Prior to the imaging process, samples were gold-sputtered with BAL-Tec SCP 050 Sputter Coater (Leica Instruments, Wetzlar, Germany) to minimise charging effects. All images were taken with an acceleration voltage of 10 kV using a backscatter detector (magnitudes are specified in the figure description).

2.6. Measurement of residual moisture (RM)

An infrared-balance (MA 45, sartorius, Gottingen, Germany) was utilised to quantify the amount of residual moisture in the powder samples. Approximately two grams of powder

sample were weighed into an aluminium pan and heated by infrared rays until a decrease in sample mass was no longer measurable. We performed the measurement at room temperature. The calculation of residual moisture content was carried out following equation (1).

$$RM = \frac{m_{moist} - m_{dried}}{m_{dried}} \times 100\% \quad (1)$$

2.7. Quantification of drug content

High-performance liquid chromatography (HPLC, Waters Corporation, Milford, United States) was used for quantification of drug content. The analytical method was based on a cyanopropyl-substituted stationary phase (LiChrospher® 100 CN, Merck), using premixed solvents (71% aqua bidest., 29% acetonitrile, 1.42 g/L heptanesulfonic acid) adjusted to pH 3.2 as mobile phase. A method validation was carried out covering system suitability, specificity, precision, repeatability and linearity. The limit of quantification was calculated based on the corresponding ICH guideline (CPMP/ICH/381/95) to be 0.08 µg/mL. An external standard calibration curve was prepared and analysed prior to every HPLC analytical procedure to enable quantification calculations over a con- centration range from 0.21 µg/mL to 104.8 µg/mL ($R^2 > 0.99$). All values used were within the calibrated range. All solvents used were chromatographic grade and supplied by Honeywell Riedel-de Haën (Chromasolv, Seelze, Germany).

2.8. Preparation of interactive blends

All interactive blends in this study were prepared using the high- shear mixer module of the Picoline® platform (Hosokawa Alpine, Augsburg, Germany). The mixing process was divided in two mixing steps at 500 rpm and one sieving step (mesh size: 250 µm) in between. The blend preparation was conducted at monitored environmental conditions (RH: 45% ± 15%; temperature 20 °C to 25 °C). For ternary blends, the fine excipients were added to the carrier in the first mixing step (7.5% w/w) followed by the addition of drug (1% w/w) in the second step. Each blend batch contained 30 g and was tested for homogeneity by analysing ten randomly picked samples via HPLC. Blend homogeneity was reached with a relative standard deviation of drug content below 5% and recovery of 90% – 110%.

2.9. Aerodynamic assessment

The aerodynamic assessment was carried out using the Next Generation Pharmaceutical Impactor (NGI, Copley Scientific, Nottingham, United Kingdom). The DPI blends were filled

into a Novolizer® device (MEDA Pharma GmbH & Co. KG, Bad Homburg, Germany) and dispersed at a flow rate corresponding to 4 kPa pressure drop over the inhaler (78.3 L/min). All results are shown as average of three measurements with eight emitted doses per measurement. All NGI experiments took place in a climate chamber with constant environmental conditions of 21 °C and 45% RH. Deposited drug was quantified with high performance liquid chromatography. The calculation of fine particle fraction was performed using CITDAS Software V3.1 (Copley Scientific).

2.10. Statistical evaluation

All statistical calculations (*p*-value calculations) were carried out with Microsoft Excel 2016 (Microsoft Corporation, Redmond, United States). Depending on the calculated *p*-value, results were categorised as significant (*p*-value < 0.05; *), very significant (*p*-value < 0.005; **) or highly significant (*p*-value < 0.001; ***).

3. Results and discussion

3.1. Surface energy of added fines influences the respective aerodynamic performance

The first part of this work covers the importance of surface energy considerations of fine lactose in ternary blends. Therefore, this dataset is based on one type of carrier, which was combined with several different qualities of fine lactose. These lactose qualities principally differ in surface energies, due to their production route and storage [17,18]. As there is a known influence of size on aerodynamic performance of DPI formulations [19,20], one focus of this comprehensive study was on comparability of particle size distributions.

Figure 2 shows the PSDs of all used fines, which were characterised by particle sizes essentially below 37 µm (mean d_{90} values < 37 µm). To eliminate effects of available intrinsic fines in the carrier bulk (IH230rF), all particles below 32 µm were removed by sieving. Laser diffraction measurements verified the absence of intrinsic fines in the carrier quality (Figure 2).

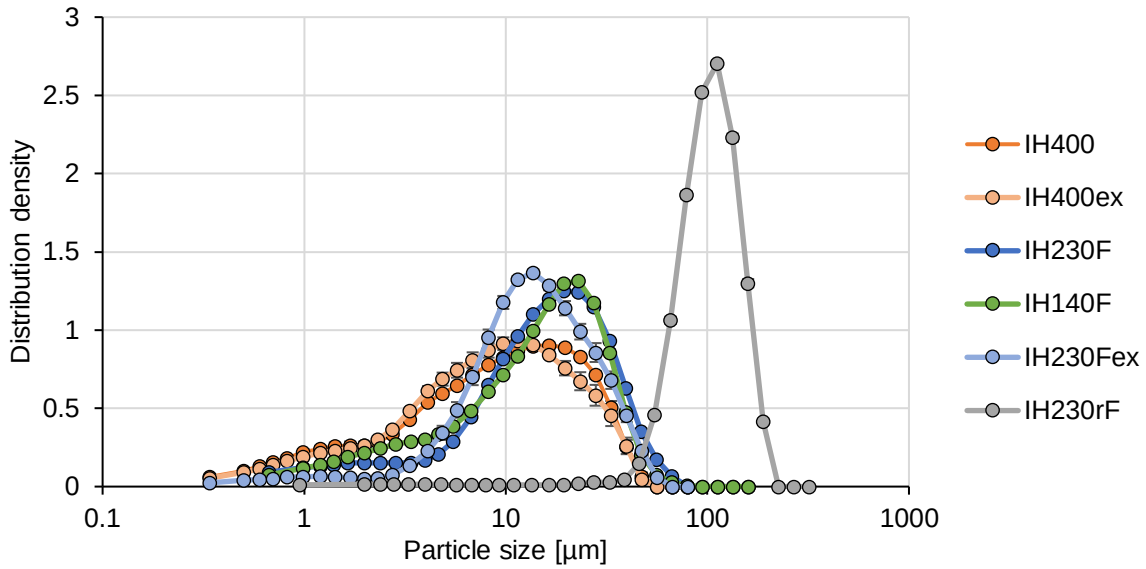

Figure 2: Particle size distributions of the carrier sieve fraction and all used fine lactose qualities. n=3, error bars denote standard deviation.

Moisture is another performance influencing parameter, as capillary forces can lead to considerably strong interactions [21].

Table 1: Residual moisture (RM) of all lactose qualities used. n=3, standard deviations in parentheses.

	IH400		IH400ex		IH230F		IH230Fex		IH140F		IH230rF	
RM [%]	1.2	(0.3)	0.9	(0.1)	1.1	(0.1)	0.8	(0.0)	0.9	(0.4)	0.4	(0.2)

To ensure equal conditions of possible particle interactions residual moisture was determined, and for none of the used powders was considerably above 1% (Table 1). No statistically significant difference was observed between the residual moistures of the fines (*p*-value > 0.05). Moisture content served as an indication of equal conditions in this work. Another powerful powder characterisation technique is the inverse gas chromatography (iGC), which can be used to gain expressive insights into surface interaction properties. Modern iGC approaches comprise the measurement over a range of different sample surface coverages, which enables interpretation of the interaction capabilities (e.g., van-der-Waals interaction) depending on the area involved. Furthermore, the distribution of surface energies allows insights on whether a material surface is mainly homogeneous or heterogeneous. Figure 3 shows the distribution of the total surface energy in dependence of the surface coverage for all used fines. IH400 as commercially available lactose fines exhibited the highest surface energy of 78.2 mJ/m^2 (at 20% surface coverage). This kind of lactose is produced by milling.

Mechanical stress and energy input can lead to substantial changes in the surface condition (e.g., crystal defects, process-induced disorder), which in turn can lead to SE changes [22].

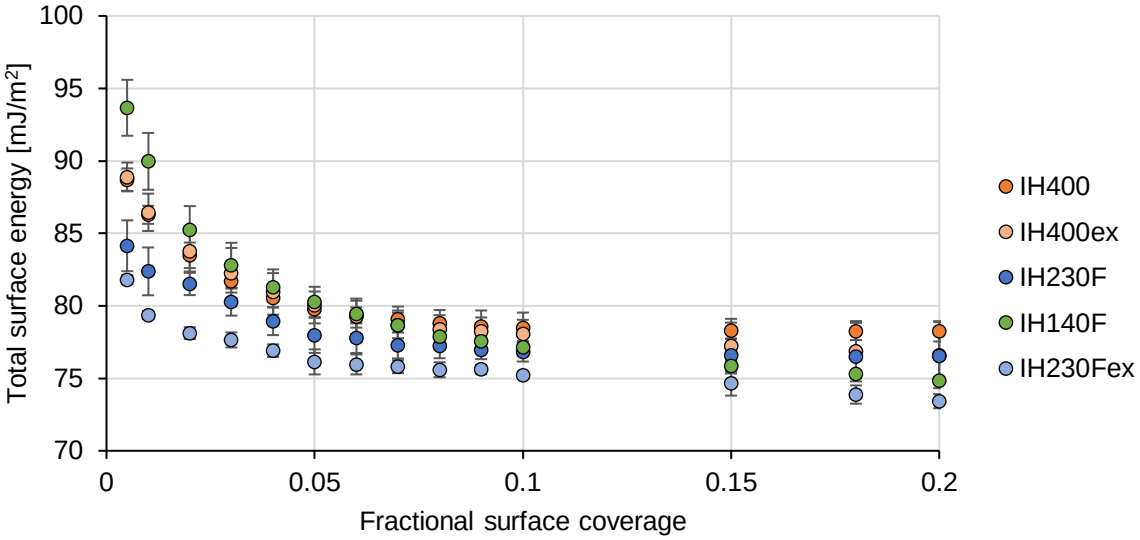

Figure 3: Energy distributions of the total surface energy measured up to 20 % fractional surface coverage. n=3, error bars show standard deviation.

The SE energy trend continued with intrinsic fines of InhaLac 230 more or less on the same level with expired batches of IH400 (76.5 mJ/m^2 and 76.6 mJ/m^2). The heterogeneous IH140F sample exhibited a SE of 74.9 mJ/m^2. Expired intrinsic fines of IH230 reached lowest SE levels of 73.4 mJ/m^2. Both investigated expired batches showed an overall less energetic surface in comparison to fresh batches. The observation of decreased surface energies after in- use long-time storage could potentially be attributed to rearrangement of manufacturing-induced disorders on the surface. The surface of the carrier quality exhibited the lowest surface energy of 56.8 mJ/m^2 (not shown in Figure 3 and 4 for clarity).

Surface energies below 5% fractional surface coverage are not directly interpretable due to differing distribution heterogeneities. SE below 5% fractional coverage represent small shares of the surface with high energy but may be less conclusive if relatively high amounts of the surface are involved in interactions like particle adhesion.

Figure 4 displays the surface energy distributions, as a point-by-point integration first introduced by Ho et al. [23]. The graph visualises interpolated data of 15 measured surface coverages ranging from 0.05% up to 20% for each sample.

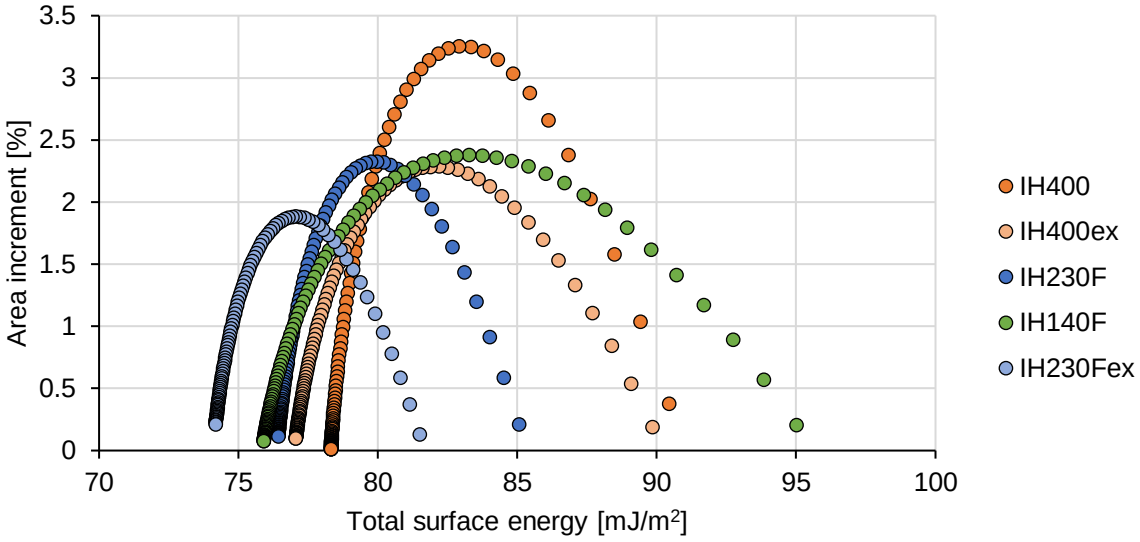

Figure 4: Total surface energy distribution for all fine lactose qualities investigated in this study. Data is shown as average of three measurements.

The peak width correlates with the surface energy heterogeneity and the peak position correlates with the surface energy value. The assumptions made in this work are based on the SE order of higher surface area contributions.

The surface energy of solids is used for calculating the work of adhesion. The work of adhesion is the energy required to separate two interacting surfaces. It consists of the dispersive (non-polar) and the acid-base (polar) part. While the dispersive part mainly represents long- range van-der-Waals interaction, the polar part composes of interactions due to H-bondings [24], dipole interaction or electrostatic forces [25]. In carrier-based blends, the operating principle is substantially based on adhesion and cohesion [26,27]. One could assume that changes in the surface energy of solids, and therefore in adhesion, will cause fundamental changes in dispersion properties, i.e., aerodynamic performance of adhesive mixtures [28].

The work of adhesion (WAdh) between two solid surfaces (s1, s2) is calculated based on equation (2) [29].

$$W_{Adh}^{Total} = W_{Adh}^{dispersive} + W_{Adh}^{acid-base} = 2 \times \sqrt{\gamma_{s1}^{d} \times \gamma_{s2}^{d}} + \sqrt{\gamma_{s1}^{-} \times \gamma_{s2}^{+}} + \sqrt{\gamma_{s1}^{+} \times \gamma_{s2}^{-}} \qquad (2)$$

The study design comprises the specific alteration of one part of the formulation, while other parts are kept constant. Hence, changes in the surface energies of the tested fines (dataset one) will directly influence the resulting adhesion strength, which will follow the same trend as

observed for the surface energies. The calculated work of adhesion of drug-lactose interactions are displayed in Table 2, calculated for 20% surface coverage.

Table 2: Calculated work of adhesion between ipratropium bromide and respective lactose qualities based on triplicate measurements at 20% fractional surface coverage.

IP adhesion to	IH230rF (carrier)	IH230Fex	IH230F	IH140F	IH400ex	IH400
W_{Adh} [mJ/m^2]	123.3	148.5	151.8	150.1	151.7	153.0

The values obtained by a measurement at 20% surface coverage represent the energetic levels of the surface majority. Higher injection concentrations could lead to measuring errors due to probe-probe interactions, whereas smaller surface coverages would depict extremely low surface shares [30]. The lowest W_{Adh} is calculated for carrier-drug interactions (123.3 mJ/m^2). The drug-carrier interaction being inferior to the drug-fine interaction could be a required parameter for significantly enhanced performance by additional fines (not investigated in this study). This W_{Adh} is valid for all investigated blends, since carrier and drug were the same in all experiments of the first data set. Higher W_{Adh} between drug and fines leads to stronger interaction, or stronger agglomerates respectively. Furthermore, in an agitated system of all three substances in a blending vessel, it could be assumed, that agglomerates of drug and fines are less likely to break up again and adhere to other available particle surfaces. In this study, higher W_{Adh} is therefore interpreted as preferred formation of drug-fines agglomerates.

Kinnunen et al. proposed, that if agglomerates of drug particles and fines are formed, they will detach more easily from the carrier compared to the pure drug [31]. It could be assumed, the higher the work of adhesion between those agglomerates, the higher the enhancement on the aerodynamic performance of the respective ternary blend.

As shown in Figure 5, the presence of drug-fines agglomerates was discernible on NGI stages with low aerodynamic cut-offs. The chemical composition was determined using energy-dispersive X-ray to identify whether the visible particles are drug or lactose.

Begat et al. suggested in 2005 to focus on the relationship of drug cohesion and adhesion instead of just considering adhesive mechanisms between drug and carrier [32]. The particle interactions within an interactive blend can be pictured as a delicate equilibrium, which needs to be in a specific position (depending on formulation, device and patient) to work as desired.

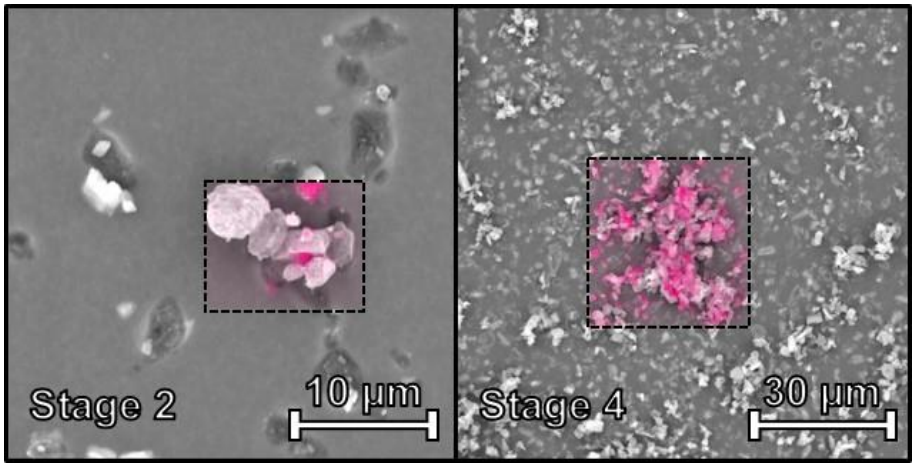

Figure 5: Agglomerates of drug (ipratropium bromide) and fines (IH400) on Stage 2 (3500x magnification), pure drug on stage 4 (2500x magnification) using EDS analysis. Bromide coloured in pink.

In turn, small changes can force the system out of the equilibrium and therefore, decrease aerodynamic performance. In this study, all calculations of the cohesive-adhesive balance (CAB) were based on thermodynamic work of adhesion at 20% surface coverage following equation (3).

$$CAB = \frac{Work\ of\ cohesion\ (A)}{Work\ of\ adhesion\ (B)} \quad (3)$$

Carrier-API: A = Ipratropium bromide; B = Ipratropium bromide and carrier

Carrier-Fines: A = Fines; B = Fines and carrier

API-Fines: A = Ipratropium bromide; B = Ipratropium bromide and fines

Since this work investigated ternary blends, we extended the CAB calculations to display the interactions between all types of components. Therefore, three different CABs represented carrier-drug, carrier-fines and drug-fines interactions. The calculated CAB of carrier-drug interaction was the same for all investigated blends. The calculations for carrier-fines and drug-fines interactions are displayed in Figure 6. For both interactions, a clear trend was observable. For the blend containing IH400, the fines were more likely to agglomerate than adhere to the coarse carrier. Furthermore, the formation of drug-fine agglomerates was preferred within this mixture as shown by a CAB value < 1.0. The trend continued with decreasing surface energies of the raw materials. The only ternary blend, which shows slight tendency to pure drug agglomerates over drug-fine agglomerates contained expired IH230 fines, similar to the control, i.e., binary blend.

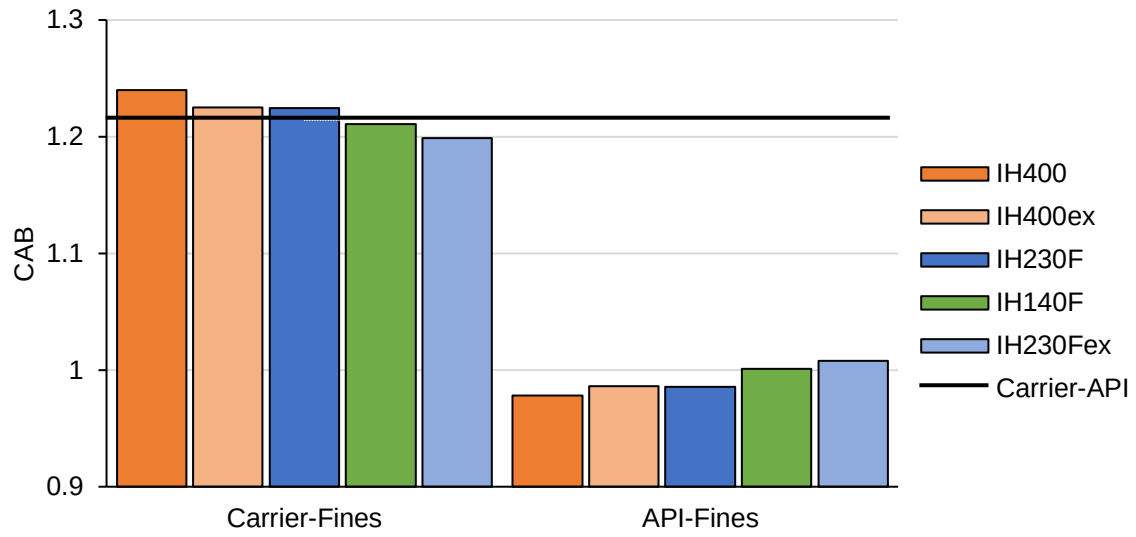

Figure 6: Cohesive-adhesive balance calculated based on the work of adhesion at 20 % surface coverage. The calculations are based on triplicate measurements.

To proof the previously stated hypothesis of FPF enhancement with high-energy fines, all blends were assessed in the Next Generation pharmaceutical Impactor. The results are displayed in Figure 7.

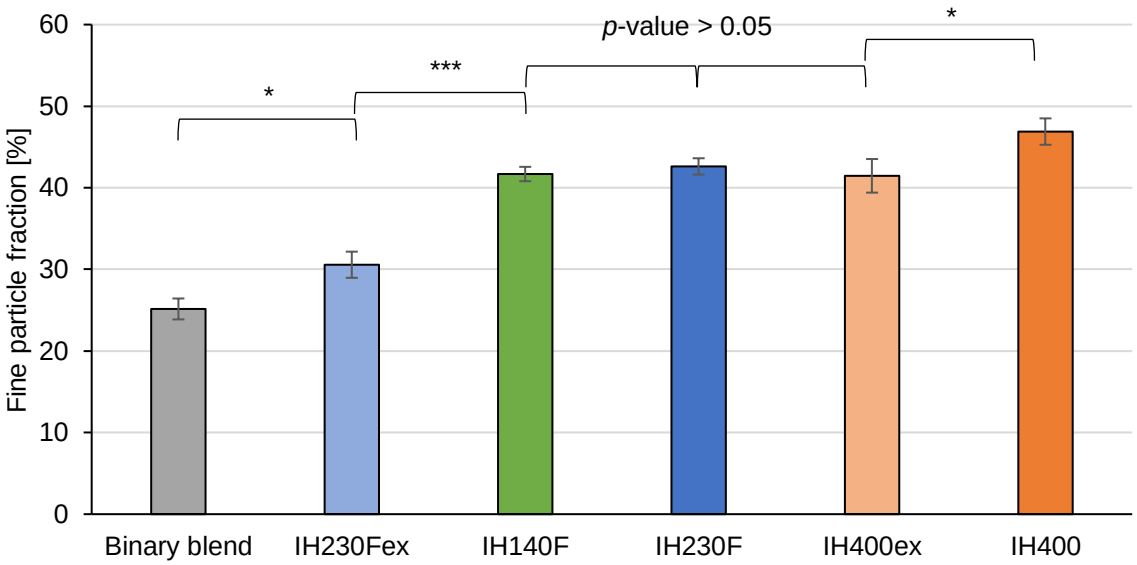

*Figure 7: Results of the aerodynamic assessment in the NGI (IH230rF in combination with different additional fines or as binary blend). All displayed FPF data is calculated for a cut-off at five micrometers. n=3, error bars show standard deviation. Significance denoted as *: p-value < 0.05; **: p-value < 0.005.*

The binary blend reached the smallest FPF value. The initially removed intrinsic fines of the carrier material, representing sieved fines, increased the FPF of the control blend from 25.1%

up to 30.6% fine particle fraction. The fine lactose material which originates from an already expired batch, led to significantly lower FPF than intrinsic fines, which were extracted from a fresh batch of the carrier material (*p*-value < 0.005). We also observed a similar trend for the milled InhaLac 400 batches (*p*-value < 0.05). Three of the five investigated fines showed similar adhesion properties based on their surface energy (IH230F, IH140F, IH400ex). All interactive blends using these fines indicated no statistic difference from each other in terms of FPF (*p*-value > 0.05), whereas fines with distinctly different surface energies led to statistically different (*p*-value < 0.05) FPFs. To summarise, the results showed a correlation of surface energy levels of the fine material with the FPF of the corresponding adhesive mixture.

3.2. Superior drug-fine agglomerates define aerodynamic performance

W_{Adh} values as indicator of particle–particle interactions were examined with the second dataset. This dataset uses three coarse lactose sieve fractions of different origin. All carriers varied in specific surface area, surface energy (Table 3), surface morphology and roughness, but exhibit essentially the same particle sizes (Figure 8). The model API, as well as the fine excipient quality were kept constant for all experiments of dataset two.

Table 3: Particle characteristics of carrier substances used in dataset two. n=3, standard deviations in parentheses.

Carrier quality	IH230S		IH140S		FL90S	
γ^{Total} maximum [mJ/m^2]	81.1	(0.4)	94.7	(4.3)	89.5	(2.4)
γ^{Total} minimum [mJ/m^2]	64.2	(1.0)	74.8	(2.7)	69.1	(0.7)
SSA [m^2/g]	0.10	(0.0)	0.19	(0.1)	0.23	(0.0)

To eliminate size-dependent influences, this study achieved comparable sizes for the coarse lactose qualities in dataset two by sieving, which was verified by laser diffraction (< 10% deviation between all d_{50} values). Figure 8 shows particle size distributions with d50 values in the range of 100.5 µm to 106.6 µm for the coarse lactose qualities. SEM images of original material and sieve fractions were used to determine carrier integrity and sufficient removal of intrinsic fines (Figure 9).

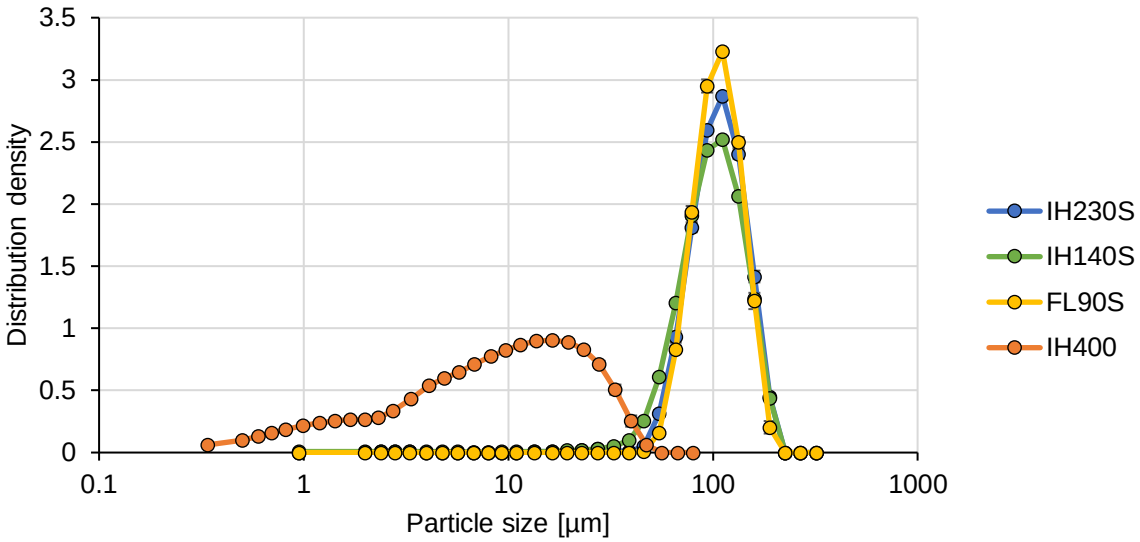

Figure 8: Particle size distributions fines and carriers used in binary and ternary blends. n=3, error bars denote standard deviation.

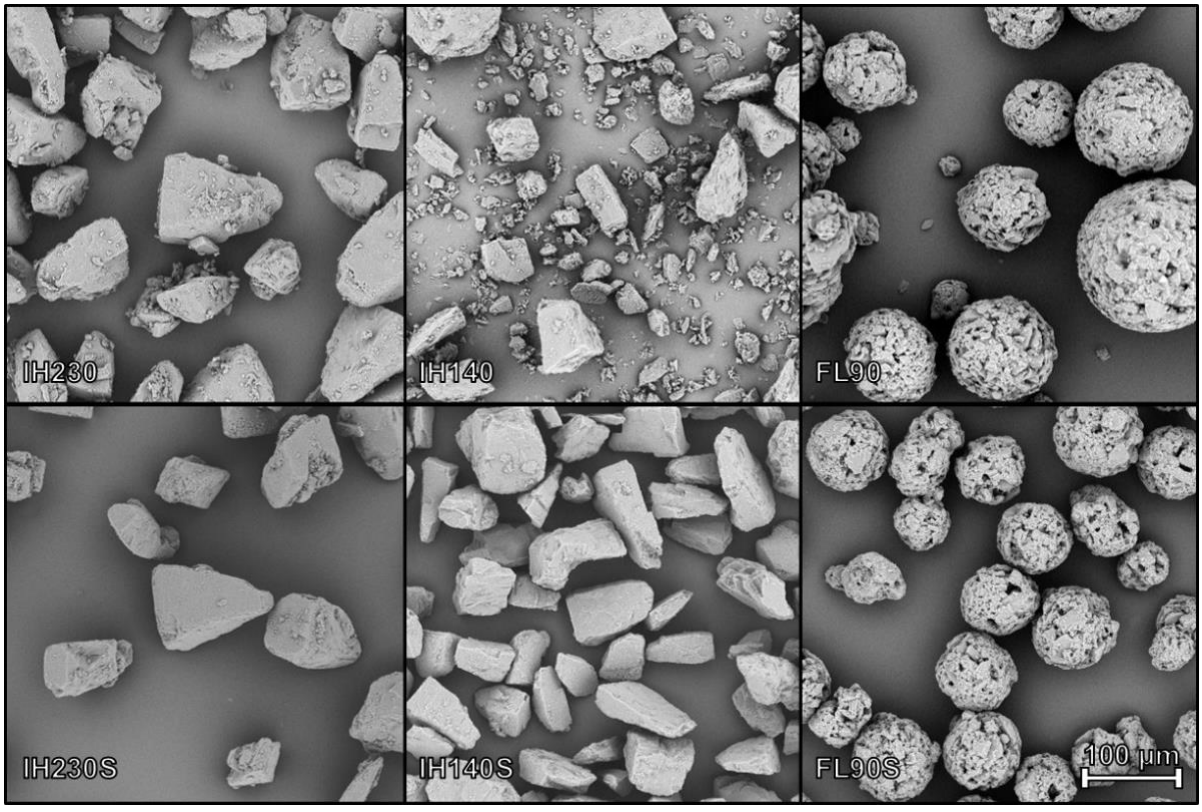

Figure 9: SEM (500x magnitude) images of coarse lactose qualities (InhaLac 230, InhaLac 140, FlowLac 90) of different origins before and after sieving.

Table 4 provides a summary of the values determined for the work of adhesion at 20% surface coverage between ipratropium bromide and possible interaction partners. The highest

interaction energy (153.0 mJ/m^2) is calculated for the IH400-IP adhesion, regardless of the carrier quality. Referring to the hypothesis stated in the previous section, agglomerate formation of the drug and fine lactose are thus preferred compared to other partners.

Table 4: Calculated work of adhesion between ipratropium bromide and respective lactose qualities based on triplicate measurements at 20 % fractional surface coverage.

IP adhesion to	IH230S	IH140S	FL90S	IH400	IP
W_{Adh} [mJ/m^2]	142.0	150.0	144.0	153.0	149.6

The results of the NGI assessment (Figure 10) showed that all binary blends resulted in different FPFs as expected due to different morphologies and origins. The milled lactose quality IH140S reached the highest FPF. The worst performance in this setting was shown by the spray-dried lactose FL90S. All binary blends differed significantly from each other in their FPFs (*p*-value < 0.005). Since the FPF is a multi-factor dependent characteristic, the differences may be based on a combination of SSA, SE, morphology and many more [33].

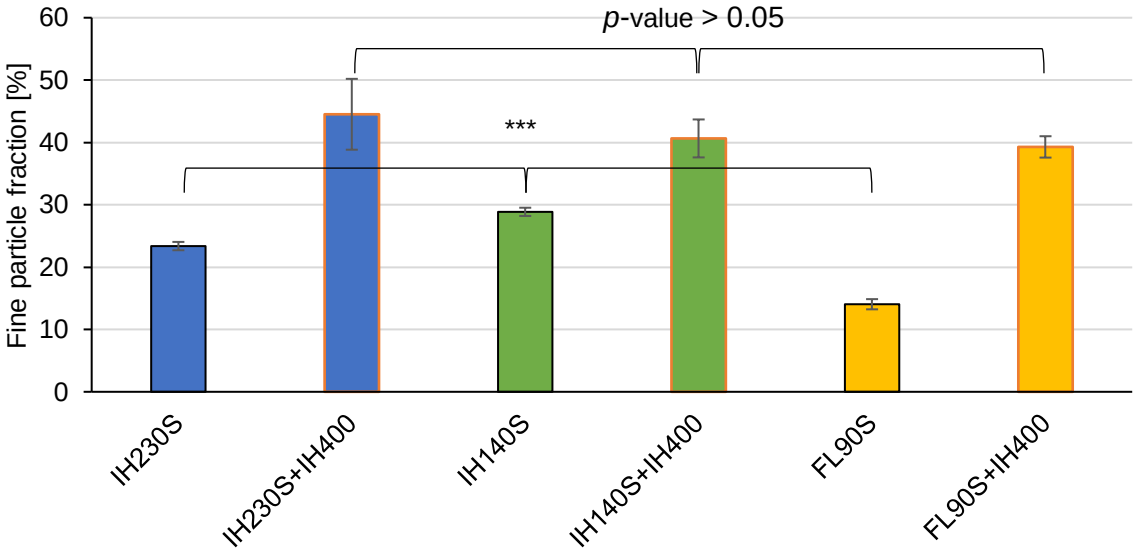

*Figure 10: Results of the aerodynamic assessment in the NGI (binary (columns without border) and ternary blends (columns with orange border) based on different carrier substances). All displayed FPF data is calculated for a cut-off at five micrometers. n=3, error bars show standard deviation. Significance denoted as ***: p-value < 0.001.*

The same carriers, in turn, used in ternary blends, performed without a statistically significant difference (*p*-value > 0.05). The single altered parameter was the addition of IH400 (7.5% w/w) as extrinsic fines. Based on the starting points, we assume a levelling of FPFs due to

superiority of fine-drug interactions over carrier-drug interactions (Table 4). Especially since the carrier morphology showed crucial differences (e.g., in terms of roughness), an alignment of FPFs shows the shrinking influence of the carrier on aerodynamic performance in such a ternary system.

4. Conclusion

This study investigated ternary blends for inhalation with regard to their surface energy. As the results show, surface energy and derived thermodynamic adhesion strength crucially influenced the effect of fines in DPI formulations. Lactose fines from different origins and with distinct surface energies led to significant changes in aerodynamic performances of the respective ternary blends. Therefore, formulation scientists should consider the origin of the fines used as a crucial parameter besides the amount added.

Furthermore, we summarise, that the use of fines on fundamentally different carriers led to FPFs, which were not statistically different. Based on the work of adhesion calculations, this can be explained by superior adhesion strength of fines to drug compared to fines-carrier or drug-carrier interactions.

This work also substantiates the need to monitor storage and expiry date of the used substances, since fines above their use-by period per- formed significantly worse than fresh ones. Extensive storage stability tests are needed to make a clear statement on expiry mechanisms influencing surface energies.

Moreover, this study highlighted the use of inverse gas chromatography as powerful tool for characterisation of pharmaceutical powder applications. Formulation scientists should consider the surface energy of their raw materials to gain insights in adhesion behaviour measured as a bulk parameter.

Nevertheless, adhesion of solids is a very complex interaction and surface energy interaction is just one of many interacting factors, like mechanical interlocking, roughness or electrostatic interactions, which need to be considered. Even though this experimental setup detected surface energy related trends, many more interactions have to be taken into account in a formulation development approach.

References Chapter 3

[1] S. Ramakrishnan, D. v Nicolau, B. Langford, M. Mahdi, H. Jeffers, C. Mwasuku, K. Krassowska, R. Fox, I. Binnian, V. Glover, S. Bright, C. Butler, J.L. Cane, A. Halner, P.C. Matthews, L.E. Donnelly, J.L. Simpson, J.R. Baker, N.T. Fadai, S. Peterson, T. Bengtsson, P.J. Barnes, R.E.K. Russell, M. Bafadhel, Inhaled budesonide in the treatment of early COVID-19 (STOIC): A phase 2, open-label, randomised controlled trial, The Lancet Respiratory Medicine. 395 (2021) 497. https://doi.org/10.1016/S2213-2600(21)00160-0.

[2] A.H.L. Chow, H.H.Y. Tong, P. Chattopadhyay, B.Y. Shekunov, Particle engineering for pulmonary drug delivery, Pharmaceutical Research. 24 (2007) 411–437. https://doi.org/10.1007/s11095-006-9174-3.

[3] A. J. Hickey, S. R. da Rocha, Pharmaceutical Inhalation Aerosol Technology, 3rd ed., CRC Press, 2021.

[4] R. Scherließ, C. Etschmann, DPI formulations for high dose applications - Challenges and opportunities, International Journal of Pharmaceutics. 548 (2018) 49–53. https://doi.org/10.1016/j.ijpharm.2018.06.038.

[5] M. Hoppentocht, P. Hagedoorn, H.W. Frijlink, A.H. de Boer, Technological and practical challenges of dry powder inhalers and formulations, Advanced Drug Delivery Reviews. 75 (2014) 18–31. https://doi.org/10.1016/j.addr.2014.04.004.

[6] N.T.Q. Ngoc, L. Chang, X. Jia, R. Lau, Experimental investigation of design parameters on dry powder inhaler performance, International Journal of Pharmaceutics. 457 (2013) 92–100. https://doi.org/10.1016/j.ijpharm.2013.08.072.

[7] N. Bungert, M. Kobler, R. Scherließ, In-Depth Comparison of Dry Particle Coating Processes Used in DPI Particle Engineering, Pharmaceutics. 13 (2021) 580. https://doi.org/10.3390/pharmaceutics13040580.

[8] Q.T. Zhou, L. Qu, I. Larson, P.J. Stewart, D.A.V. Morton, Improving aerosolization of drug powders by reducing powder intrinsic cohesion via a mechanical dry coating approach, International Journal of Pharmaceutics. 394 (2010) 50–59. https://doi.org/10.1016/j.ijpharm.2010.04.032.

[9] M.D. Jones, R. Price, The influence of fine excipient particles on the performance of carrier-based dry powder inhalation formulations, Pharmaceutical Research. 23 (2006) 1665–1674. https://doi.org/10.1007/s11095-006-9012-7.

[10] F. Grasmeijer, A.J. Lexmond, M. van den Noort, P. Hagedoorn, A.J. Hickey, H.W. Frijlink, A.H. de Boer, New mechanisms to explain the effects of added lactose fines on the dispersion performance of adhesive mixtures for inhalation, PloS One. 9 (2014) e87825. https://doi.org/10.1371/journal.pone.0087825.

[11] H.D.C. Smyth, A.J. Hickey, Carriers in Drug Powder Delivery, American Journal of Drug Delivery. 3 (2005) 117–132. https://doi.org/10.2165/00137696-200503020-00004.

[12] M. Hertel, E. Schwarz, M. Kobler, S. Hauptstein, H. Steckel, R. Scherließ, The influence of high shear mixing on ternary dry powder inhaler formulations, International Journal of Pharmaceutics. 534 (2017) 242–250. https://doi.org/10.1016/j.ijpharm.2017.10.033.

[13] M.D. Louey, P. Mulvaney, P.J. Stewart, Characterisation of adhesional properties of lactose carriers using atomic force microscopy, Journal of Pharmaceutical and Biomedical Analysis. 25 (2001) 559–567. https://doi.org/10.1016/S0731-7085(00)00523-9.

[14] E. Emery, J. Oliver, T. Pugsley, J. Sharma, J. Zhou, Flowability of moist pharmaceutical powders, Powder Technology. 189 (2009) 409–415. https://doi.org/10.1016/j.powtec.2008.06.017.

[15] Anett Kondor Daryl R. Williams Daniel J. Burnett, Determination of Acid-Base Component of the Surface Energy by Inverse Gas Chromatography: iGC SEA Application Note 227, (2014). https://www.surfacemeasurementsystems.com/downloads/sea-application-notes/.

[16] P.P. Ylä-Mäihäniemi, J.Y.Y. Heng, F. Thielmann, D.R. Williams, Inverse Gas Chromatographic Method for Measuring the Dispersive Surface Energy Distribution for Particulates, Langmuir. 24 (2008) 9551–9557. https://doi.org/10.1021/la801676n.

[17] S. Das, I. Larson, P. Young, P. Stewart, Understanding lactose behaviour during storage by monitoring surface energy change using inverse gas chromatography, Dairy Science & Technology. 90 (2010) 271–285. https://doi.org/10.1051/dst/2009051.

[18] F. Thielmann, D.J. Burnett, J.Y.Y. Heng, Determination of the surface energy distributions of different processed lactose, Drug Development and Industrial Pharmacy. 33 (2007) 1240–1253. https://doi.org/10.1080/03639040701378035.

[19] M.J. Telko, A.J. Hickey, Dry powder inhaler formulation, Respiratory Care. 50 (2005) 1209–1227.

[20] X.M. Zeng, G.P. Martin, S.-K. Tee, A.A. Ghoush, C. Marriott, Effects of particle size and adding sequence of fine lactose on the deposition of salbutamol sulphate from a dry powder formulation, International Journal of Pharmaceutics. 182 (1999) 133–144. https://doi.org/10.1016/S0378-5173(99)00021-6.

[21] D. Dopfer, S. Palzer, S. Heinrich, L. Fries, S. Antonyuk, C. Haider, A.D. Salman, Adhesion mechanisms between water soluble particles, Powder Technology. 238 (2013) 35–49. https://doi.org/10.1016/j.powtec.2012.06.029.

[22] H.E. Newell, G. Buckton, D.A. Butler, F. Thielmann, D.R. Williams, The Use of Inverse Phase Gas Chromatography to Measure the Surface Energy of Crystalline, Amorphous, and Recently Milled Lactose, Pharmaceutical Research. 18 (2001) 662–666. https://doi.org/10.1023/A:1011089511959.

[23] R. Ho, M. Naderi, J.Y.Y. Heng, D.R. Williams, F. Thielmann, P. Bouza, A.R. Keith, G. Thiele, D.J. Burnett, Effect of Milling on Particle Shape and Surface Energy Heterogeneity of Needle-Shaped Crystals, Pharmaceutical Research. 29 (2012) 2806–2816. https://doi.org/10.1007/s11095-012-0842-1.

[24] F.M. Fowkes, Role of acid-base interfacial bonding in adhesion, Journal of Adhesion Science and Technology. 1 (1987) 7–27. https://doi.org/10.1163/156856187X00049.

[25] N.M. Ahfat, G. Buckton, R. Burrows, M.D. Ticehurst, An exploration of inter-relationships between contact angle, inverse phase gas chromatography and triboelectric charging data, European Journal of Pharmaceutical Sciences. 9 (2000) 271–276. https://doi.org/10.1016/S0928-0987(99)00063-9.

[26] G. Saint-Lorant, P. Leterme, A. Gayot, M.P. Flament, Influence of carrier on the performance of dry powder inhalers, International Journal of Pharmaceutics. 334 (2007) 85–91. https://doi.org/10.1016/j.ijpharm.2006.10.028.

[27] J.N. Staniforth, J.E. Rees, F.K. Lai, J.A. Hersey, Interparticle forces in binary and ternary ordered powder mixes, The Journal of Pharmacy and Pharmacology. 34 (1982) 141–145. https://doi.org/10.1111/j.2042-7158.1982.tb04210.x.

[28] I. Saleem, H. Smyth, M. Telko, Prediction of dry powder inhaler formulation performance from surface energetics and blending dynamics, Drug Development and Industrial Pharmacy. 34 (2008) 1002–1010. https://doi.org/10.1080/03639040802154905.

[29] D. R. Williams, Particle Engineering in Pharmaceutical Solids Processing: Surface Energy Considerations, Current Pharmaceutical Design. (2015) 2677–2694.

[30] A. Kondor, Infinite Dilution and Surface Energy Heterogeneity Profile by iGC-SEA: iGC-SEA Technical Note 807, (2020).

[31] H. Kinnunen, G. Hebbink, H. Peters, D. Huck, L. Makein, R. Price, Extrinsic lactose fines improve dry powder inhaler formulation performance of a cohesive batch of budesonide via agglomerate formation and consequential co-deposition, International Journal of Pharmaceutics. 478 (2015) 53–59. https://doi.org/10.1016/j.ijpharm.2014.11.019.

[32] P. Begat, R. Price, H. Harris, D.A. v Morton, J.N. Staniforth, The Influence of Force Control Agents on the Cohesive-Adhesive Balance in Dry Powder Inhaler Formulations, KONA Powder and Particle Journal. 23 (2005) 109–121. https://doi.org/10.14356/kona.2005014.

[33] F. Grasmeijer, N. Grasmeijer, P. Hagedoorn, H. Willem Frijlink, A. Haaije de Boer, Recent advances in the fundamental understanding of adhesive mixtures for inhalation, Current Pharmaceutical Design. (2015) 5900–5914.

Introduction to Chapter 4

In chapter two of this thesis, the methodological possibilities for a surface energy decrease of carriers were discussed.

Chapter three in turn, emphasises the benefits of using high-energy fines to complement the excipient bulk. Therefore, it seems obvious to find a method to increase particle surface energy, instead of decreasing. This could potentially enable the production of superior fine excipients in terms of (aerodynamic) performance enhancement.

High-shear mixer processing of host and additive (guest) particle may result in different coatings, depending on additive properties and processing parameters. A prerequisite for such dry particle coatings is that the guest particle is considerably smaller than the host particle or that the guest particle is able to spread over the host particle during the process, based on material properties (e.g., lubricious material) [1]. Within the first phase of that high-shear mixer process, the additive gets distributed throughout the host bulk. A well distributed guest particle will adhere to the exhibited host particle surface resulting in an ordered mixture. Now in dependence of additive content and/or additive properties it can be distinguished into I) a porous coating or II) a continuous film. The latter occurs more likely for additives which tend to soften at the given process environment (mechanical stress, temperature). A porous coating describes the occupancy of the host particle with guest particles.

So, to achieve a sufficient coating on the surface of small excipients (lactose fines) an additive is needed, which is either in a proximately submicron size or spreads easily during processing. Magnesium stearate probably fulfils both requirements, but it results in decreased surface energies. That is why a trial-and-error approach was conducted. I tested polylactic acid and poloxamer 188 as polar model additives. Polylactic acid was unfortunately not spreading on the surface of the guest particle (carrier lactose), resulting in no firmly bound additive after processing. Poloxamer 188 in turn, was coatable onto the lactose surface. The results of both a high-energy carrier coating, as well as modifying fines' surface energy are reported in chapter four.

References

[1] M. Gera, V. Saharan, M. Kataria, V. Kukkar, Mechanical Methods for Dry Particle Coating Processes and Their Applications in Drug Delivery and Development, Recent Patents on Drug Delivery & Formulation. 4 (2010) 58–81. https://doi.org/10.2174/187221110789957200.

Chapter 4: Proof-of-concept for adjusted surface energies and modified fines as a novel concept in particle engineering for DPI formulations

This chapter is published as:
Bungert, N., Kobler, M., Scherließ, R.: Proof-of-concept for adjusted surface energies and modified fines as a novel concept in particle engineering for DPI formulations.
Pharmaceutics **2022**, 14(5), 951.
https://doi.org/10.3390/pharmaceutics14050951

Abstract

Current marketed dry powder inhaler (DPI) medicine lacks drug delivery performance, due to insufficient powder dispersion. In carrier-based blends, incomplete drug detachment is typically attributed to excessive adhesion forces between carrier and drug particles. Adding force control agents (FCA) is known to increase drug detachment. Several researchers accounted this effect to a decrease in carrier surface energy (SE). In turn, an increase in SE should impede drug detachment. In this proof-of-concept study, we investigated the influence of the SE of the carrier material in binary blends by intentionally inverting the FCA approach. We increased SEs by dry particle coating utilising high shear mixing, which resulted in decreased respirable fractions of the respective blends. Thus, we confirmed SE of the carrier influences drug delivery and should be considered in formulation approaches. Complementing engineering techniques on the carrier level, we evaluated a method to modify SE of extrinsic fines in ternary powder blends for inhalation. By co-milling of fine lactose and additive, we tailored the SE and hence the adhesiveness of additional fine excipients. Thus, the extent and the strength of drug-fines agglomerates may be controllable. For ternary DPI formulations, this work highlights the potential benefits of matching the SE of both fines and drug.

1. Introduction

Dry powder drug delivery into the deep lung is a challenging task. Branching of pulmonary structures with decreasing diameters needs drug particles to be micronised, typically smaller than 5 µm. Micronisation increases surface area and surface energy [1], which leads to high co- and adhesiveness. To enable reproducible dosing, scientists combine the drug with a coarser carrier, formulating interactive blends or adhesive mixtures [2]. The adhesion between drug and carrier is typically excessively strong, resulting in incomplete drug detachment from the carrier. Force-control agents (FCA) are a well-known tool in carrier-based DPI formulation development [3–5]. They shall de-crease the adhesion between drug and carrier particle in adhesive mixtures for inhalation and hence increase drug detachment during inhalation. Magnesium stearate is one of the best-studied additives for DPI application [6–9]. It is FDA (Food and Drug Administration) approved as safe for pulmonary application and already utilised in marketed products (e.g., Breo® Ellipta®) [10]. Due to the complexity of particle-particle interactions in adhesive mixtures, the underlying principle of FCAs remains partly unsolved. It is reported that the mechanism of action bases on a combination of carrier smoothening [11] and the decrease of adhesion forces [12]. However, it remains challenging to distinguish which principle primarily causes the specific effect. Fundamental adhesion properties (thermodynamic adhesion, surface energy interaction) are determinable by inverse gas chromatography. Several researchers found the surface energy of magnesium stearate-treated powders to be decreased compared to untreated material [13]. Since magnesium stearate is the only well-investigated example, it remains unclear if this is a causal relationship and valid for other additives.

The aim of this study was to highlight the surface energy of solids as a main influence in adhesion, which will translate into an influence on aerodynamic performance. Herewith, we investigated if observed effects of modified DPI carrier SEs on respirable fractions are invertible. Furthermore, we examined particle engineering towards tailored SE of fine excipients their respective influence.

As a proof-of-concept, we prepared DPI carrier particles with artificially increased SEs by dry particle coating. As a continuation of published data [14], we used previously applied methods and compared the SE impact of carriers with high SEs with carriers being treated with magnesium stearate (decreased SEs). According to the hypothesis that aerodynamic performance of adhesive blends increases with decreasing carrier SE (e.g., after processing with magnesium stearate), we expect the contrary for the high-energy carriers. The second part of this study translates this finding to fine excipients in ternary blends for inhalation. Ternary powder blends are DPI formulations, which contain additional fine excipient fractions

(fines) to improve drug detachment and hence drug de-livery. Grasmeijer et al., as well as Jones and Price extensively reviewed the principles with which additional fines are likely to improve aerodynamic performances [15,16]. One of the main theories is the formation of agglomerates of drug and fines. These agglomerates are prone to detach more easily from the carrier compared to the pure drug [17]. Furthermore, fines may adhere to higher-energy binding sites on the carrier, forcing the drug to bind on weaker adhesion spots. In 2021, we published a study on the influence of SEs in ternary powder blends. We found high SE fines to be superior and concluded higher SE will preferentially lead to more agglomeration with the drug and consequently higher drug detachment from the carrier. The different fine qualities originated from different manufacturing routes or storage conditions [18]. To evaluate and substantiate this theory, we engineered particles in the size level of fine lactose by co-milling. The resulting novel compound fines in this study were then assessed for their performance-affecting properties. Apart from specific SE modifications, the effect of intrinsic SE levels of different drugs is also part of this work. The surface energy interaction depends always on both interacting surfaces, emphasising the importance of the drugs' surface energy level.
We assume that there is an optimum of SE interaction in dependency of the drug. When the interaction strength exceeds an optimum, we postulate that the drug-fines-agglomerates do not disperse sufficiently during inhalation.

2. Materials and Methods

2.1. Materials

The first section of this study covers the carrier modification of a specific respiratory grade, sieved lactose quality, namely InhaLac® 230 (IH230, Meggle, Wasserburg, Germany), using magnesium stearate (MgSt, Parteck® LUB MST, Merck, Darmstadt, Germany) and poloxamer 188 (Pol, Lutrol® micro 68, BASF, Ludwigshafen, Germany). To produce engineered fine excipients, we used the micronised, respiratory grade lactose InhaLac 400 (IH400, Meggle) in combination with MgSt or Pol. IH230 after the removal the present intrinsic fines (IH230rF) served as carrier material. Ipratropium bromide (d_{90} < 5 µm, Boehringer Ingelheim, Ingelheim, Germany) and fenoterol hydrobromide (d_{90} < 5 µm, Boehringer Ingelheim) were used as model drugs.

2.2. Particle size distributions

Laser diffraction measurements provided particle size distributions (PSD) of all used excipients. We used the Helium Laser Optical System (HELOS®, Sympatec, Clausthal-Zellerfeld, Germany) equipped with the dry dispersion unit (RODOS®) and an automatic feeder

(VIBRI®). The samples were dispersed by pressurised air (primary dispersion pressure of 2 bar for carrier samples and 3 bar for extrinsic fines). Depending on the sample, we used either an R1, R3 or an R4 lens. All data is shown as average of triplicate measurements. The respective standard deviation is depicted accordingly.

2.3. Particle engineering of DPI carriers

We modified the carrier lactose using dry particle coating in the high shear mixing unit of the Picoline® (Picomix®, Hosokawa Alpine, Augsburg, Germany). The process comprised multiple steps. First, pre-sieving of additive (mesh size: 180 µm) and carrier (mesh size: 250 µm). Second, weighing both substances into the mixing vessel using the sandwich method. Third, a coating period of 15 minutes at 500 rpm. Each batch was 30 g containing 2% (w/w) of the additive, in line with earlier studies [14]. The dry particle coating was conducted at monitored lab conditions (21 °C ± 5 °C; 45% RH ± 15%).

2.4. Removal of intrinsic fines

To exclude the effect of present intrinsic fines in ternary blends, we removed particles < 32 µm (equates the mesh size) from IH230 using an air-jet sieving technique (e200LS®, Hosokawa Alpine) at 4 kPa negative pressure for 29 min. The resulting material (IH230rF) served as carrier material for ternary interactive blends containing engineered fines.

2.5. Particle engineering of extrinsic fines

Particle engineering of fine lactose was conducted by co-milling using the Jet-O-Mizer® (Fluid Energy Processing and Equipment Company, Bethlehem Pike Telford, PA, USA) air jet mill. We premixed IH400 with the respective additive (MgSt or Pol) at 10% (w/w) concentration for 45 min at 42 rpm in the Turbula® blender (Willy A. Bachofen Maschinenfabrik, Basel, Switzerland) prior to co-milling.

The obtained pre-blends were fed manually to the air jet mill. The feed pressure was 9 bar for all milling procedures. The grinding pressure and the number of grinding cycles was adjusted to fit the PSD of IH400 being processed at 9 bar grinding pressure.

In order to meet these PSD requirements (InhaLac 400 after one grinding cycle at 9 bar), IH400 + 10% MgSt needed one grinding cycle at 7.5 bar, whereas IH400 + 10% Pol needed two cycles: The first at 9 bar and a second at 7 bar grinding pressure. The batch size of the co-milling was approximately 10 g and the milling was performed at monitored lab conditions (21 °C ± 5 °C; 45% RH ± 15%).

2.6. Surface area and surface energy determination

To determine the specific surface area (SSA) and SE distributions of all materials, we used the Surface Energy Analyser (SEA, Surface measurement Systems, London, UK), an inverse gaschromatograph (iGC). The sample preparation included transferring the powder into silanised glass columns (4 mm inner diameter for carriers and 3 mm inner diameter for drugs and fines) and fixing the sample on both ends using silanised glass wool. The magnesium stearate processed fines needed a stepwise column filling. Due to their greasy nature, we inserted multiple glass wool spacers between small amounts of sample (approx. one spacer every 25 mg). A tapping procedure using the SMS Column Packer Accessory (Surface Measurement Systems) excluded voids within the sample columns. Experiments were performed as triplicate, meaning three separately prepared columns per sample. To purge any volatile contamination, we conditioned samples ahead of the respective experiment for one hour (at 0% RH and 10 cm^3/min nitrogen flow, equated to the general measurement conditions). Furthermore, the double injection of methane to determine the dead volume at the beginning and the end was part of all experiments.

Prior to a SE assessment, we conducted the SSA determination by injecting octane concentrations (pressure range (p/p^0) 0.05 − 0.35) leading to an adsorption isotherm. The SSA was hence calculated using the BET theory. Knowing the respective monolayer capacity of a sample allowed for SE determinations at specific fractional surfaces coverages. We used homologous alkanes from heptane to undecane as non-polar probes, as well as chloroform and toluene to determine acid-base properties of the sample. The injected concentrations led to specific surface coverages from 0.5% up to 20% of the monolayer capacity. The SEA Analysis software (Surface Measurement Systems) enabled the calculation of the SE properties based on the raw data (retention of probes). All calculations based on the DellaVolpe scale [19], the Dorris and Gray method (dispersive SE) and the polarisation method (specific SE) [20,21]. SE raw data was analysed regarding the peak centre of mass, whereas SSA calculations based on peak maxima. SE data in this work is depicted as the average of three parallels with their respective standard deviation.

2.7. Production of interactive blends

The interactive blends in this study were obtained by blending respective drug and carrier (and eventual extrinsic fines) in a high-shear mixer (Picomix®, Hosokawa Alpine) for 60 seconds twice at 500 rpm, with a sieving step in between (mesh size: 250 µm). All the excipients underwent pre-process sieving at respective mesh sizes (drug: 180 µm; fines: 180 µm; carrier:

250 µm) to avoid large agglomerates. The production process of binary blends consists of weighing-in the drug (1% w/w) using the sandwich method, followed by the blending steps and a post-process sieving (mesh size: 250 µm). For ternary blends in turn, we added the fine excipient (7.5% w/w) in the first mixing step and the drug (1% w/w) within the second, complemented with post-process sieving (mesh size: 250 µm). The drug content was matched to earlier studies and the respective batch size was 30 g [14,18]. High-performance liquid chromatography (HPLC) analysis of 10 randomly picked samples provided data on blend homogeneity. We considered a blend homogeneous at a drug recovery of 90% – 110% and a relative standard deviation of less than 5%. Prior to further tests, we conditioned all homogeneous blends at 44% RH and room temperature for one week.

2.8. Aerodynamic assessment

Impaction analysis using the Next Generation pharmaceutical Impactor (NGI; Copley Scientific, Nottingham, UK) of conditioned blends provided information on aerodynamic particle size distributions and fine particle fractions (FPF) of the respective blends. FPF is defined as the percentage of the emitted dose with an aerodynamic diameter smaller than 5 µm. Delivered doses are defined as the mass of drug per shot, which was emitted from the device upon actuation. The blends were manually filled into reservoirs of Novolizer® devices (MEDA Pharma, Bad Homburg, Germany). We set the flow rate through the NGI to 78.3 L/min to generate a pressure drop of 4 kPa over the inhaler and actuated the device 8 times per run. Each aerodynamic assessment consisted of three runs per blend and all tests took place at controlled environmental conditions of 45% RH and 21 °C. Drug quantification was performed using HPLC. After quantification, we used CITDAS Software V3.1 (Copley Scientific) to calculate aerodynamic particle size distributions and hence resulting FPFs. NGI assessments were performed in triplicate; reported values are the respective averages in combination with the standard deviations.

2.9. Quantification of drug content

The HPLC (Waters Corporation, Milford, United States) method for fenoterol hydrobromide comprised using a reverse stationary phase (LiChrospher® 100 RP-18, Merck, Darmstadt, Germany) and a solvent mixture consisting of 88% bidestilled water adjusted to pH 3.0 (with phosphoric acid) and 12% acetonitrile as mobile phase. We conducted a method validation, which covered system suitability, specificity, precision, repeatability and linearity. The LOQ (limit of quantification) was 0.03 µg/mL (calculated according to the corresponding ICH guideline CPMP/ICH/381/95). Prior to every HPLC analysis we freshly prepared an external standard calibration curve (0.2 µg/mL to 99.9 µg/mL, $R^2 > 0.99$). All determined sample

concentrations were within that calibrated range. We used chromatographic grade solvents for all HPLC procedures, which were purchased from Honeywell Riedel-de Häen (Chromasolv, Seelze, Germany).

The HPLC method for quantification of ipratropium bromide (including validation parameters) was previously reported [14,18].

3. Results and Discussion

3.1. Proof-of-concept for carrier surface energies affecting drug detachment

3.1.1. Creating a portfolio of different carrier surface energies by dry particle coating

Prior to the blend preparation and the respective aerodynamic assessment, we characterised the compound carrier particles in terms of PSD and SE. Following the same protocol of previously published studies (utilising MgSt) [13], it was also possible to sufficiently coat the lactose carrier with poloxamer. Particle size distribution measurements served as verification for firmly bound additive. Figure 1 shows the PSDs of InhaLac® 230 before and after processing with magnesium stearate and the polar model additive (poloxamer 188) in their respective concentrations (2% w/w). The PSDs of the carriers being processed with additive are similar to the unprocessed material indicating no substantial loose additive residuals in the powder, which would result in a shoulder in the PSD.

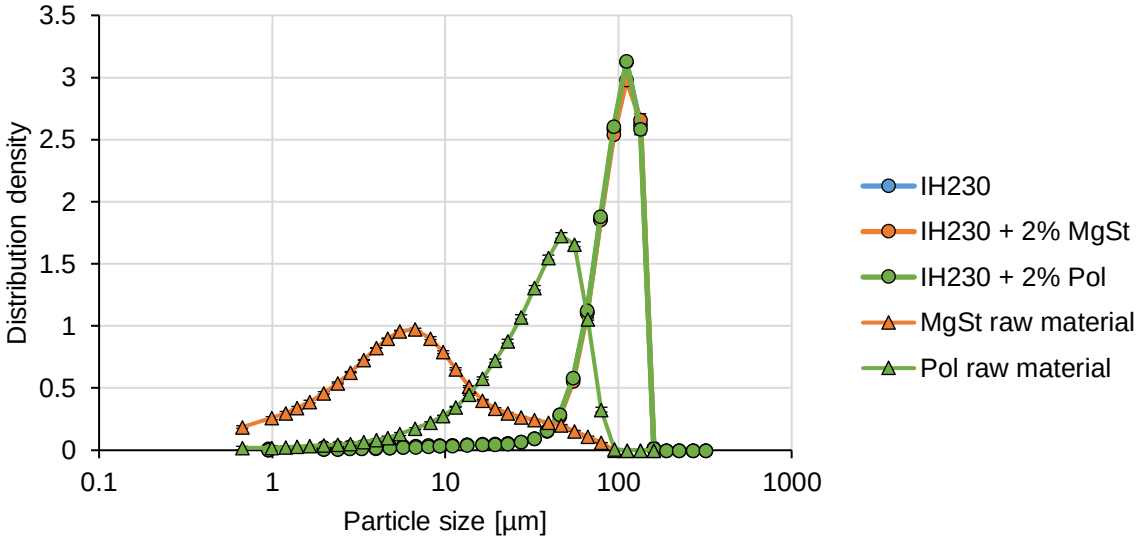

Figure 1: Particle size distribution of the carrier lactose with and without additives. N=3, error bars denote standard deviation.

The aim of this work was to demonstrate the technical feasibility of specifically altering the surface of carrier and fines (see section 3.2) and consequently the SE. Therefore, all samples

were assessed using the Surface Energy Analyser to investigate process induced SE modifications. In Figure 2 we plotted the respective dispersive, specific and total SE distributions of all three carrier batches. Figure 2A shows a small increase in dispersive SE for the MgSt coated sample compared to the unprocessed and polar-coated lactose, which is due to the non-polar properties of MgSt. Moreover, Figure 2A displays an increase in specific SE of the polar-coated sample (green triangles), whereas the SE of non-polar processed lactose indicates less polar surface properties (orange triangles).

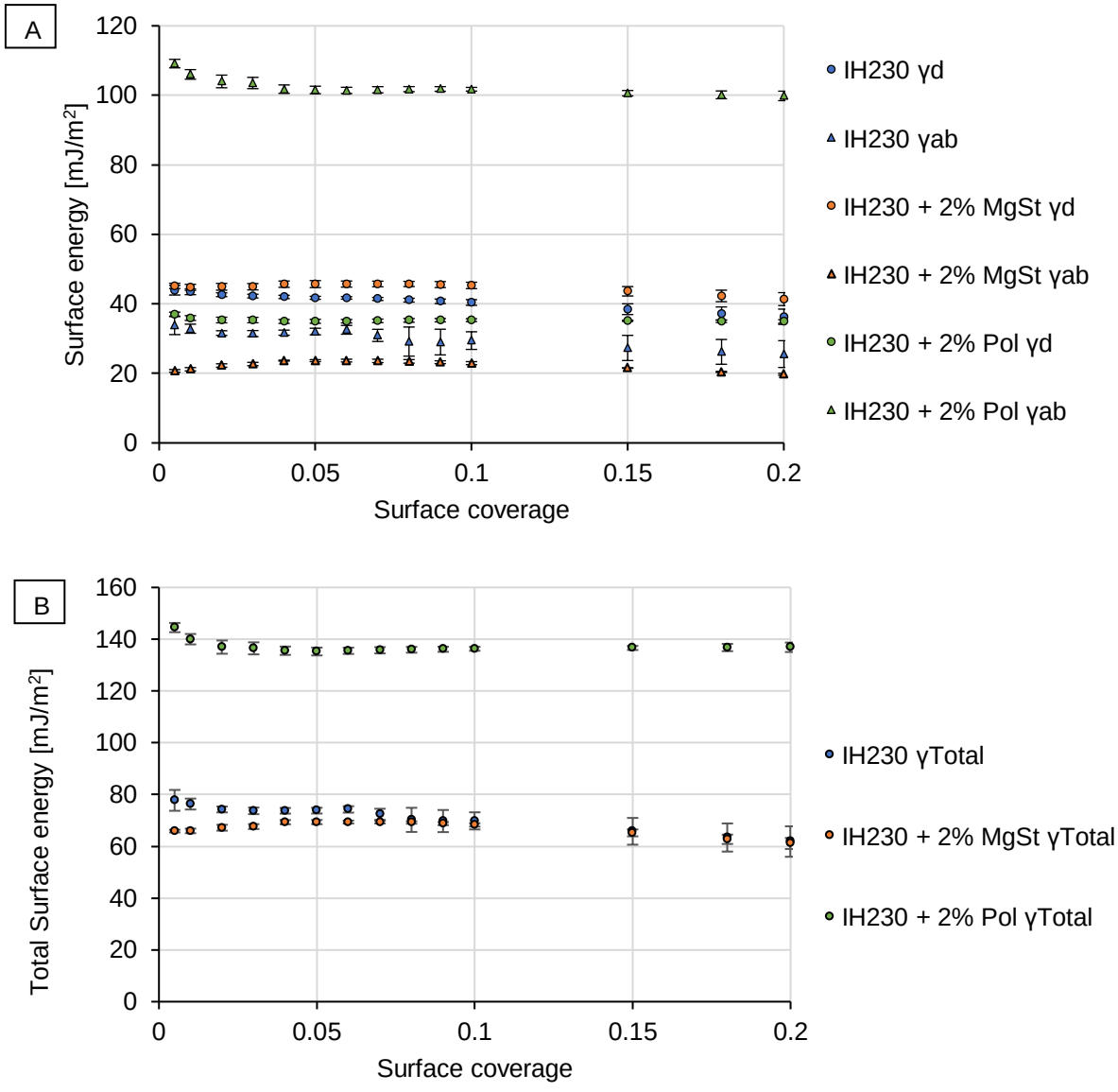

Figure 2: Surface energy distributions of lactose carriers with and without additive. 2A depicts the changes in the surface energy (γ) composition, i.e., the suffix "d" indicates the dispersive part and suffix "ab" the acid-base or specific part of the respective surface energy. Figure 2B shows the resulting total surface energies for all samples. N=3, error bars denote standard deviation.

The distributions of the resulting total surface energies (Figure 2B) give a trend of the polar sample being the one with the highest SE levels, followed by the non-processed. The lowest total SE level was exhibited by the MgSt coated samples, which agreed with our previously published findings.The absolute values of the specific surface energy, however, depend crucially on the probes used in the iGC method. Thus, specific SE and total SE provide comparative information if the same methods were used, but are limited in deriving solid, value-based conclusions.

3.1.2. Binary blends for inhalation using the engineered carrier particles

The corresponding interactive blends of all carrier batches under investigation were then examined for their aerodynamic performances (FPF). We displayed results of the impaction analysis in Table 1. For ipratropium, being the model drug with lower SE (Figure 3), the low-energy carrier performed significantly better than non-processed lactose (FPF increase of 145.7%, *p*-value < 0.05). The poloxamer-coated carrier resulted in a decreased FPF in comparison to the unmodified sample (decreased by 9.2%), although this is no statistically significant decrease (*p*-value > 0.05). De Boer et al. reported that the Novolizer device is comparably carrier-insensitive regarding the resulting FPF [22]. Thus, even if the carrier properties are detrimental for high drug delivery, the Novolizer device may cause relatively good FPFs, due to its effective dispersing principle [23]. We assume that there is a minimum (API-specific) FPF in this device, which we will not undercut by increasing thermodynamic adhesion. Although the decrease in FPF for the high-SE carrier is magnitudes lower than the increase for the low-SE carrier, this finding thus supports the hypothesis of higher SE interaction leading to stronger adhesion between drug and carrier.

Table 1: Calculated FPFs at a 5 µm cut-off, derived from NGI assessments. N=3, standard deviation in parentheses.

Carrier	FPF ipratropium [%]		FPF fenoterol [%]	
IH230	23.2	(1.9)	11.9	(2.1)
IH230 + 2% MgSt	57.0	(0.1)	56.1	(0.6)
IH230 + 2% Pol	21.1	(1.6)	11.1	(0.7)

To verify this hypothesis, we also investigated the effect of using a drug with higher SE, namely fenoterol (Figure 3). According to equation (1), the increase of the SE of any of both interacting

surfaces (s1 and s2) will increase the overall SE interaction (SEI, WAdh), and hence the adhesion strength [24].

$$W_{Adh}^{Total} = W_{Adh}^{dispersive} + W_{Adh}^{acid-base} = 2 \times \left[\sqrt{\gamma_{s1}^{d} \times \gamma_{s2}^{d}} + \sqrt{\gamma_{s1}^{-} \times \gamma_{s2}^{+}} + \sqrt{\gamma_{s1}^{+} \times \gamma_{s2}^{-}}\right] \quad (1)$$

Figure 3 displays the surface energy distribution of fenoterol hydrobromide in relation to ipratropium bromide. The overall higher surface energy level should cause stronger interaction with the carrier particle (Equation 1).

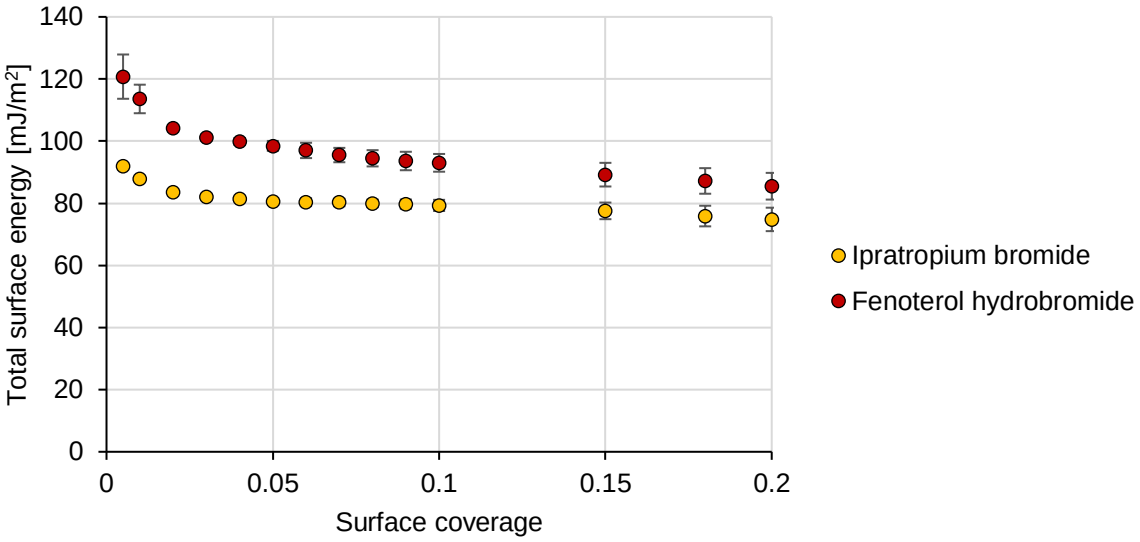

Figure 3: The distribution of total surface energies from the respective model APIs of this study. N=3, error bars denote standard deviation.

All resulting FPFs of interactive blends based on the above-mentioned carriers formulated with fenoterol as API were lower compared to the ones using a lower energy drug (ipratropium bromide; Table 1). Aiming for a decreased FPF has no practical use but serves as a proof of the general influence of SE alterations.

We conclude, if the SEI is increased in a binary system, the FPF will decrease due to increased adhesion between drug and carrier. This can be achieved by either exchanging one of the substances or altering their surface.

3.2. Particle engineering of extrinsic fines enables surface energy matching with the drug

3.2.1. Evaluation of particle engineering methods

According to our preceding work, SE differences (induced by manufacturing route) of fine excipients will cause differences in the resulting FPFs of ternary blends for inhalation. In our extensive study of a range of fine lactose qualities, we found that higher SE of fines led to higher FPFs of the respective adhesive blends. We explained the results with higher

agglomeration tendency of high-energy fines with the drug and more efficient saturation of active sites. Therefore, particle engineering on the fine additives level (here InhaLac 400) should probably enable to extend that beneficial effect.

Previously reported engineering methods (i.e., high-shear mixing, medium green triangles in Figure 4) were not suitable to coat high amounts of additive onto the surface of fine lactose. The PSDs of InhaLac 400 processed with 10% additive (w/w) indicated an insufficient coating by a shoulder (black arrow) matching the d_{50} of pure poloxamer 188 at approximately 30 µm (Figure 4).

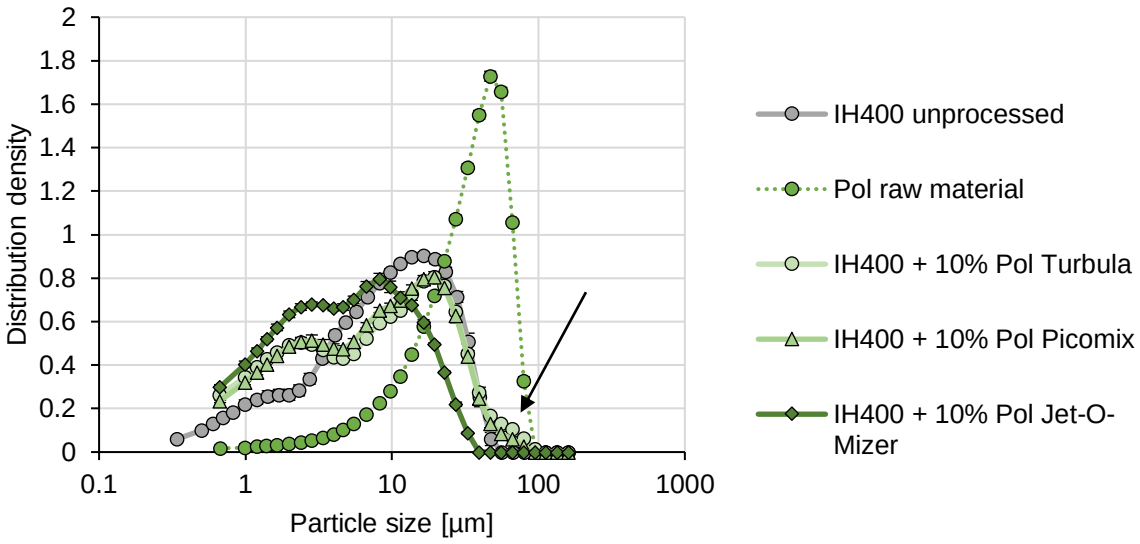

Figure 4: Resulting PSDs from the evaluation of particle engineering methods, which are unsuitable for extrinsic fines (exemplary shown for poloxamer processes). Turbula blender as low-shear blending shown in light green circles, Picomix exemplary for high-shear mixing depicted in medium green triangles and the Jet-O-Mizer as co-milling approach is coloured in dark green squares. The black arrow points at the shoulder in PSD as a result of loose, residual additive. N=3, error bars denote standard deviation.

Thus, we evaluated another particle engineering method, which is more suitable to produce compound fines. Co-milling can apply high energy (particle - particle and particle - wall collisions) and hence merging or coating [25,26] of the substances in the grinding chamber. After optimising the grinding conditions, the process resulted in similar particle sizes (Figure 5).

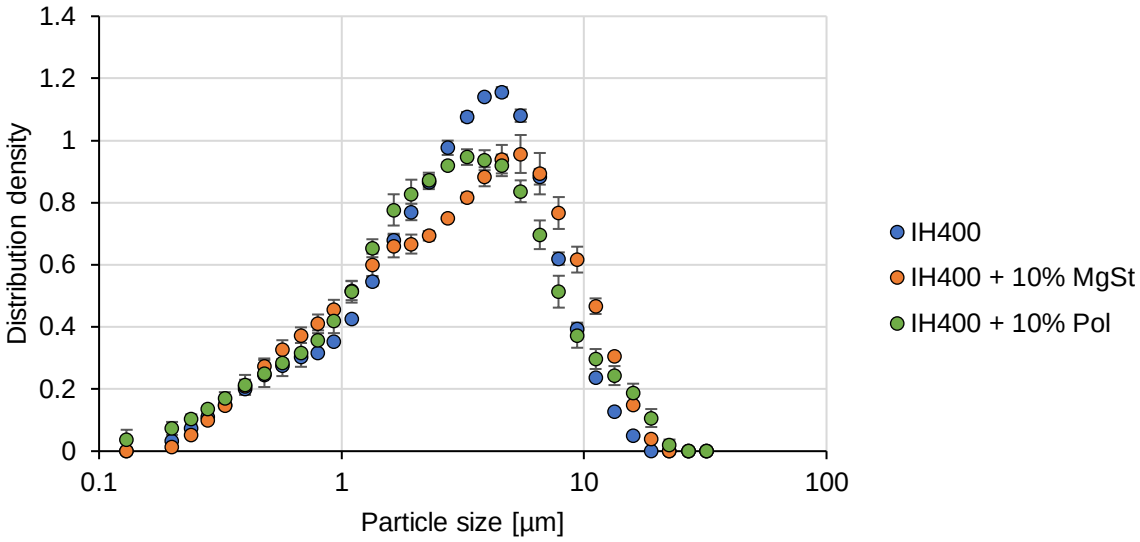

Figure 5: Particle size distribution after the optimisation of grinding pressures in the air jet mill. N=3, error bars denote standard deviation.

To test our hypothesis, we measured the respective SE distributions of the novel compound fines. As clearly visible in Figure 6, processing with either high- or low-energy additives led to crucial changes in the fines' SE levels. Showing the same trends as for processed carriers, merging with MgSt resulted in decreased total surface energies, whereas co-milling with poloxamer led to significantly increased SE.

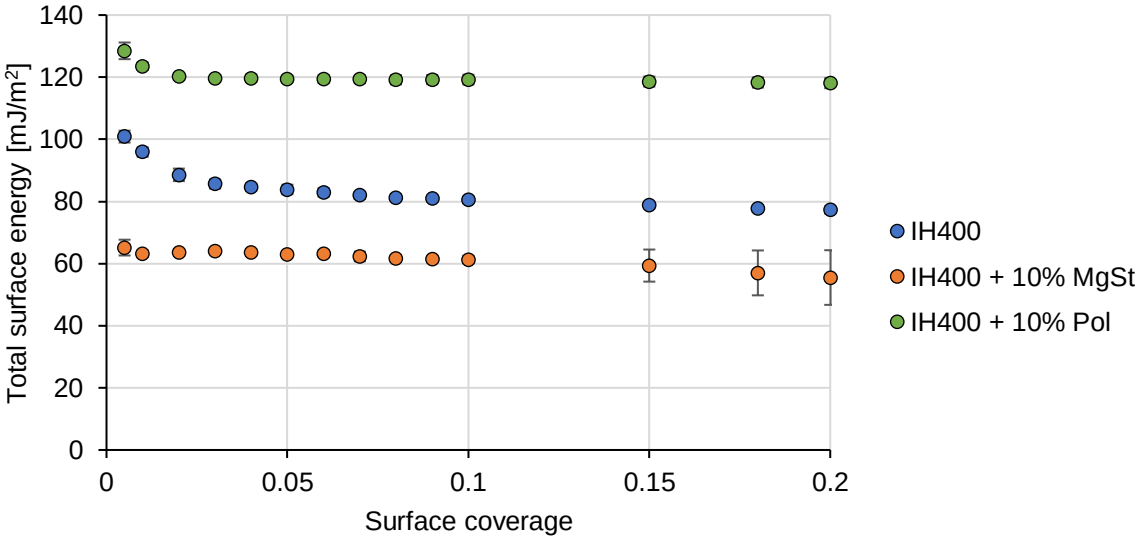

Figure 6: Distribution of total surface energies of fines engineered by co-milling. N=3, error bars denote standard deviation.

3.2.2. Ternary blends for inhalation using the engineered fines

Within a ternary blend, a high-energy fine particle should exhibit higher adhesion forces and hence result in increased saturation of active sites and increased agglomeration with the API. These agglomerates are known to increase drug detachment from the carrier and to result in higher fine particle fractions, if readily dispersible [27].

Therefore, we determined the FPF of the respective ternary blends, containing the novel compound fines (Table 2). Contrary to our expectations, the blends with fines processed without additive resulted in the highest FPF. Both compound fines performed worse, with the high-energy fines being statistically significant inferior to the additive-free fines (*p*-value < 0.05).

Table 2: FPF at a 5 µm cut-off for ternary blends containing engineered fines. "IH400" herewith means that the fines base on the processed IH400 quality, if stated, with the respective additive. N=3, standard deviation in parentheses.

Blend	FPF ipratropium [%]		FPF fenoterol [%]	
IH230rF + IH400	50.5	(2.4)	46.9	(1.3)
IH230rF + IH400 + 10% MgSt	47.9	(2.5)	62.9	(0.8)
IH230rF + IH400 + 10% Pol	45.0	(1.8)	38.9	(2.5)

All ternary blends were additionally prepared using fenoterol hydrobromide as API with higher SE levels (Figure 3). The FPFs decreased again compared to ipratropium bromide blends. This finding further substantiates the hypothesis that higher SE of drugs results in higher adhesion and hence less drug detachment and the formation of API-fines agglomerates, which are hard to disperse. The only exception was the ternary blend containing MgSt, which showed higher FPF for fenoterol than for ipratropium. All blends prepared with fenoterol differed statistically significant from each other (*p*-value < 0.05). Since the combination of the low energy fines with the high-energy API resulted in the best performance, it seems reasonable that there is an optimal SEI for a given drug-carrier combination and device.

This is further substantiated by evaluating statistic differences of FPFs between the respective drugs per fine quality. The high-energy drug (fenoterol) performed significantly better (*p*-value < 0.05) in combination with low-energy fines (MgSt). Ipratropium bromide as low-energy drug in turn, reached significantly higher FPFs (*p*-value < 0.05) combined with high-energy fines (Pol). Both drugs led to FPFs without statistically significant difference (*p*-value > 0.05) if formulated with non-modified (medium-energy) fine excipients.

The drug is usually a fixed parameter in formulation development and modifications should be evaluated extremely critically. As the specific alteration of drug particles by particle engineering could result in changes in the respective clinical effect, scientists typically focus on excipient modifications. The obtained data indicated that matching the drugs' SE with the SE of fines could be beneficial. In doing so, a high SE drug may be compensated with low SE fines for instance. Furthermore, the co-milling approach we introduced in this study enables the tailoring of fines in dependence of the drugs' SE.

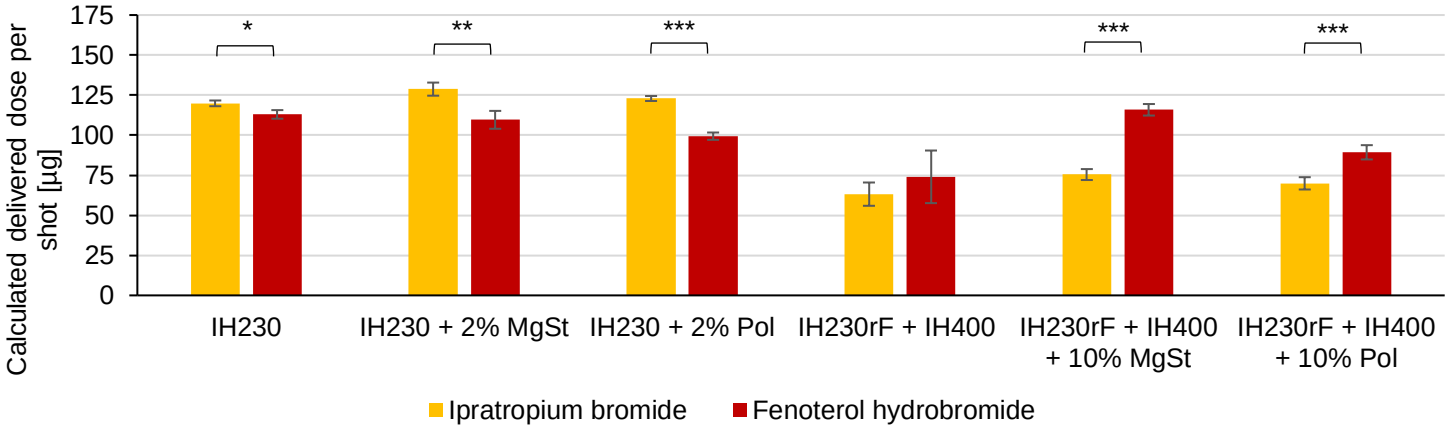

*Figure 7: Calculated delivered doses of all assessed formulations in µg. N=3, error bars denote standard deviation. Significance depicted as: * p-value < 0.05; ** p-value < 0.01; *** p-value < 0.005.*

Additionally, we assessed the changes in delivered doses (DD) when switching from ipratropium (lower SE) to fenoterol (higher SE) in Figure 7. The DD decreased in the binary blends due to increased adhesion forces between carrier and drug. The trend in DD matches the trend in FPFs. In ternary blends in contrast, the DD increased in fenoterol blends, even though the FPF decreased. This is due to a higher emission of drug, probably based on more drug-fine agglomerates, which detach more easily from the carrier, but are hardly dispersed into individual particles < 5 µm

4. Conclusion

Based on the experimental data we conclude that systematically modified surface energies in binary blends work according to fundamental adhesion (thermodynamic adhesion) theories. This means that both an increased adhesion of drug by a SE increase of the carrier and a decreased adhesion of drug to carrier by reduction of carrier SE are feasible. We showed that decreased carrier SE after processing with MgSt is not just an artefact, but a causal relation. This highlights SE assessments to keep track of changed adhesion properties after particle engineering. Substantiating the influence of thermodynamic adhesion, changing the drug to one with higher SEs also resulted in decreased drug detachment.

Engineering of high- and low-energy extrinsic fines for DPI formulations was also feasible, but the results of aerodynamic assessment were not fully matching earlier stated hypotheses. Usually, practical adhesion forces are larger than just thermodynamic adhesion forces (surface energy interactions) [28]. Thus, trends in SE will just transfer to trends in adhesion if a major part of the particle properties does not change. We assume that by fundamentally altering the particle properties by jet mill processing, the properties influencing practical adhesion (not SE related, such as plastic or viscoelastic deformation upon the break of the adhesive joint) changed crucially. Therefore, earlier observed correlations of fines SEs and respective FPFs are not extendable due to practical adhesion.

Nonetheless, we showed that high-energy fines performed better with a low-energy drug and vice versa. This substantiated the hypothesis of SE matching as a strategy to enhance the drug delivery of ternary blends.

In general, it is not possible to correlate DPI performance with just single solid-state parameters directly. Our study emphasises the influence of the SE on adhesion, which translates into an influence in drug detachment and delivery. In a multifactorial system like DPI formulations, we must take several influencing parameters into account to enable a more purposive formulation development and optimisation.

Particle engineering in DPI formulations holds great potential to optimise overall performance. Even though modification techniques on the carrier level are well established, the engineering of extrinsic fines is a novel approach. Additional experiments and method optimisations are needed to fully develop this approach and exploit its potential towards enhanced respiratory drug delivery. The findings of this study underline the importance of surface energy considerations within DPI formulation development.

References Chapter 4

[1] U. v. Shah, Z. Wang, D. Olusanmi, A.S. Narang, M.A. Hussain, M.J. Tobyn, J.Y.Y. Heng, Effect of milling temperatures on surface area, surface energy and cohesion of pharmaceutical powders, International Journal of Pharmaceutics. 495 (2015) 234–240. https://doi.org/10.1016/j.ijpharm.2015.08.061.

[2] S. Marek, H.D.C. Smyth, L. Garcia-Contreras, D.J. Cooney, R.J. Garmise, L.D. Jones, A.J. Hickey, Medicinal and Pharmaceutical Aerosols, in: Aerosols Handbook: Measurement, Dosimetry, and Health Effects, 2nd ed., CRC Press, 2013.

[3] P. Begat, D.A.V. Morton, J. Shur, P. Kippax, J.N. Staniforth, R. Price, The Role of Force Control Agents in High-Dose Dry Powder Inhaler Formulations, Journal of Pharmaceutical Sciences. 98 (2009) 2770–2783. https://doi.org/10.1002/jps.21629.

[4] P. Begat, R. Price, H. Harris, D.A. v Morton, J.N. Staniforth, The Influence of Force Control Agents on the Cohesive-Adhesive Balance in Dry Powder Inhaler Formulations, KONA Powder and Particle Journal. 23 (2005) 109–121. https://doi.org/10.14356/kona.2005014.

[5] P. Mehta, Imagine the Superiority of Dry Powder Inhalers from Carrier Engineering, Journal of Drug Delivery. 2018 (2018) 1–19. https://doi.org/10.1155/2018/5635010.

[6] M. Kumon, S. Machida, M. Suzuki, A. Kusai, E. Yonemochi, K. Terada, Application and Mechanism of Inhalation Profile Improvement of DPI Formulations by Mechanofusion with Magnesium Stearate, Chemical and Pharmaceutical Bulletin. 56 (2008) 617–625. https://doi.org/10.1248/cpb.56.617.

[7] S.S. Desai, A.A. Aher, P.T. Kadaskar, Methods for reduction of cohesive forces between carrier and drug in DPI formulation, Drug Development and Industrial Pharmacy. 39 (2013) 1589–1598. https://doi.org/10.3109/03639045.2012.728229.

[8] M. Kumon, M. Suzuki, A. Kusai, E. Yonemochi, K. Terada, Novel approach to DPI carrier lactose with mechanofusion process with additives and evaluation by IGC, Chem Pharm Bull (Tokyo). 54 (2006) 1508–1514. https://doi.org/10.1248/cpb.54.1508.

[9] R. Guchardi, M. Frei, E. John, J.S. Kaerger, Influence of fine lactose and magnesium stearate on low dose dry powder inhaler formulations, Int J Pharm. 348 (2008) 10–17. https://doi.org/10.1016/j.ijpharm.2007.06.041.

[10] S. Hou, J. Wu, X. Li, H. Shu, Practical, regulatory and clinical considerations for development of inhalation drug products, Asian Journal of Pharmaceutical Sciences. 10 (2015) 490–500. https://doi.org/10.1016/j.ajps.2015.08.008.

[11] J. Koskela, D.A. v Morton, P.J. Stewart, A.M. Juppo, S. Lakio, The effect of mechanical dry coating with magnesium stearate on flowability and compactibility of plastically deforming

microcrystalline cellulose powders, Int J Pharm. 537 (2018) 64–72. https://doi.org/10.1016/j.ijpharm.2017.11.068.

[12] P.M. Young, D. Cocconi, P. Colombo, R. Bettini, R. Price, D.F. Steele, M.J. Tobyn, Characterization of a surface modified dry powder inhalation carrier prepared by "particle smoothing," Journal of Pharmacy and Pharmacology. 54 (2010) 1339–1344. https://doi.org/10.1211/002235702760345400.

[13] S.C. Das, Q. Zhou, D.A.V. Morton, I. Larson, P.J. Stewart, Use of surface energy distributions by inverse gas chromatography to understand mechanofusion processing and functionality of lactose coated with magnesium stearate, European Journal of Pharmaceutical Sciences. 43 (2011) 325–333. https://doi.org/10.1016/j.ejps.2011.05.012.

[14] N. Bungert, M. Kobler, R. Scherließ, In-Depth Comparison of Dry Particle Coating Processes Used in DPI Particle Engineering, Pharmaceutics. 13 (2021) 580. https://doi.org/10.3390/pharmaceutics13040580.

[15] M.D. Jones, R. Price, The influence of fine excipient particles on the performance of carrier-based dry powder inhalation formulations, Pharm Res. 23 (2006) 1665–1674. https://doi.org/10.1007/s11095-006-9012-7.

[16] F. Grasmeijer, A.J. Lexmond, M. van den Noort, P. Hagedoorn, A.J. Hickey, H.W. Frijlink, A.H. de Boer, New mechanisms to explain the effects of added lactose fines on the dispersion performance of adhesive mixtures for inhalation, PLoS One. 9 (2014) e87825. https://doi.org/10.1371/journal.pone.0087825.

[17] H. Kinnunen, G. Hebbink, H. Peters, D. Huck, L. Makein, R. Price, Extrinsic lactose fines improve dry powder inhaler formulation performance of a cohesive batch of budesonide via agglomerate formation and consequential co-deposition, Int J Pharm. 478 (2015) 53–59. https://doi.org/10.1016/j.ijpharm.2014.11.019.

[18] N. Bungert, M. Kobler, R. Scherließ, Surface energy considerations in ternary powder blends for inhalation, Int J Pharm. 609 (2021) 121189. https://doi.org/10.1016/j.ijpharm.2021.121189.

[19] C. della Volpe, S. Siboni, Acid–base surface free energies of solids and the definition of scales in the Good–van Oss–Chaudhury theory, Journal of Adhesion Science and Technology. 14 (2000) 235–272. https://doi.org/10.1163/156856100742546.

[20] Anett Kondor Daryl R. Williams Daniel J. Burnett, Determination of Acid-Base Component of the Surface Energy by Inverse Gas Chromatography: iGC SEA Application Note 227, (2014). https://www.surfacemeasurementsystems.com/downloads/sea-application-notes/.

[21] P.P. Ylä-Mäihäniemi, J.Y.Y. Heng, F. Thielmann, D.R. Williams, Inverse Gas Chromatographic Method for Measuring the Dispersive Surface Energy Distribution for Particulates, Langmuir. 24 (2008) 9551–9557. https://doi.org/10.1021/la801676n.

[22] A.H. de Boer, P. Hagedoorn, D. Gjaltema, J. Goede, H.W. Frijlink, Air classifier technology (ACT) in dry powder inhalation, International Journal of Pharmaceutics. 310 (2006) 81–89. https://doi.org/10.1016/j.ijpharm.2005.11.029.

[23] A. DeBoer, P. Hagedoorn, D. Gjaltema, J. Goede, K. Kussendrager, H. Frijlink, Air classifier technology (ACT) in dry powder inhalation Part 2. The effect of lactose carrier surface properties on the drug-to-carrier interaction in adhesive mixtures for inhalation, International Journal of Pharmaceutics. 260 (2003) 201–216. https://doi.org/10.1016/S0378-5173(03)00264-3.

[24] D. R. Williams, Particle Engineering in Pharmaceutical Solids Processing: Surface Energy Considerations, Current Pharmaceutical Design. (2015) 2677–2694.

[25] M. Lau, P.M. Young, D. Traini, A review of co-milling techniques for the production of high dose dry powder inhaler formulation, Drug Dev Ind Pharm. 43 (2017) 1229–1238. https://doi.org/10.1080/03639045.2017.1313858.

[26] K. Stank, H. Steckel, Physico-chemical characterisation of surface modified particles for inhalation, Int J Pharm. 448 (2013) 9–18. https://doi.org/10.1016/j.ijpharm.2013.03.009.

[27] H. Kinnunen, G. Hebbink, H. Peters, J. Shur, R. Price, An investigation into the effect of fine lactose particles on the fluidization behaviour and aerosolization performance of carrier-based dry powder inhaler formulations, AAPS PharmSciTech. 15 (2014) 898–909. https://doi.org/10.1208/s12249-014-0119-6.

[28] David E. Packham, Theories of Fundamental Adhesion, Springer, 2017.

Introduction to Chapter 5

Surface energies of lactose particles are not solely differing if modificated or manufactured differently. Indeed, the surface energy may also change during the storage of excipients. The risk within this process is that surface energy assessments are, to date, not part of typical batch release tests or retestings in pharmaceutical quality control. If stored at room conditions, moisture may adsorb on the surface of the excipients or may get absorbed. Absorbed humidity increases the molecular mobility, which could cause the reorientation of molecules to lower energy states. Hence, the surface energy would decrease [1]. Typically, DPI formulations contain highly crystalline carrier particles to prevent recrystallisation related stability issues. Such carriers may still adsorb moisture, which then covers parts of the surface and consequently determines the interaction with the surroundings. If humidity condenses on the particles‘ surface, capillary forces may occur [2]. Furthermore, if two particles in contact are surrounded stored at humid conditions and both show a (limited) solubility in water, they may start fusing in dependence of their storage time at these conditions. As a result, the particles will be hardly separable.

I found long-time stored lactose batches to perform significantly worse as carriers in DPI formulations than fresh batches. Although particle size distributions seemed similar, the *in vitro* drug delivery was considerably decreased. Chapter 5 comprises the study I designed to figure out the reason for the decreased performance after long time storage of inhalation grade lactose.

References

[1] H.E. Newell, G. Buckton, D.A. Butler, F. Thielmann, D.R. Williams, The use of inverse phase gas chromatography to study the change of surface energy of amorphous lactose as a function of relative humidity and the processes of collapse and crystallisation, International Journal of Pharmaceutics. 217 (2001) 45–56. https://doi.org/10.1016/S0378-5173(01)00589-0.

[2] H.-J. Butt, M. Kappl, Normal capillary forces, Advances in Colloid and Interface Science. 146 (2009) 48–60. https://doi.org/10.1016/j.cis.2008.10.002.

Chapter 5: The role of intrinsic fines in the decreasing performance of expired lactose carriers for DPI applications

This chapter is published as:
Bungert, N., Kobler, M., Scherließ, R.: The role of intrinsic
fines in the decreasing performance of expired lactose carriers for DPI applications.
International Journal of Pharmaceutics and *Biopharmaceutics* **2022**, Vol. 175, 7-12.
https://doi.org/10.1016/j.ejpb.2022.04.006

Abstract

Dry powder inhalation offers a well-established administration route for either local or systemic drug delivery. Lactose-based powder blends still build the basis of respiratory drug delivery, despite of numerous emerging formulation approaches. The amount of fine lactose excipients, either extrinsic or intrinsic, crucially influences the aerodynamic performance of the corresponding blend. This study highlights the role of intrinsic fines as a fundamental performance affecting parameter during storage and expiry of lactose carrier bulk. We showed that intrinsic fines play an inferior role after expiring compared to fresh batches. If strongly adhering or even merged fines regain their mobility and contribute to the dispersion (by removal and re-addition), it will significantly enhance drug delivery. Furthermore, we provide evidence for decreased mobility of intrinsic fines caused by humidity (e.g., during inappropriate storage) resulting in decreased powder fluidisation.

1. Introduction

Although well-established in the treatment of respiratory diseases, research on dry powder inhalation (DPI) still reveals new insights. There is ongoing research regarding new formulation strategies [1], digitalisation-focused therapeutic optimisations [2] or sustainability considerations [3]. Regardless of these future-oriented approaches, the quality of the current orally inhaled drug products needs to be constantly evaluated as well. Currently, most marketed products (US and EU) are lactose-based interactive blend [4]. These formulations are therapeutic cornerstones of the more than 500 million asthma and COPD patients worldwide [5].

Lactose serves as a carrier particle to enable the processing and dose metering of the micronised (< 5 µm), highly cohesive active pharmaceutical ingredient (API) particles. These interactive blends are obtained by mixing drug and carrier. This straightforward formulation strategy enables respiratory drug delivery but has still room for improvement regarding drug delivery performance [6]. The reason for insufficient drug delivery is mainly due to too high adhesion between drug and carrier [7]. To decrease this adhesion, scientists use particle engineering techniques such as dry particle coatings or modify carrier roughness and hence contact area [8,9]. A different approach to enhancing formulation performance is to use fine lactose excipients to create ternary blends for inhalation. Those ternary blends are known to be superior in terms of aerodynamic performance compared to the respective binary blends [10]. But adding a ternary component to the bulk carrier represents an additional processing step, which needs quality control and is money- and time-consuming.

Carrier materials initially contain fines to a certain extent, depending on the production technique of the inhalation grade lactose. These intrinsic fines are known to enhance delivery performance following the same principles as added extrinsic fines [11]. Therefore, intrinsic fines are a critical quality attribute of lactose for inhalation.

This study highlights the role of intrinsic fines in lactose-based blends for inhalation. Furthermore, we investigated how intrinsic fines influence the performance of their corresponding interactive blends depending on age and storage.

2. Materials and Methods

2.1. Materials

The carrier material investigated in this study was a highly crystalline, inhalation grade lactose (InhaLac® 230, IH230, Meggle, Wasserburg, Germany). In the following sections, we refer to a fresh batch as a batch that was still ahead of its retest date (< 12 months) and stored in its

commercial packaging (sealed aluminium bag) at non-monitored benchtop conditions. Furthermore, we used an expired batch of the same carrier quality. “Expired” refers to InhaLac 230, which was stored outside of its commercial packaging (wide neck screw top drum) at non-monitored benchtop conditions (IH230 (ex)) for more than 36 months.

To investigate the role of intrinsic fines in the expiry process, we removed and re-added intrinsic fines in this study. Lactose batches with removed intrinsic fines are denoted with the suffix “rF”; the ones where we added the initially removed fines in their initial concentration are denoted with “rF-F”. In all interactive blends we used ipratropium bromide as a model drug (d_{90} < 5 µm, Boehringer Ingelheim, Ingelheim, Germany).

2.1.1. Stressed lactose storage

We stored fresh IH230 samples in open aluminium jars at different conditions for 4 months in different conditioning units (Weiss Umwelttechnik, Reiskirchen-Lindenstruth, Germany) to recreate the condition of the IH230 (ex) sample. The conditions were constantly monitored using data loggers (TFA Dostmann, Wertheim-Reicholzheim, Germany). We chose the conditions according to the ICH guideline CPMP/QWP/ 609/96/Rev 2 as I) long term (25 °C, 60% RH) II) accelerated (40 °C, 75% RH and III) high humidity (25 °C, 90% RH). The high humidity conditions were chosen separately from the well-established ICH guideline to provide information on humidity influence dissociated from higher temperatures.

2.2. Measurement of particle size distributions

We analysed all batches using laser diffraction to ensure similar particle size distributions (PSD) and adequate removal of intrinsic fines. The automatically fed powder (VIBRI) was dispersed using compressed air within the dry powder dispersion unit (RODOS) of the helium-neon laser optical system (HELOS®, Sympatec, Clausthal-Zellerfeld, Germany) at a dispersion pressure of 2 bar for carrier batches and 4 bar for the fines, respectively. We used the R4 lens for all measurements and evaluated the raw data based on the Fraunhofer enhanced equation using the PAQXOS software. Displayed data is average of three measurements.

2.3. Extraction and removal of intrinsic fines

IH230 and IH230 (ex) were both sieved on a sieve shaker (mesh size: 32 µm, RETSCH, Haan, Germany) to extract and collect the corresponding intrinsic fines. Due to high agglomeration tendencies of such small excipients, we additionally used an air-jet sieve (mesh size: 32 µm, Hosokawa Alpine, Augsburg, Germany) with a negative pressure of 4 kPa and 29 min sieving time to ensure complete removal of loose intrinsic fines in the respective carrier batches.

2.4. Assessment of specific surface area (SSA)

We measured the SSA using octane adsorption isotherms in the Surface Energy Analyser (SEA, Surface Measurement Systems, London, UK). Samples were packed into silanised glass columns (inner diameter: 4 mm) and fixed with silanised glass wool on both ends. By tapping the columns using the SMS Column Packer Accessory (Surface Measurement Systems) for 5 min, we excluded voids within the powder bed. The packed columns were conditioned for 60 min at 0% RH and 10 cm^3/min nitrogen flow prior to the SSA measurement. After a double injection of methane (determination of dead volume) we conducted a range of octane injections, which resulted in an adsorption isotherm. The SEA Analysis software (Surface Measurement Systems) enabled the calculation of the SSA according to the BET theory.

2.5. Preparation of interactive blends

All interactive blends in this study were prepared using the Picomix® high-shear mixer (Hosokawa Alpine). All excipients were pre-sieved (mesh size carrier: 250 µm; mesh size drug: 180 µm; mesh size fines: 180 µm) to remove agglomerates. Ahead of the blending process, the excipients were weighed into the mixing vessel using the sandwich-weighing method (1% w/w drug concentration). The mixing process comprised two mixing steps at 500 rpm as well as a sieving step (mesh size: 250 µm) in between. For ternary blends, fines were added in the first mixing step and the drug in the second one. All blends were tested for homogeneity using high-performance liquid chromatography (HPLC, see section 2.7). A blend was considered homogeneous at a drug content of 90% − 110% and a relative standard deviation of drug content < 5%. Prior to the following experiments, we conditioned the blends at 44% RH for at least one week to decrease process-induced electrostatic charging.

2.6. Aerodynamic assessment

The assessment for aerodynamic performance was conducted using the Next Generation Pharmaceutical Impactor (NGI, Copley Scientific, Nottingham, United Kingdom). The powder blends were transferred into Novolizer® devices (MEDA Pharma, Bad Homburg, Germany) and dispersed at an airflow which corresponds to a 4 kPa pressure drop over the device (78.3 L/min). After emitting eight doses, the drug content was quantified using HPLC (see section 2.7). We evaluated the raw data using the CITDAS software (V3.1, Copley Scientific). All data displayed as an average of triplets.

2.7. Quantification of drug content

To quantify drug content in this study, we used HPLC. The analytical method comprised a cyanopropyl-substituted stationary phase (LiChrospher® 100 CN, Merck) and a mobile phase consisting of 71% bidistilled water, 29% acetonitrile and 1.42 g/L heptane sulfonic acid, adjusted to pH 3.2. We validated the method in terms of system suitability, specificity, precision, repeatability, and linearity and calculated the limit of quantification according to the ICH guideline CPMP/ICH/ 381/95 as 0.08 µg/mL. All drug concentrations used for further calculations were within a calibrated range (external standard calibration curve ranging from 0.21 µg/mL to 104.80 µg/mL. Solvents used in this study were supplied by Honeywell Riedel-de Haën (Chromasolv, Seelze, Germany) as chromatographic grade solvents.

2.8. Powder rheometry

Different powder properties were measured using the FT4 Powder Rheometer (Freeman Technology, Tewkesbury, United Kingdom). We used two different methods: The aeration method and powder permeability tests.

2.8.1. Aeration method

The aeration setup comprised an aeration base (perforated base connected to an air control unit), a borosilicate vessel and a stirring blade. The powder sample passes different conditioning and test phases during this test with increasing air flow through the powder bed. The instrument monitors the force which is needed to stir through the powder in helical movements. The range of air velocities needs to be adjusted to the powder behaviour, resulting in an energy plateau at the end of the corresponding method (aeration energy). We used 10 g sample mass per measurement and increased the air velocity up to 20 mm/s to ensure a complete fluidisation for all samples. In contrast to the aeration energy (plateau energy), the aeration ratio allows levelling out of parameters like sample mass deviations. The aeration ratio (AR) is calculated following equation (1).

$$AR = \frac{Total\ energy\ at\ 0\ \frac{mm}{s}\ air\ velocity}{Aeration\ energy\ at\ 20\ \frac{mm}{s}\ air\ velocity} \quad (1)$$

2.8.2. Permeability method

The permeability setup uses the same aeration base as the aeration energy test. In contrast to aeration, the powder sample is filled into a borosilicate split vessel. This split vessel allows (after conditioning by the stirring blade) a levelled sample surface. The conditioned sample was compressed at different pressures by a vented piston. During compression, air passes through the sample and the instrument measures the pressure drop over the powder bed.

Using the pressure drop at 15 kPa compaction pressure, we calculated the permeability according to equation (2).

$$Permeability = \frac{Air\ velocity \times Air\ viscosity \times Length\ of\ the\ powder\ bed}{Cross\text{-}sectional\ area\ of\ the\ powder\ bed \times Pressure\ drop} \quad (2)$$

All FT4 data in this work is based on triplicate measurements.

2.9. Carrier surface morphology

2.9.1. Scanning electron microscopy (SEM)

A Hitachi TM3030 tabletop SEM (Hitachi, Chiyoda, Japan) equipped with a backscatter detector was used to depict lactose surface appearance at 5 kV acceleration voltage. Ahead of SEM imaging, samples were fixed onto carbon stickers and sputter-coated with gold to minimise charging effects (Cressington 108, Tescan, Dortmund, Germany).

2.9.2. Atomic force microscopy (AFM)

Morphology mapping of lactose particles has been conducted using a cypher atomic force microscope (Oxford Instruments, Abingdon, United Kingdom) in tapping mode. The scan size was 25 µm^2 at a scan rate of 1 Hz and a resolution of 256 x 256 pixel. The spring constant of the cantilever was 457.5 pN/nm. AFM raw data was processed using Igor Pro software (Wavemetrics, Lake Oswego, OR, USA). We probed at least two different spots on the surface of three different particles. Shown data is picked as representative for these particle qualities.

2.10. Statistical evaluation

Statistical calculations were performed using Microsoft Excel 2016 (Microsoft Corporation, Redmond, WA, USA). We stated differences between measurement results to be significant at a *p*-value < 0.05 (depicted as "*").

3. Results and Discussion

3.1. Air-jet sieving could remove intrinsic fines without changing carrier particle size

This study is based on different sieve fractions. We removed the intrinsic fines of inhalation grade lactose batches to investigate if and how this will affect carrier performance in the corresponding interactive blends. To obtain valid results, we verified the success of the sieving process by measuring the PSDs. The PSDs of the carrier substances used are displayed in Fig. 1.

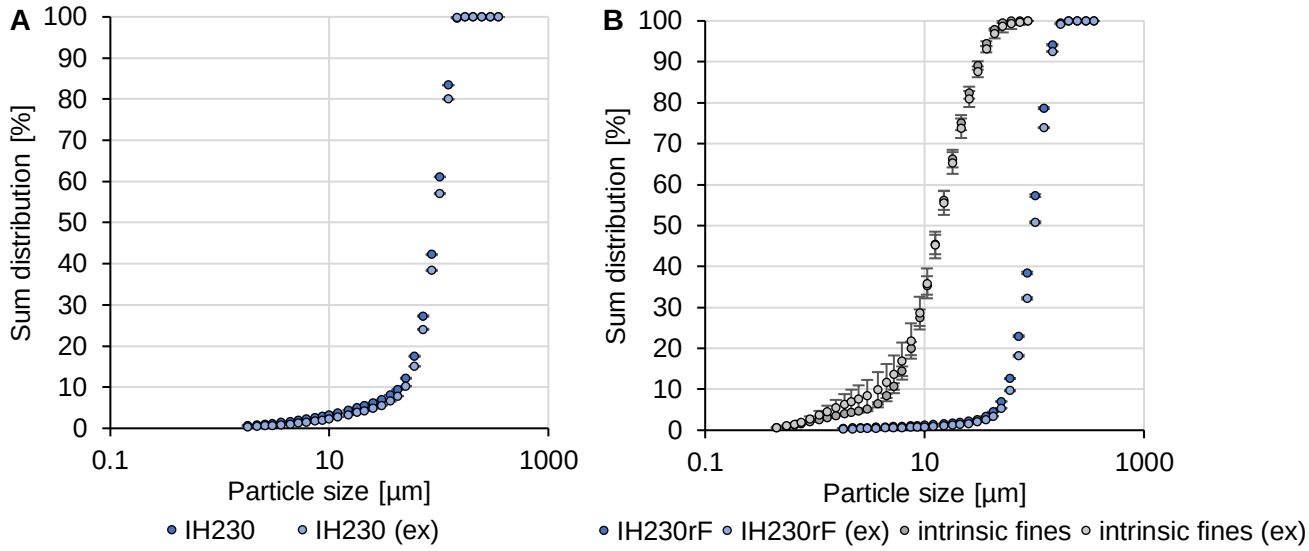

Figure 1: PSDs of A) InhaLac 230 and InhaLac 230 (ex) as bulk and B) after the removal of the respective intrinsic fines. n=3, error bars show SD.

Based on Fig. 1, we state that the PSDs within the lactose batches before and after sieving were equivalent (IH230 = IH230 (ex)). Furthermore, the PSDs (Fig. 1 A and B) served as proof for the successful removal of intrinsic fines. Table 1 displays the d_{10}, d_{50} and d_{90} values before and after air-jet sieving. The values did not differ statistically significant before the removal of intrinsic fines (p-value > 0.05), whereas they did after (p-value < 0.05). The mass concentration of the removable fines (via air-jet sieving) was higher for the fresh batch (IH230: 3.2%) compared to the expired batch (IH230 (ex): 2.2%), which is in line with the differing d-values. Nevertheless, the differences in PSD of the “rF” batches have no influence on the comparability in section 3.2, since we are comparing changes within batches, not total values.

Table 1: Particle size parameters before and after removing intrinsic fines via air-jet sieving. n=3, SD in parentheses.

Material	IH230		IH230 (ex)		IH230rF		IH230rF (ex)	
d_{10} [µm]	44.2	(4.0)	49.2	(0.2)	55.3	(0.2)	60.5	(0.2)
d_{50} [µm]	93.4	(3.2)	96.0	(0.1)	95.8	(0.3)	101.3	(0.2)
d_{90} [µm]	134.2	(0.0)	134.1	(0.1)	139.5	(0.3)	142.7	(0.1)
Particles < 30 µm [%]	6.9	(0.1)	5.6	(0.0)	2.6	(0.0)	2.0	(0.0)

Furthermore, Table 1 presents the percentage of particles smaller than 30 µm. Both batches decreased by approximately 65% in particles < 30 µm after air-jet sieving, even though the removed mass concentration was different. This hints at fines, which were not removable by air-jet sieving, but dispersible at high pressures in HELOS measurements. It must be stated that particle sizing by laser diffraction differs from the results obtained by sieving. The reason is a lack of precision for small sizes when using laser diffraction, different measurement principles and crucially different dispersion forces between air-jet sieving and laser diffraction [12].

Using the original bulk materials and these sieve fractions, we produced adhesive mixtures for inhalation. We additionally rebuild the original batches by adding the previously removed intrinsic fines in their initial concentration to the carrier sieve fractions without intrinsic fines, respectively. We proportioned the re-added concentration to the removable fines' concentrations.

3.2. Removal of intrinsic fines caused changes of fine particle fraction depending on the carrier storage

All six blends were homogeneous (RSD < 3%) after blending and assessed for their aerodynamic performance after conditioning. We refer to aerodynamic performance as fine particle fraction (FPF). We depicted the results of the NGI assessments in Fig. 2. After removing the intrinsic fines of IH230, the FPF of the corresponding blend decreased significantly from 39.9% to 33.6%. Since fines crucially influence the aerodynamic performance of an interactive blend [10], the significant performance decrease can be explained solely by the absence of fines. But performing the same removal step with the IH230 (ex) batch, the performance did not change statistically significant. Hence, we concluded that the fines in the expired batch did not significantly contribute to the blend performance of IH230 (ex).

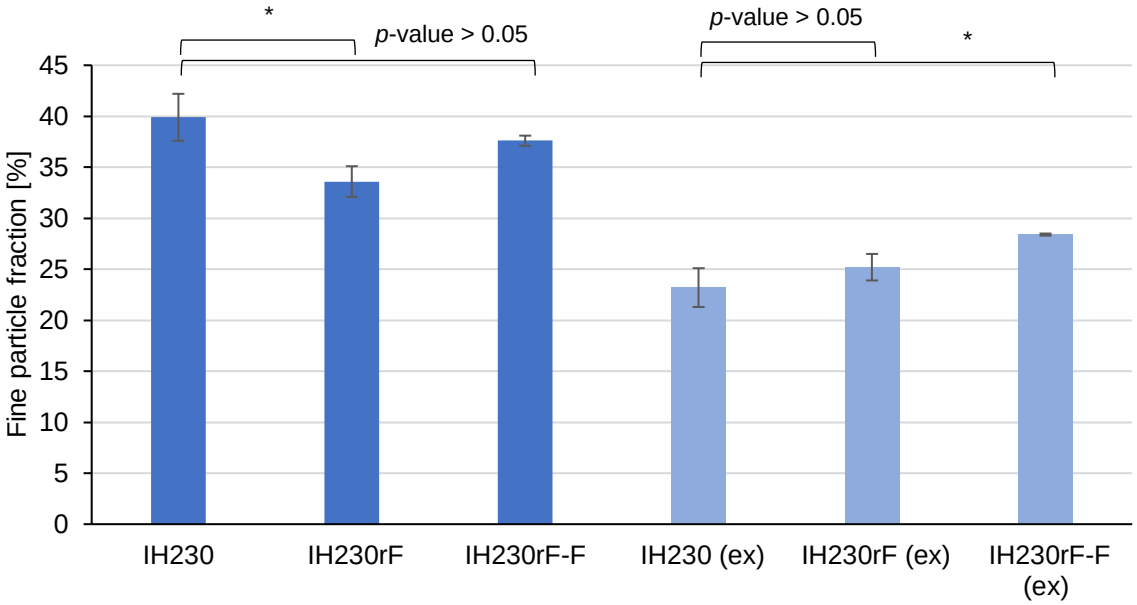

Figure 2: Results of NGI assessment (FPF at a cut-off of 5 µm). IH230 batches coloured in dark blue, IH230 (ex) batches coloured in light blue. n=3, error bars indicate SD.

When re-adding the removed fines of IH230 to IH230rF, we reached a comparable FPF as before the removal (no significant difference, *p*-value > 0.05). This indicates that the fines had the same performance-enhancing characteristics in the original bulk as in the IH230rF-F blend. Contrarily, the addition of the initially removed fines to the IH230rF (ex) batch resulted in a significantly enhanced FPF. Restoring the same concentration and type of fines present in the original IH230 (ex) batch, the FPF increased from 23.2% to 28.4%.

Based on these observations, we assume the intrinsic fines in the expired batch to be strongly bound to the carrier or even fused. Nevertheless, it is possible to remove (at least parts of) them using high dispersion pressures (during the laser diffraction measurements) or extensive dispersion times (during air-jet sieving). Comparably low pressures within short timeframes during aerodynamic assessment were not able to loosen the fines to include them into the dispersion mechanism. But if these fines are removed and then blended with the initial carrier, they will be available again to meet their role as contributors in the dispersion of the blend.

Additionally, we observed a statistically significant higher FPF for IH230 blends compared to IH230 (ex) or IH230rF-F (ex) blends. This hints at FPF influencing factors apart from the content and availability of intrinsic fines. Fused fines (Fig. 3) may lead to a micro-roughness, which was shown to decrease drug detachment, due to mechanical interlocking [8].

3.3. Powder rheometry detected changes in fines-related blend characteristics

We performed powder aeration tests to check on the hypothesis of worse fluidisation with or without available intrinsic fines. A worse fluidisation may indicate a worse dispersion of the

respective powder blend and thus a worse FPF. Multiple properties influence the aeration behaviour of a powder sample: Particle adhesion/cohesion, surface texture, morphology, and particle size distribution. As adhesion should be comparable (expired and fresh batches are still chemically identical), as well as PSD, morphology and the availability of intrinsic fines could mainly influence aeration. In this study, we used the aeration ratio (AR) as a representative value for the aeration behaviour. Based on previously published data [13], a lower aeration ratio correlates with higher amounts of (available) fines and higher FPFs of the corresponding interactive blends, respectively. We displayed the measured AR in Table 2. When comparing IH230 and IH230 (ex), one can observe increased ARs after expiry. Increased ARs can be caused by decreased availability of fines resulting in decreased fluidisation and dispersion characteristics. The batches with removed fines, in turn follow the same trend, whereas it will be most likely caused by fused fines on the carrier surface of IH230rF (ex). Since the aeration method is based on a blade stirring through the air-penetrated powder bed, the friction of particles will affect the measured energy. In the scenario of particles without intrinsic fines and comparable PSDs, the fused fines could result in increased surface roughness causing more friction while stirring through the powder bed, resulting in higher ARs of the IH230rF (ex) sample.

The permeability of a powder bed depends on the particle size distribution, particle morphology and interaction strength of the particles. If a powder is little cohesive and has narrowly distributed, large, smooth particles, air will penetrate the powder bed easily. A low permeability, in opposite, will lead to the powder being lifted by the dispersing airflow as a plug, fractured and subsequently dispersed [14]. In the past, Hertel et al. used the permeation method in powder rheometry to figure out the ideal amount of extrinsic fines [13]. They reported decreasing permeability with an increasing percentage of extrinsic fines. If the particle size distribution is comparable (as shown in Fig. 1 for InhaLac 230 and InhaLac 230 (ex)), the permeability should be mainly dependent on the carrier morphology. In Table 2, we displayed the permeability of the respective powder samples.

Table 2: Results of FT4 powder rheometer tests of the carrier materials in terms of aeration energy and permeability. Also, permeability data on lactose samples after stressed storage is shown. n=3, SD in parentheses.

Material	IH230		IH230 (ex)		IH230rF		IH230rF (ex)	
AR	9.3	(0.4)	11.3	(2.2)	10.2	(0.6)	13.0	(1.5)
Permeability [•10^{-9} cm^2]	94.2	(0.8)	134.8	(3.4)	112.8	(0.9)	131.8	(3.9)

Material (conditioned)	IH230 60% RH		IH230 75% RH		IH230 90% RH	
Permeability [•10^{-9} cm^2]	108.0	(3.0)	127.0	(1.4)	133.7	(11.2)

Even though the PSDs of IH230 and IH230 (ex) are comparable (Fig. 1), the permeabilities showed significant differences.

We assume due to solid bridges between intrinsic fines and coarse carrier particles, the sample surface area decreased in the stored sample and hence the opportunities for interaction between air and lactose (see section 3.5; Fig. 3).

Furthermore, permeability is a measure of the void space in the powder if the fines are not able to move freely and thus do not occupy voids, the permeability increases.

We observed the same pattern for the batches with removed intrinsic fines. The permeability increased for IH230rf (ex) due to the irregularly shaped carriers being fused with fines. Fines that are fused could work as spacers between the particles which results in increased permeability. The fresh lactose batch without intrinsic fines, in turn, should contain less fused fines and hence resulted in less permeability.

An assessment of the SSA gave further insights into surface properties of the lactose samples. Table 3 contains the respective SSA values before and after removal of intrinsic fines of fresh and expired lactose batches. Especially the differences after air-jet sieving are interesting, since the fresh batch shows a significant decrease of SSA by removal of intrinsic fines. The SSA of the expired batch in turn, changed not statistically significant (less fines were removable). In general, the expired batch exhibited a smaller SSA compared to the fresh batch, indicating fused fines and potentially a carrier smoothening by humidity [15].

Table 3: Results of SSA assessments using octane adsorption isotherms before and after removing intrinsic fines from the respective lactose batches. n=3, SD in parentheses.

Material	IH230		IH230 (ex)		IH230rF		IH230rF (ex)	
SSA [m^2/g]	0.22	(0.00)	0.15	(0.02)	0.10	(0.01)	0.09	(0.00)

3.4. Storage stability tests reveal the reason for changes upon storage

Following the findings of the NGI assessments and powder rheometry, we started storage tests to elucidate the conditions causing transfer the fresh lactose batch into the condition of the expired batch. Therefore, InhaLac 230 samples were stored at three different conditions and assessed for their powder properties afterwards. The permeability results of the stored samples are displayed in Table 2.

One can observe, that the permeabilities approached the value measured for IH230 (ex) with increasing storage humidity. The permeability of the sample stored at 90% RH showed no statistically significant difference to IH230 (ex). The RH most likely caused the fusion of adhering fines with the carrier surface. Based on this observation, it was possible to reproduce the condition of IH230 (ex) permeability-wise.

3.5. SEM and AFM detected fused fines

To check on the hypothesis of intrinsic fines being fused on the carrier surface, we used SEM and AFM. Since neither SEM imaging nor the tapping mode of the AFM allows a clear differentiation between fines being fused or just loosely adhering, we investigated the surfaces of IH230rF and IH230rF (ex). The SEM images in Fig. 3 A and B indicate fewer residual fines on the surface of IH230rF than on the surface of IH230rF (ex).

AFM provides 3-dimensional morphology maps of the non sputter-coated carrier surface. For the sake of comparability and feasibility, we always probed the same crystal facets of tomahawk shaped, flat-lying lactose crystals (Fig. 3 C). In Fig. 3 D and E, the surface of IH230rF (ex) exhibits protrusions that can be caused by fused intrinsic fines. The surface of IH230rF showed comparably small protrusions and to a lesser extent. Furthermore, the analysis software provides RMS values (root mean square of a surface) by calculating the average height deviations from the mean height line of the mapped area [16]. The higher the RMS value, the rougher the surface. The RMS values supported the SEM and AFM measurements as the fresh batch resulted in crucially lower roughness values (IH230: 3.92 nm) than the expired batch (IH230 (ex): 10.16 nm).

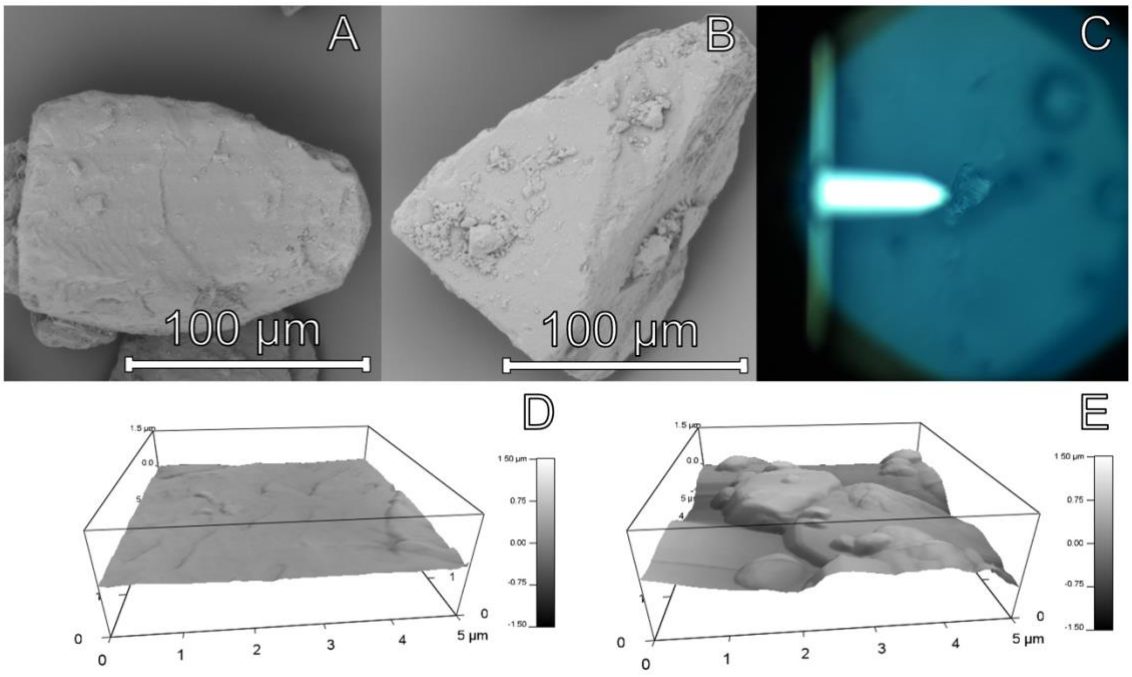

Figure 3: SEM and AFM images of IH230rF (A, D) and IH230rF (ex) (B, E). C shows a light microscopic picture of an exemplary lactose crystal under investigation by AFM.

4. Conclusion

In this study, we assessed the decreasing aerodynamic performance of expired lactose batches and attributed this behaviour to the availability of intrinsic fines. We were able to show that FPFs of old, expired batches did not change significantly after removing their intrinsic fines.

The shrinking role of intrinsic fines after expiry in powder fluidisation was confirmed in powder rheometric measurements. Furthermore, we were able to reproduce the powder characteristics of the IH230 (ex) batch by high RH storage. We hypothesised, fines began to fuse with the carrier particle in a humid environment, which prevents the respective fines from contributing to the powder dispersion [17].

This work highlights the need to control the storage conditions of excipients used in DPI applications. Even though it was possible to release strongly bound fines by means of high-pressure dry dispersion (e.g., in laser diffraction measurement), the expired batches still reached significantly lower FPFs than the fresh ones. Consequently, the intrinsic fines are not the only detrimental change after long-time storage. Nevertheless, our study emphasises the present risk of solely relying on well-established characterisation techniques such as PSD measurement in quality control or re-test analysis as this may show fines that, however, are

not able to contribute to the aerodynamic performance. PSD measurements at more realistic dispersion pressures may be a promising approach in future studies and eventually to be implemented in quality control.

Additionally, this study provides further insights into the crucial role of fine excipient fractions in lactose for inhalation. Whether to work with qualities containing higher ratios of intrinsic fines, or to manually add micronised lactose to a quality without intrinsic fines, is multifactorial: Depending on regulatory requirements, device specifications and many more, formulation scientist will make their choice. Both strategies allow for a full exploitation of the beneficial effects of fine excipients. Nevertheless, we conclude from this study that both strategies may be vulnerable to humidity dependent performance loss. Thus, lactose carriers containing fine fractions should always be used as fresh as possible.

References Chapter 5

[1] M.M. Chogale, S.B. Dhoble, V.B. Patravale, A triple combination 'nano' dry powder inhaler for tuberculosis: in vitro and in vivo pulmonary characterization, Drug Delivery and Translational Research. 11 (2021). https://doi.org/10.1007/s13346-021-01005-5.

[2] S. Xiroudaki, A. Schoubben, S. Giovagnoli, D.M. Rekkas, Dry Powder Inhalers in the Digitalization Era: Current Status and Future Perspectives, Pharmaceutics. 13 (2021). https://doi.org/10.3390/pharmaceutics13091455.

[3] B. Fulford, K. Mezzi, A. Whiting, S. Aumônier, Life-Cycle Assessment of the Breezhaler® Breath-Actuated Dry Powder Inhaler, Sustainability. 13 (2021). https://doi.org/10.3390/su13126657.

[4] H.-G. Lee, D.-W. Kim, C.-W. Park, Dry powder inhaler for pulmonary drug delivery: human respiratory system, approved products and therapeutic equivalence guideline, Journal of Pharmaceutical Investigation. 48 (2018). https://doi.org/10.1007/s40005-017-0359-z.

[5] G. Viegi, S. Maio, S. Fasola, S. Baldacci, Global Burden of Chronic Respiratory Diseases, Journal of Aerosol Medicine and Pulmonary Drug Delivery. 33 (2020). https://doi.org/10.1089/jamp.2019.1576.

[6] A.H. de Boer, P. Hagedoorn, M. Hoppentocht, F. Buttini, F. Grasmeijer, H.W. Frijlink, Dry powder inhalation: Past, present and future, Expert Opin Drug Deliv. 14 (2017) 499–512. https://doi.org/10.1080/17425247.2016.1224846.

[7] M.D. Jones, H. Harris, J.C. Hooton, J. Shur, G.S. King, C.A. Mathoulin, K. Nichol, T.L. Smith, M.L. Dawson, A.R. Ferrie, R. Price, An investigation into the relationship between carrier-based dry powder inhalation performance and formulation cohesive–adhesive force balances, European Journal of Pharmaceutics and Biopharmaceutics. 69 (2008). https://doi.org/10.1016/j.ejpb.2007.11.019.

[8] N. Renner, H. Steckel, N. Urbanetz, R. Scherließ, Nano- and Microstructured model carrier surfaces to alter dry powder inhaler performance, International Journal of Pharmaceutics. 518 (2017) 20–28. https://doi.org/10.1016/j.ijpharm.2016.12.052.

[9] Q.T. Zhou, L. Qu, I. Larson, P.J. Stewart, D.A.V. Morton, Improving aerosolization of drug powders by reducing powder intrinsic cohesion via a mechanical dry coating approach, International Journal of Pharmaceutics. 394 (2010) 50–59. https://doi.org/10.1016/j.ijpharm.2010.04.032.

[10] M.D. Jones, R. Price, The influence of fine excipient particles on the performance of carrier-based dry powder inhalation formulations, Pharm Res. 23 (2006) 1665–1674. https://doi.org/10.1007/s11095-006-9012-7.

[11] F. Grasmeijer, A.J. Lexmond, M. van den Noort, P. Hagedoorn, A.J. Hickey, H.W. Frijlink, A.H. de Boer, New mechanisms to explain the effects of added lactose fines on the dispersion performance of adhesive mixtures for inhalation, PLoS One. 9 (2014) e87825. https://doi.org/10.1371/journal.pone.0087825.

[12] K. Thalberg, E. Berg, M. Fransson, Modeling dispersion of dry powders for inhalation. The concepts of total fines, cohesive energy and interaction parameters, International Journal of Pharmaceutics. 427 (2012) 224–233. https://doi.org/10.1016/j.ijpharm.2012.02.009.

[13] M. Hertel, E. Schwarz, M. Kobler, S. Hauptstein, H. Steckel, R. Scherließ, Powder flow analysis: A simple method to indicate the ideal amount of lactose fines in dry powder inhaler formulations, Int J Pharm. 535 (2018) 59–67. https://doi.org/10.1016/j.ijpharm.2017.10.052.

[14] J. Shur, H. Harris, M.D. Jones, J.S. Kaerger, R. Price, The Role of Fines in the Modification of the Fluidization and Dispersion Mechanism Within Dry Powder Inhaler Formulations, Pharmaceutical Research. 25 (2008). https://doi.org/10.1007/s11095-008-9538-y.

[15] A. Boshhiha, The influence of relative humidity on the carrier particle surface characteristics used in dry powder inhalation formulation, 7 (2018).

[16] E.R. Beach, G.W. Tormoen, J. Drelich, R. Han, Pull-off Force Measurements between Rough Surfaces by Atomic Force Microscopy, Journal of Colloid and Interface Science. 247 (2002). https://doi.org/10.1006/jcis.2001.8126.

[17] S. Das, I. Larson, P. Young, P. Stewart, Surface energy changes and their relationship with the dispersibility of salmeterol xinafoate powders for inhalation after storage at high RH, European Journal of Pharmaceutical Sciences. 38 (2009). https://doi.org/10.1016/j.ejps.2009.08.007.

Chapter 6: Overall summary, conclusion and outlook

Formulation development in DPI formulation remains a highly complicated task. Unpredictable interdependencies impede deriving formulation properties based on excipient properties. Superior excipient properties (e.g., particle size distribution) may allow for simple, experience-based prognoses in regard of their suitability in a specific combination. But even though a fine powder is expected to exhibit poor flowability, a fine powder after particle engineering may be free flowing despite its small particle size. Therefore, to obtain realistic assumptions of bulk and formulation behaviour a combination of particle properties is needed.

Within this thesis I highlighted the use of the surface energy of solids in DPI formulations, more specifically in interactive blends for inhalation. To do so, I divided these blends in three components: The carrier (substantially between 50 µm to 150 µm), fine excipients (substantially smaller than 32 µm) and drug (smaller than 5 µm). Every fraction has its specific requirements to lead to optimised formulation performance. Since I was focussing on adhesion properties, I did not cover unrelated properties (e.g., morphology-dependent flight behaviour of particles).

I hypothesised the presence of optimal surface energies per fraction. The surface energy interaction (or work of adhesion) is dependent of both interacting surfaces. Therefore, the hypothesis of higher carrier surface energies leading to higher drug adhesion and hence less drug detachment, is also applicable *vice versa*. Thus, a drug should preferentially exhibit lower surface energies, to ease drug detachment from the carrier.

Different surface energy carriers of binary blends were investigated in **Chapter 2** and **Chapter 4**. After an extensive investigation of particle and blend properties, I concluded high-shear mixing as being superior over mechanofusion. The key outcomes were a more sufficient coating of the force-control agent, as well as enhanced drug detachment after high-shear mixing the carrier with magnesium stearate. Magnesium stearate is well-known for its ability to decrease adhesion forces along with or indicated by a surface energy decrease. In the case of this specific additive, the decreasing adhesion is partly attributed to a particle smoothening [1]. This complicates narrowing down observed aerodynamic performance effects to the surface energy changes. As proof for the causal relationship of carrier surface energy and drug detachment, **Chapter 4** introduced an attempt for a proof-of-concept for artificially changed surface energies. A hitherto unexploited additive for carrier modifications, poloxoamer 188, allowed for systematically increased carrier energy levels. The additive was coated onto lactose carrier particles using the coating technique which was found to be superior in **Chapter 2**. After the high-shear mixer coating, carrier surface energies increased crucially, mainly due to an increase in the polar component of the surface energy, as expected. The blend performance (FPF) indicated an increased carrier-drug adhesion, which matched the hypothesis (**Chapter 4**).

I therefore derive the conclusion that systematically decreased or increased carrier surface energies will accordingly influence carrier-drug adhesion in binary blends. Further studies should evaluate additional additives to decrease the carrier surface energy, which is the preferred modification (higher drug detachment). Research mainly relies on magnesium stearate, but probably there are other additives, which hold even greater potential. Inverse gas chromatography may serve as an adhesion benchmark in these studies.

As an additional strategy of proof, drug particles with different surface energies were used in **Chapter 4**. I found high-energy drug substances to result in decreased drug detachment and dispersion, measured as fine particle fraction. This finding also matches the theory mentioned above, that an increase of either of the contributing surface energies will cause stronger thermodynamic work of adhesion. Since drugs are chosen based on their pharmacological properties, this finding met the expectations, but I cannot provide a recommendation for action. If drug modification is acceptable in the respective formulation, a dry particle coating attempt to decrease drug's surface energy should enhance drug detachment from a carrier particle. Additives need therefore to be evaluated for their safety when administered into the lung, since they will deposit together with the drug at the targeted lung region. Furthermore, pharmacological changes such as delayed onset of action due to hydrophobisation need to be considered. Additives on carriers in contrast, will mainly impact in the upper throat region and be swallowed.

I assume that there is an optimum of adhesion forces; strong enough to ensure a stable formulation, but as weak as possible to reach the highest drug detachment rate. Typically, the drug is adhesive enough after micronisation that even after decreasing the surface energy of the carrier crucially, the formulation remains stable. At the moment, the modification of both, drug and carrier, is not established. If further effort will be put in formulation optimisation in terms of adhesion strength matching, alternatives to magnesium stearate would be needed. In this scenario, one would need a portfolio of suitable additives for carrier (and probably drug) to reach the optimum of the respective adhesion strength.

Regarding fine excipients in turn, my hypothesis bases on some theories of their action principle. In short, the agglomeration theory and the active site theory claim that fines adhere to a specific surface. That surface is either the carrier (active site theory) or drug (agglomerate theory). Since these events should be influenced by surface energy changes, a portfolio of fines that were distinguishable in terms of surface energies, was investigated in **Chapter 3**. Higher surface energy levels were expected to build stronger agglomerates with the drug and to occupy high-energy sites on the carrier more likely. The study shows that additional fines exhibiting higher surface energies led to higher fine particle fractions of the respective ternary blends. Again, I assume an optimum of fines' surface energies. Due to the different proposed

working principles, it's hard to predict which surface energy level should be preferred. Excessive surface energies could cause hardly dispersible drug-fines agglomerates, whereas the occupation of high-energy sites on the carrier surface could be more sufficient. I hypothesise, a surface energy order as follows would result in the best fine particle fraction: Carrier < drug < fines. The fines would adhere to drug and carrier preferably. Thus, the higher energy sites on the carrier would be occupied. If the surface energy of the drug is then matched with the fines, leading to dispersible agglomerates, the formulation should reach its maximum performance. This assumption can solely be proven, if most other particle properties are levelled out, so that fundamental adhesion (thermodynamic work of adhesion) changes determine the changes in practical adhesion.

In **Chapter 4** a novel approach was introduced, with which surface modification of fine excipients in respiratory formulations is possible. I extended the hypothesis of Chapter 3, which just covered one drug substance in combination with different fines. Hence, I produced high-energy fines to further increase respective fine particle fractions. The results did not fully match the expectations. This could be due to two reasons: By fundamentally changing particle properties using co-milling, practical adhesion does not follow trends of fundamental adhesion anymore. Or alternatively, using these novel fine excipients shows the expected optimum of surface energy interaction, leading to the highest fine particle fraction only for the medium surface energy levels. Higher surface energies (poloxamer processed) in contrast caused excessive drug-fine adhesion and lower surface energies were just inferior based on the earlier stated hypothesis (Chapter 3). Poloxamer processed fines may also lead to sufficient occupation of active sites on the carriers' surface, but I assume that this beneficial effect may be levelled out by detrimental, excessive adhesion with the drug. Especially since the fines offer more surface area for interaction and typically higher adhesiveness than the carrier, their adhesion properties define the interactions between drug and excipients.

The theory of SE optima is further substantiated by superiority of low-energy fines combined with a high-energy drug over low-energy fines with low-energy drugs. Fines exhibiting lower SEs may need the higher adhesiveness of the drug to sufficiently form agglomerates. High-energy fines in turn worked significantly better with low-energy drugs. A combination of high surface energies for both, drug and fines, might have resulted in poorly dispersible agglomerates (always dependent on the dispersion effectiveness of the device) and less agglomerates detaching from the carrier. The medium-energy fine excipients showed no statistically significant difference between both drugs.

An additional theory to explain the enhanced drug delivery of ternary blends (including fine excipient) is the fluidisation theory. It describes the role of fines within the fluidisation and hence dispersion process of a powder bulk. Fines lead to an increase of tensile strength of

the respective powder bulk. Thus, the more compact powder gets aerated more easily. After observing crucial differences between long-time stored lactose batches and fresh ones, I set up a study, which addresses some of these differences. **Chapter 5** presents one approach to investigate the role of intrinsic fines in the diminishing performance of long-time stored lactose. On first sight both investigated batches looked similar, i.e., in terms of PSD. The respective interactive blends in contrast, performed significantly different. I traced this observation back to the availability of intrinsic fines within the powder bed. Fines being merged with the carrier (most likely due to humidity) are not contributing to the dispersion process. Just at high dispersion pressures (during laser diffraction) I was able disperse the bulk into coarser carrier and intrinsic fines. Thus, this holds the risk of scientists being misled by apparently “matching” size distributions.

In the former chapters it was also observed that long-time stored lactose exhibited lower surface energies compared to fresh batches. Therefore, inverse gas chromatography is able to provide hints on batch-to-batch variations and storage-induced changes, where conventional methods are limited.

The surface energy of solids is a valuable information for formulation development. Nonetheless, it remains just one of many parameters to consider. Some particle properties may have more significant influences on the aerodynamic performance (PSD, roughness, surface area), but one cannot derive everything from these. That is when “inferior” solid state parameters gain importance. Thus, in a scenario of similar particle properties the surface energy unfolds its influence and helps with explaining adhesion related events. Also, the categorisation of engineered particles after production benefits from knowledge of surface energy parameters, since it fills a gap which is left by conventional particle characterisation techniques.

The engineering and thus tailoring of particles for respiratory formulations matches the flexibility we gained with emerging device design strategies. In the next years, we are probably able to match device and formulation to the patient needs. But to reach this target, scientists need a filled toolbox for therapy optimisations. Subsequent studies should put their focus on further developing engineered fines. While carrier and drug modifications are already established, engineered fines are mostly unexplored. They could evolve into a powerful formulation tool by offering new optimisation strategies. In my opinion, modified fines are more promising than drug modifications, when it comes to clinical relevance. Drug particles which are modified to be less adhesive are consequently less wettable (both surface energy related). Hence, they will dissolve slower in the lung fluid and result in a later onset of action.

Especially the modification of the polar surface energy component remains challenging. I highly recommend using a range of polar probe gases in inverse gas chromatography instead

of just using one Lewis acid and one Lewis base. In my studies I confined to always using the same probes for the sake of comparability between all performed studies. If one puts focus on polar energy modifications, a range of polar probe gases will provide more detailed information on the introduced changes. The already mentioned magnitude difference between dispersive and polar component could thereby potentially be levelled out.

Additionally, surface energy analysis can provide useful information on DPI formulations apart from interactive blends. In spheronised powders, the use of inverse gas chromatography is already under investigation [2]. Surface energies can serve as benchmarks if the attractive forces of the drug itself are too strong for a sufficient deagglomeration. If that is the case, one can apply a suitable force control agent to modify the agglomeration strength of the drug particles. Hence, scientists can avoid the complex production process for just checking if force control agents are necessary. Other applications could be the production process setup. Depending on the surface energy and hence cohesiveness, process parameters like rounding repetitions can be adjusted (if using a Vibro-pelletiser [2]).

In terms of engineered particles in DPI formulations, surface energy again provides adhesion indications and additionally parameters of clinical relevance as well. Especially wetting behaviour is crucial for particles, which are intended to dissolve in the lung fluid.

Particle engineering of the future may need the support of valid numerical simulations of particles in contact, to figure out which morphology to engineer [3]. The surface energy is a material property which needs to be included into these models to obtain realistic results.

References

[1] Q. (Tony) Zhou, L. Qu, T. Gengenbach, J.A. Denman, I. Larson, P.J. Stewart, D.A.V. Morton, Investigation of the extent of surface coating via mechanofusion with varying additive levels and the influences on bulk powder flow properties, International Journal of Pharmaceutics. 413 (2011) 36–43. https://doi.org/10.1016/j.ijpharm.2011.04.014.

[2] C. Etschmann, Development of a Softpellet Formulation for Inhaled High-Dose Therapy, 2021. Dissertation Kiel University.

[3] S. Bock, T. Rades, J. Rantanen, R. Scherließ, Additive manufacturing in respiratory sciences – Current applications and future prospects, Advanced Drug Delivery Reviews. 186 (2022) 114341. https://doi.org/10.1016/j.addr.2022.114341.

Synopsis: Bibliographic abstracts

1. Abstract (English)

Dry powder inhalers (DPI) build the fundament of anti-inflammatory therapy for respiratory diseases like asthma and COPD. To reach the target tissue in the lung, the drug particles need to be micronised (< 5 µm), or at least have a corresponding flight behaviour. Particles in that size range come with detrimental properties like high cohesiveness and increased electrostatic charge. Hence, the pure drug is hard to handle, and reproducible dose metering is impossible. Consequently, the drug needs excipients to form a suitable formulation. The most common one is the interactive blend, also referred to as adhesive mixture. It bases on a drug carrier with micronised drug adhering on its surface. During inhalation, the drug is intended to detach and follow the inhalation airstream to the targeted site of absorption. The carrier mainly impacts in the upper throat region, ending up being swallowed and eliminated.

The main challenge with interactive blends is the excessive adhesion of drug to the carrier and hence insufficient drug detachment. Since adhesion is mainly dependent on the intrinsic material properties and on the area of contact, its modifiable either by changing the former using chemical modification or the latter by roughness or morphology alteration. These engineering techniques are mostly applied to the carrier.

Introduced modifications can be characterised by a range of physico-chemical analytical methods. Methods like particle size determinations provide information on general fragmentation during processing, surface area assessment can hint on roughness changes and amorphous content indicates stability. Many more methods may provide useful information, but the fewest address adhesion itself.

Inverse gas chromatography allows for calculating the surface energy of solids (SE), which is the fundament of thermodynamic adhesion. By using the surface energy, adhesion influencing differences can be detected. Within this work I want to highlight the benefits of considering the SE of different formulation components in DPI formulations.

This thesis is divided into six chapters, of which two are the introduction and the overall conclusion. Chapter two deals with the evaluation of suitable methods to specifically modify carrier surface energy. After high-shear mixing was found to be most suitable in terms of coating quality and resulting adhesion decrease, I used this method to prove the causal connection between drug detachment and carrier surface energy in chapter four. By applying a high-energy coating to a lactose carrier, I was able to compare high-, medium- and low energy carriers in terms of aerodynamic performance of the respective blend. The lower the carrier surface energy was, the better performed the respective blend.

Another component of DPI blends are fine excipients. Since their working principal bases on adhesion, I created a portfolio of fine excipients, which were mainly distinguishable in terms of

surface energy. Chapter three comprises the study of the respective blends. Here I found the higher the SE of the fines, the higher the aerodynamic performance of the DPI formulation.
Chapter four continued this approach, by creating a portfolio of different fines using particle engineering and preparing blends with APIs, which also exhibited different SEs. It was shown that high-energy fines worked best with low-energy drug and *vice versa*. This leads to the conclusion that one needs to match the SEs of the respective formulation components.
Since I observed different SEs and performances of fines in chapter three depending on their expiry status, the last study in this thesis addressed expiry mechanisms of inhalation grade lactose.
Chapter five covers a systematic approach to show that fines start to merge with the carrier during expiry. Hence, they were not fully available to contribute to the dispersion process of the respective ternary blend. Both batches, fresh and expired, were similar in terms of typical particle properties like size distribution. The differences that nevertheless exist between those batches are detectable using inverse gas chromatography.
In conclusion, the influence of SE as solid-state parameter was investigated for every component of interactive blends for inhalation. In general, it met the expectations of high surface energy being correlated with increased adhesion and its respective influence on aerodynamic performance. Since all adhesive interactions in DPI formulations have an optimum, SE matching of formulation components may be a promising approach for the future. Therefore, I introduced suitable methods to modify particles in different size ranges and methods to track the introduced modifications.
Here, the surface energy is an easily measurable bulk parameter and adhesiveness benchmark for future formulation development.

2. Abstract (German)

Trockenpulverinhalation bildet das Fundament der Therapien für Krankheiten wie Asthma oder COPD. Um tiefere Lungenregionen zu erreichen, müssen die Wirkstoffpartikel mikronisiert sein (< 5 µm), oder zumindest das entsprechende Flugverhalten aufweisen um dem Atemluftstrom ausreichend tief in die Lunge zu folgen. Partikel in dieser Größe zeichnen sich durch erhöhte Kohäsivität und elektrostatische Aufladung aus, wodurch sie praktisch nicht reproduzierbar zu dosieren oder zu verarbeiten sind. Die interaktive Pulvermischung ist die heutzutage am häufigsten auf dem Markt vertretene Formulierungsstrategie, um dieses Problem zu adressieren. Der mikronisierte Wirkstoff wird mit einem gröberen Träger gemischt, wodurch der Wirkstoff am Träger adhäriert. Während des Inhalationsvorganges soll sich dann der Wirkstoff wieder von dem Trägerpartikel lösen und dem Atemstrom in die tieferen Lungenregionen folgen. Der Träger hingegen impaktiert im Rachen, wird geschluckt und ausgeschieden.

Der Hauptnachteil dieser Formulierungsstrategie ist die zu starke Adhäsion zwischen Wirkstoff und Träger, was zu unzureichendem Ablösen während der Inhalation führt. Da Adhäsion grundlegend von den Materialeigenschaften der Oberflächen und der Kontaktfläche abhängig ist kann man entweder ersteres durch Beschichtungen verändern oder letzteres durch Veränderung der Rauigkeit oder Morphologie. Meistens beschränkt man sich bei diesen Modifikationen auf die Trägersubstanz. Solche Änderungen können dann mit einer Reihe physiko-chemischer Methoden charakterisiert werden; leider messen die wenigsten analytischen Methoden die Adhäsion selbst.

Die inverse Gaschromatographie hingegen ermöglicht die Berechnung der Oberflächenenergie von Feststoffen. Diese ist die Grundlage der thermodynamischen Adhäsion. Durch diese Methode können folglich Änderungen detektiert werden, die die Adhäsionseigenschaften von Stoffen beeinflussen. Das Ziel der Arbeit ist es, den Einfluss der Oberflächenenergie auf verschiedene Bestandteile von Pulverformulierungen zur Inhalation zu beleuchten und somit den Einsatz der inversen Gaschromatographie in der Formulierungsentwicklung zu fördern.

Diese Arbeit gliedert sich in sechs Kapitel, wovon das erste Kapitel eine Einleitung in die Thematik darstellt und das letzte alle durchgeführten Studien abschließend verknüpft. Das zweite Kapitel evaluiert verschiedene Methoden für Oberflächenbeschichtungen mit dem Augenmerk auf einer möglichst gezielten Senkung der Oberflächenenergie von Laktoseträgern. Die Beschichtung im Zwangsmischer war dabei der Mechanofusion überlegen. Die entscheidenden Parameter waren dabei insbesondere die effizientere Beschichtung und die bessere Wirkstoffablösung der korrespondierenden interaktiven Pulvermischungen.

Da viele Publikationen dem Additiv aus Kapitel zwei (Magnesiumstearat) zuschreiben die Wirkstoffablösung zu erhöhen, kommt die Frage auf, ob die gleichzeitig sinkende Oberflächenenergie nur ein Artefakt darstellt.

In Kapitel vier wurde deshalb als Vergleich ein Träger mit einem Additiv beschichtet, das die Oberfächenenergie erhöht, anstatt zu senken. Die Performance der entsprechenden Pulvermischung war erniedrigt gegenüber der nicht veränderten Laktose. Daraus wurde abgeleitet, dass ein kausaler Zusammenhang zwischen der Oberflächenenergie des Trägers und der Wirkstoffablösung von eben jenem während der Inhalation bestätigt werden kann.

Kapitel drei evaluiert die Oberflächenenergie von Laktosefeinanteilen in ternären Pulvermischungen zur Inhalation. Hier wurden Feinanteile verschiedenster Herkunft verglichen, um zu untersuchen, welche Oberflächenenergie optimale Ergebnisse hervorruft. Abgesehen von unterschiedlichen Oberflächenenergien, waren alle Feinanteilqualitäten vergleichbar. In ternären Mischungen mit dem Wirkstoff Ipratropiumbromid konnte geschlussfolgert werden, dass je höher die Oberflächenenergie des Feinanteils, desto besser die Performance der Pulvermischung.

Kapitel vier umfasst neben den neuen Trägerbeschichtungen auch die gezielte Veränderung von Laktosefeinanteilen. Drei Feinanteile mit unterschiedlichen Oberflächenenergien wurden mit je einem von zwei Wirkstoffen unterschiedlicher Oberflächenenergie kombiniert und getestet. Das Ergebnis war, dass Feinanteile mit höheren Energien bessere inhalierbare Fraktionen mit Wirkstoffen niedrigerer Energie erzielten als mit Wirkstoffen hoher Energie und andersherum. Daraus lässt sich schließen, dass es optimale Kombinationen aus Oberflächenenergien zu geben scheint.

Das fünfte Kapitel untersucht lagerungsbedingte Veränderungen von Trägerlaktosen. Es wurde herausgefunden, dass abgelaufene Chargen weniger frei verfügbare, intrinsische Feinanteile besitzen. Diese sind teilweise mit dem Träger verschmolzen und nehmen somit nicht mehr an der Pulverdispergierung teil, was zu einer schlechteren Performance der Mischung führt. Da diese frischen und abgelaufenen Chargen sich auch in ihrer Oberflächenenergie unterscheiden, jedoch nicht in ihrer Partikelgrößenverteilung, kann die inverse Gaschromatographie hier als Ergänzung zu bereits etablierter Analytik dienen.

Zusammenfassend kann gesagt werden, dass diese Arbeit die Effekte der Oberflächenenergie verschiedener Bestandteile von Pulvermischungen zur Inhalation beleuchtet und neue Erkenntnisse hervorgebracht hat. Die Oberflächenenergie kann in der Zukunft eine wertvolle Ergänzung zu bereits routinemäßig genutzter Analytik darstellen.

Synopsis: Appendix

Statement in lieu of an oath:

Erklärungen nach § 8 und § 9 der Promotionsordnung:

Hiermit erkläre ich gemäß § 9 der Promotionsordnung der Mathematisch-Naturwissenschaftlichen Fakultät der Christian-Albrechts-Universität zu Kiel, dass ich die vorliegende Arbeit, abgesehen von der Beratung durch meine Betreuerin, nach Inhalt und Form selbstständig und ohne fremde Hilfe verfasst habe. Weiterhin habe ich keine anderen als die angegebenen Quellen oder Hilfsmittel benutzt und die den benutzten Werken wörtlich oder inhaltlich entnommenen Stellen als solche kenntlich gemacht. Die vorliegende Arbeit ist unter Einhaltung der Regeln guter wissenschaftlicher Praxis entstanden und wurde weder ganz noch in Teilen an einer anderen Stelle im Rahmen eines Prüfungsverfahrens vorgelegt, veröffentlicht oder zur Veröffentlichung eingereicht. Weiterhin wurde mir weder ein akademischer Grad entzogen, noch habe ich an dieser oder einer anderen Fakultät einen früheren Promotionsversuch unternommen. Teile der Arbeit sind in wissenschaftlichen Zeitschriften veröffentlicht oder zur Veröffentlichung akzeptiert. Die dies betreffenden Abschnitte sind entsprechend gekennzeichnet. Die vorliegende Dissertation wurde als kumulative Arbeit verfasst. Im Folgenden wird der Eigenanteil des Promovenden an den veröffentlichten oder zur Veröffentlichung angestrebten Kapiteln gemäß § 8 Absatz 2 der Promotionsordnung dargestellt.

Nicholas Bungert

Darstellung des Eigenanteils nach § 8 Abs. 2 der Promotionsordnung:

Nicholas Bungert, Mirjam Kobler, Regina Scherließ
In-Depth Comparison of Dry Particle Coating Processes Used in DPI Particle Engineering
Pharmaceutics **2021**, 13, 580.

Nicholas Bungert: Conceptualization, Methodology, Validation, Formal analysis, Investigation, Writing – original draft, Visualization.
Mirjam Kobler: Conceptualization, Writing – review & editing.
Regina Scherließ: Conceptualization, Resources, Writing – review & editing, Supervision, Project administration.

Nicholas Bungert, Mirjam Kobler, Regina Scherließ
Surface energy considerations in ternary powder blends for inhalation
International Journal of Pharmaceutics **2021**, 609, 121189.

Nicholas Bungert: Conceptualization, Methodology, Validation, Formal analysis, Investigation, Writing – original draft, Visualization.
Mirjam Kobler: Conceptualization, Writing – review & editing.
Regina Scherließ: Conceptualization, Resources, Writing – review & editing, Supervision, Project administration.

Nicholas Bungert, Mirjam Kobler, Regina Scherließ
Proof-of-concept for artificial surface energies and modified extrinsic fines as a novel particle engineering approach in DPI formulations
Pharmaceutics **2022**, 14(5), 951.

Nicholas Bungert: Conceptualization, Methodology, Validation, Formal analysis, Investigation, Writing – original draft, Visualization.
Mirjam Kobler: Conceptualization, Writing – review & editing.
Regina Scherließ: Conceptualization, Resources, Writing – review & editing, Supervision, Project administration.

Nicholas Bungert, Mirjam Kobler, Regina Scherließ
The role of intrinsic fines in the decreasing performance of expired lactose carriers for DPI applications
European Journal of Pharmaceutics and Biopharmaceutics **2022**, Vol. 175, 7-12.

Nicholas Bungert: Conceptualization, Methodology, Validation, Formal analysis, Investigation, Writing – original draft, Visualization.
Mirjam Kobler: Conceptualization, Writing – review & editing.
Regina Scherließ: Conceptualization, Resources, Writing – review & editing, Supervision, Project administration.

Danksagung

Diese Arbeit markiert den Endpunkt meiner prägenden Zeit in Kiel und an dieser Stelle möchte ich die Möglichkeit nutzen mich bei einigen wichtigen Menschen zu bedanken.

Zuallererst danke ich meiner Doktormutter Regina für die Annahme als Doktorand in deiner Arbeitsgruppe und die Betreuung während der letzten Jahre. Durch die Freiheiten, die du mir gelassen hast, konnte ich die Arbeit in Kiel wirklich zu meiner eigenen Forschung machen.

Ohne besagte Arbeitsgruppe und Institutsmitarbeitende wäre die Zeit als Doktorand sicher deutlich weniger unterhaltsam gewesen. Ich möchte allen Kolleginnen und Kollegen danken, die mich während meiner Promotion begleitet und unterstützt haben. Einige Personen möchte ich dabei besonders hervorheben:

Als ich 2019 nach Kiel kam wurde ich unfassbar herzlich von Büro 106 aufgenommen. Schnell wurden aus Kollegen Freunde und ich bin euch sehr dankbar für die unzähligen Stunden voller Fach- & Freizeitgespräche. Ihr habt alle signifikant an meiner Arbeit mitgewirkt; und sei es „nur“ durch euren Arbeitsethos.

Weiterer Dank geht an Marie und Lena, für Feierabendbiere, Spieleabende und Kaffeekränzchen. Ihr seid ein genau so wichtiger Teil meiner Zeit in Kiel.

Und zu diesem Freundeskreis gehörst natürlich auch du, Hanna. Ich danke dir, für unzählige Gespräche, tatkräftige Unterstützung und dein offenes Ohr. Unser Rumgealber werde ich sehr vermissen!

Ich hoffe, dass unser aller Kontakt nie ganz abbricht!

Und auch wenn euch die Arbeit im Gesamten gewidmet ist, möchte ich an dieser Stelle noch einmal meiner Familie danken. Ohne die bedingungslose Unterstützung meiner Eltern, Lisa und meinen beiden Brüdern, wäre sicher vieles anders gelaufen. Für euch und unsere Beziehung zueinander bin ich unendlich dankbar.